# SYNTHESIS OF POLYCYCLIC HYDROCARBON METAL SYSTEMS AND RUTHENIUM PYRAZOLE SYSTEMS.

BY

TIMOTHY J. BEASLEY

B.Sc. (Hons). University of Leeds, 1984.

A DISSERTATION SUBMITTED IN PARTIAL FULFILMENT

OF THE REQUIREMENTS FOR THE DEGREE OF

MASTER OF SCIENCE

In the Department

of

Chemistry

ACCEPTED
FACULTY OF GRADUATE STUDIES
[redacted]
DEAN
DATE 89/02/07

We accept this dissertation as conforming to the

required standard

[redacted]

Dr. S.R. STOBART

[redacted]

Dr. A. McAULEY

[redacted]

Dr. G.W. BUSHNELL

[redacted]

Dr. C.E. PICCIOTTO



University of Victoria

January 1989

Supervisor: Dr S.R. Stobart.

## ABSTRACT

Prolonged irradiation of a mixture of $Fe(CO)_5$ and 1,4,5,8,9,10-hexahydroanthracene, HHA, results in the formation of mono- and di-iron derivatives $[(C_{14}H_{16})Fe_n(CO)_{3n}]$, n = 1,2; for n = 2, two isomers are formed, with cis and trans arrangements of (diene)-$Fe(CO)_3$ fragments. An X-ray crystal determination for the trans compound shows that the molecule possesses $C_i$ symmetry. Treatment of HHA with $Ru_3(CO)_{12}$ results in catalytic disproportionation of the organic ligand and the isolation of five major organic components.

Reaction of $RuCl_3 \cdot 3H_2O$ with HHA leads to the formation of the polycyclic arene dimer $[(\eta^6\text{-}C_{14}H_{14})Ru(\mu\text{-}Cl)Cl]_2$ which on dissolution in DMSO forms, as a result of the cleavage of the chloro bridges, the mononuclear adduct $[(\eta^6\text{-}C_{14}H_{14})RuCl_2DMSO]$. An X-ray crystal structure determination shows coordination of the DMSO ligand through the sulphur atom; substitution of the DMSO ligand by the phosphorus donor ligand, L, has yielded four mono phosphino adducts which show selective coupling of the phosphorus nucleus to two of the four coordinated arene protons; these protons are shielded by the phosphine ligands which contain phenyl rings (L = $PPh_3$ or $PPh_2Me$).

The substitution of DMSO by $Me_2pzH$, which yields $[(\eta^6\text{-}C_{14}H_{14})RuCl_2(Me_2pzH)]$, has been made the subject of a kinetic study, the results of which indicate that the reaction proceeds via an associative mechanism. A series of mononuclear ruthenium arene pyrazole species of general formula $[(\eta^6\text{-arene})RuCl_2(pzH)_n]$ arene = $C_{14}H_{14}$, n = 2; arene = $C_6H_6$, $C_{10}H_{14}$, n = 1,2, have been formed, and are non-fluxional at ambient temperature on the NMR timescale.

The ruthenium pyrazolyl bridged dimers $[(\eta^6\text{-arene})_2Ru_2(\mu\text{-pz})_2\mu\text{-Cl}]Cl$, arene = $C_6H_6$, $C_{10}H_{14}$, have been prepared. For arene = $C_6H_6$, an X-ray crystal structure determination shows a chlorine atom in a bridging position. For arene = $C_{10}H_{14}$, treatment with reducing agents, such as sodium/mercury amalgam, results in the formation of a Ru(I)-Ru(I) species, proposed to contain a metal-metal bond. A number of oxidative addition reactions have been attempted on this bimetallic system.

[redacted]

Dr. S.R. STOBART

[redacted]

Dr. M.A. McAULEY

[redacted]

Dr. G.W. BUSHNELL

[redacted]

Dr. C.E. PICCIOTTO

# TABLE OF CONTENTS

# LIST OF TABLES

# LIST OF FIGURES

# LIST OF SCHEMES

## ABBREVIATIONS

| | | |
|---|---|---|
| A | = | Absorbance. |
| Cp | = | cyclopentadienyl. |
| $Cp^*$ | = | pentamethylcyclopentadienyl. |
| $C_{10}H_{14}$ | = | para-cymene. |
| d | = | doublet. |
| $\delta$ | = | chemical shift. |
| DMSO | = | dimethylsulphoxide. |
| HHA | = | 1,4,5,8,9,10-hexahydroanthracene. |
| $HHA^*$ | = | 3,4,6,7,9,10-hexahydroanthracene. |
| IR | = | infra-red. |
| LUMO | = | lowest unoccupied molecular orbital. |
| Me | = | methyl. |
| $Me_2pzH$ | = | 3,5-dimethylpyrazole. |
| NMR | = | nuclear magnetic resonance. |
| Ph | = | phenyl. |
| ppm | = | parts per million. |
| pz | = | pyrazolyl anion. |
| pzH | = | pyrazole. |
| q | = | quartet. |
| qn | = | quintet. |
| R | = | alkyl or phenyl. |
| s | = | singlet. |
| t | = | triplet. |
| THF | = | tetrahydrofuran. |
| UV | = | ultra-violet. |

# ACKNOWLEDGEMENTS

I would like to thank Professor S.R. Stobart for his guidance and encouragement during the course of this work. I am very grateful to Mrs. Chris Greenwood and Mr. Ron Brost for assistance provided in NMR and Crystallographic analysis. The University of Victoria is acknowledged for the financial support in the form of Graduate Fellowships (1986 to 1988). Finally, I am indebted to the SRS sports club and my friends for making my stay in Victoria culturally enlightening.

# DEDICATION

To mum, dad, Mick, Doris and family.

# PART 1

## INTRODUCTION

Areas of research which have accounted for the rapid growth of organometallic chemistry include the modification of chemical reactivity of ligands through metal coordination, investigation of practical homogenous catalysis and the modelling of catalytic systems. The role of the ligand in such chemistry is threefold, being present either to impart stability on the metal centre, influence the reactivity of the metal, or to undergo reaction whilst in a coordinated mode. Although there is a plethora of hydrocarbon and related ligands, the following discussion will concentrate only on $\eta^6$-arene and $\eta^4$-conjugated diene complexes as they relate to the context of this thesis.

Many transition metals (e.g. Cr, Mo, Mn, Fe, Ru, Rh) form complexes with arenes.[1,2] The arenes of chromium have been extensively studied, particularly in relation to modification of the reactivity of the arene through coordination. Half sandwich complexes such as $\eta^6$-benzene chromium tricarbonyl were first synthesised by Ofele and Fischer in 1957,[3] and a simpler synthesis was devised by Nicholls and Whiting in 1959.[4] This latter method involved refluxing chromium hexacarbonyl in an excess of the

aromatic compound, or with a molar quantity in an inert solvent. These complexes are air stable, with good solubility properties and are easily handled.[5] The effect of coordination on the reactivity of the arene is illustrated in Fig. 1.1.[6]

Fig. 1.1: Effects of complexation of aromatic compounds to chromium tricarbonyl.

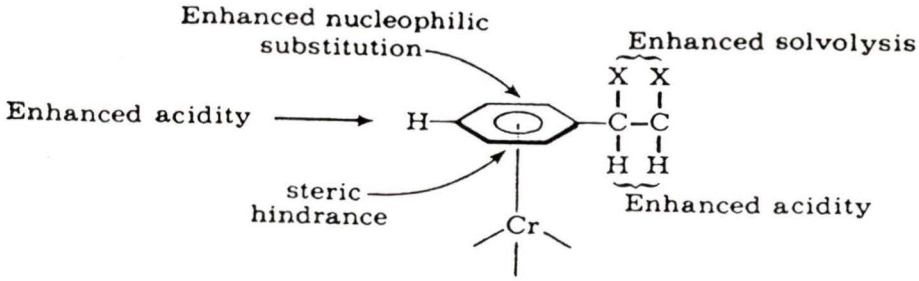


Noticeably, the coordinated arene is now susceptible to nucleophilic attack, and no longer reacts readily with electrophiles. An example of this alteration in reactivity is the reaction of $\eta^6$-chlorobenzene chromium tricarbonyl with sodium methoxide to give the $\eta^6$-anisole complex in good yield, Eqn. 1.1.

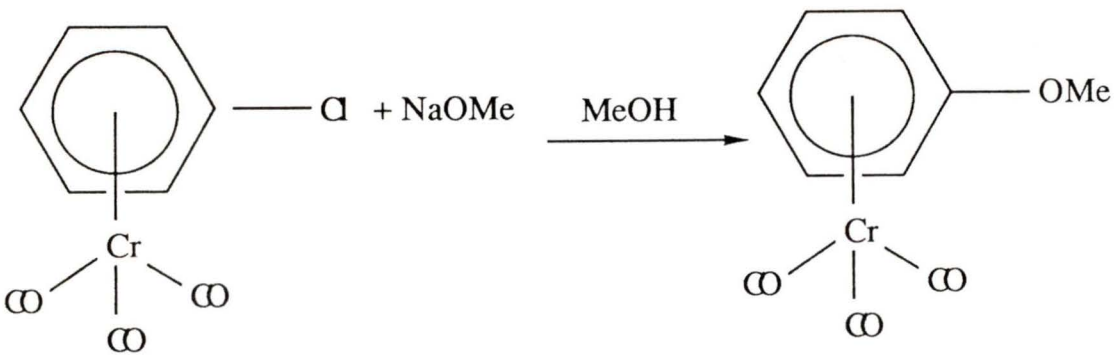


Eqn. 1.1.

There is a similarity between the rate of this reaction and the corresponding reaction involving p-nitrochlorobenzene, and a comparison between the electron withdrawing effect of the chromium tricarbonyl and nitro groups has been made.[4] Finally, the arene can be released through the action of an oxidising agent such as iodine.

Various $\eta^6$-naphthalene chromium tricarbonyl complexes have been synthesised, and the reactivity of the bound arene has been studied.[7] This reactivity is influenced by the electronic properties of the co-ligands attached to the chromium centre. For example, no reaction is observed between $(\eta^6\text{-}C_{10}H_8)Cr(P(OMe)_3)_3$ and $LiCMe_2CN$, whereas the reaction between $(\eta^6\text{-}C_{10}H_8)Cr(CO)_3$ and $LiCMe_2CN$ affords the alkylated product in good yield, Scheme 1.1.

Scheme 1.1: The effect of the co-ligand on the reactivity of two $\eta^6$-naphthalene chromium complexes.

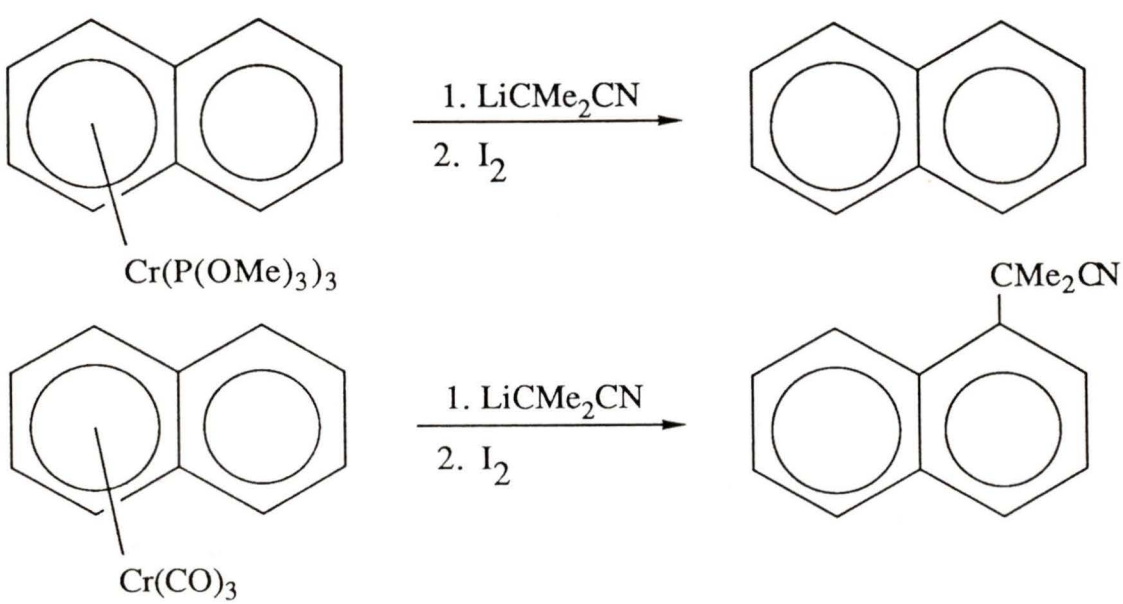

The increased donor power of $P(OMe)_3$ with respect to CO reduces the electron withdrawing effect of the chromium centre and makes the coordinated arene less susceptible to nucleophilic attack.

For group VIII metals, ruthenium accounts for the largest variety of arene complexes.[8] The reaction of ruthenium trichloride with cyclohexa-1,3-diene was first studied by Winkhaus and Singer in 1967[9] who proposed that the product of the reaction was the polymeric adduct ($\eta^4$-benzene)$RuCl_2$. Later work by Zelonka and Baird[10] and by Bennett et al[11] proved the product was dimeric in nature with all six benzene carbon atoms attached in a $\eta^6$ fashion, (1.I). Alteration of the diene in the synthesis

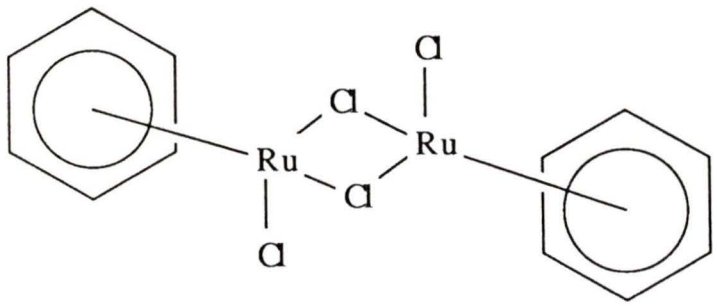


(1.I).

has allowed a variety of $\eta^6$-arene complexes to be isolated.[12] Numerous derivatives of the above complex have been formed; examples include the formation of the bromo-, iodo- and thiocyanate analogs using metathetical reactions,[13] and a range of monomeric adducts of the general formula [($\eta^6$-arene)$RuCl_2L$] (L = $PR_3$, $P(OR)_3$ and

$AsR_3$).

Treatment of $[(\eta^6\text{-benzene})RuCl_2]_2$ with $NH_4PF_6$ in methanol results in chloride abstraction and the formation of the triply halo-bridged species.[12] Similarly, treatment with aqueous sodium hydroxide gives the triply hydroxo-bridged species, (1.II).[14] Catalytic activity is shown by

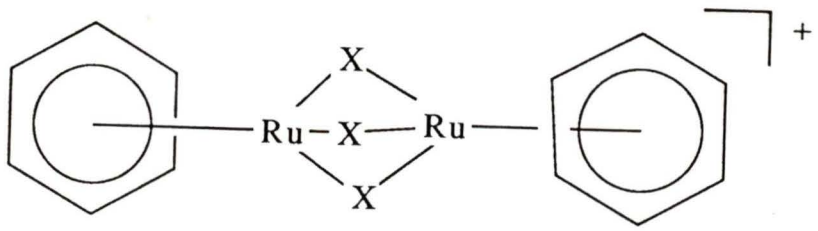


(1.II: X = Cl, OH).

$[(\eta^6\text{-benzene})RuCl_2]_2$, with respect to the hydrogenation of olefins.[15] The best results in this system are obtained in weakly coordinating solvents (S) such as benzene. The proposed reaction scheme, similar to that proposed when $(PPh_3)_3RuCl_2$ is the catalyst,[16] is shown in Scheme 1.2.

As with the chemistry of chromium arenes, coordination of Ru(II) to an arene results in enhanced reactivity of the arene to nucleophiles. However, the resulting cyclohexadienyl derivatives are often unstable; the first derivatives $[(\eta^5\text{-}C_6H_6X)RuCl_2]^{2+}$ (X = CN, OH) were observed by Zelonka and Baird[13] but isolation was unsuccessful.

Scheme 1.2: The catalytic hydrogenation of an olefin by $[(\eta^6\text{-benzene})RuCl_2]_2$.

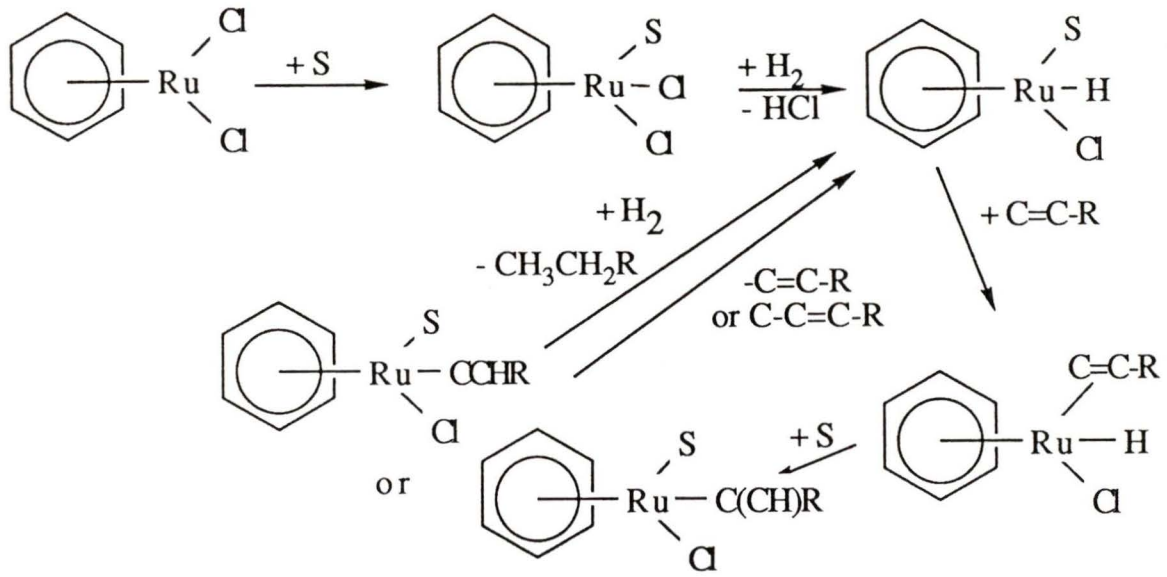


For $\eta^4$-conjugated diene complexes, the metal most commonly coordinated is iron(0). The first reported compound of this type was butadiene iron tricarbonyl formed by Rheilen et al in 1930,[17] who proposed that the butadiene fragment was chelated through the terminal carbon atoms to the iron centre, but work by Hallam and Pauson in 1958[18] showed this structure to be incorrect and they proposed a $\eta^4$-conjugated diene arrangement for the butadiene fragment which is now accepted, (1.III).

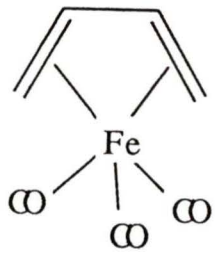


(1.III).

Various compounds, which cannot normally be isolated, are stabilised and hence can be studied upon complexation to a metal centre. An example of this is cyclobutadiene which dimerises even at very low temperature; however, the tricarbonyl iron complex is a stable pale yellow liquid.[19] The formation of this complex is shown in Eqn. 1.2.

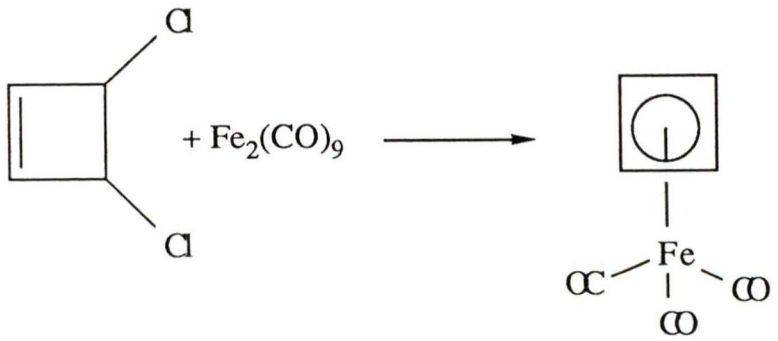


Eqn. 1.2.

Once coordinated, the cyclobutadiene fragment can be used in synthesis, such as in the formation of "cubanes"; an example of this is shown in Scheme 1.3.[20]

Scheme 1.3: The synthesis of cubane.

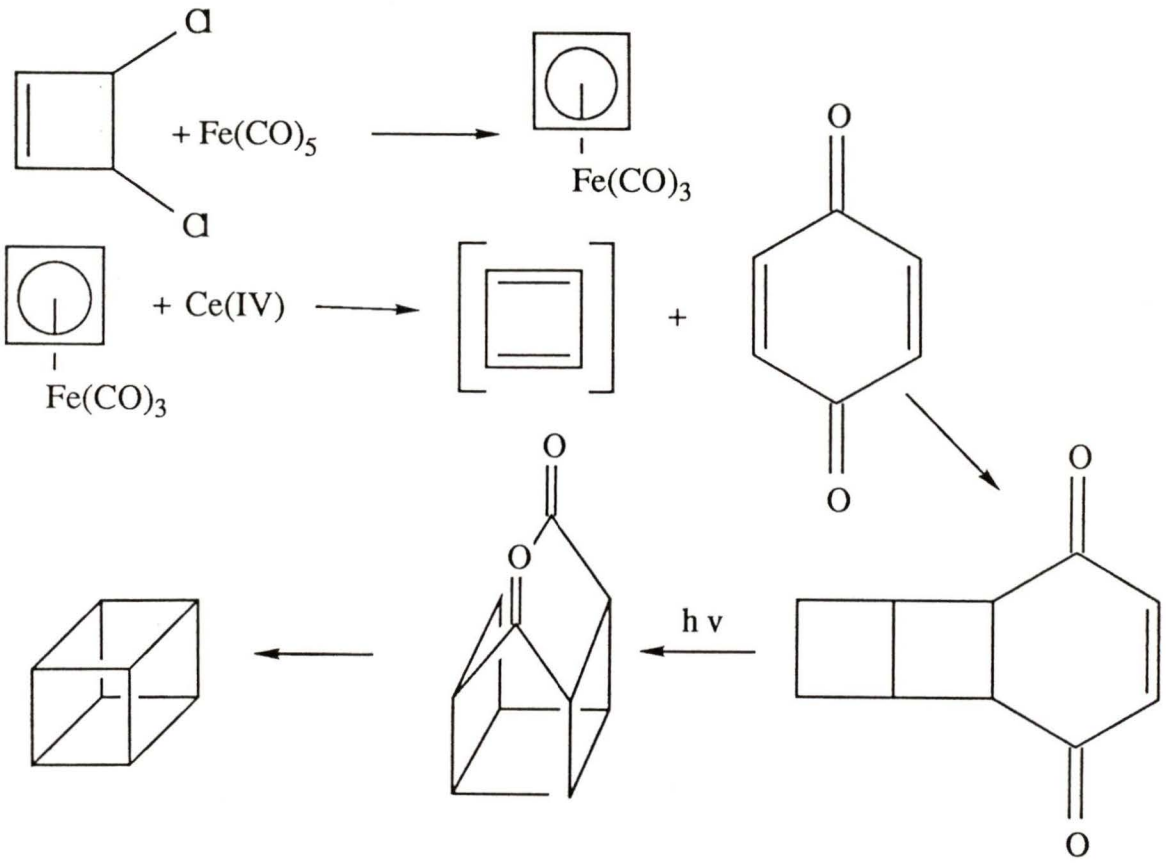


Unconjugated dienes may be isomerised to the conjugated adducts upon coordination to an iron tricarbonyl fragment and two examples are shown in Scheme 1.4.[21,22] Conjugated diene-iron complexes are stable and exhibit low reactivity. However, abstraction of a hydride generates a cationic dienyl ligand which can react with a variety of nucleophiles. The majority of the chemistry of these compounds comes from the second step which follows this initial hydride abstraction, and two examples are shown in Scheme 1.5.[23,24] Finally, the $Fe(CO)_3$ fragment is removed using strong oxidising agents such as cerium (IV).

Scheme 1.4: Two examples of olefin isomerisation on coordination to iron tricarbonyl.

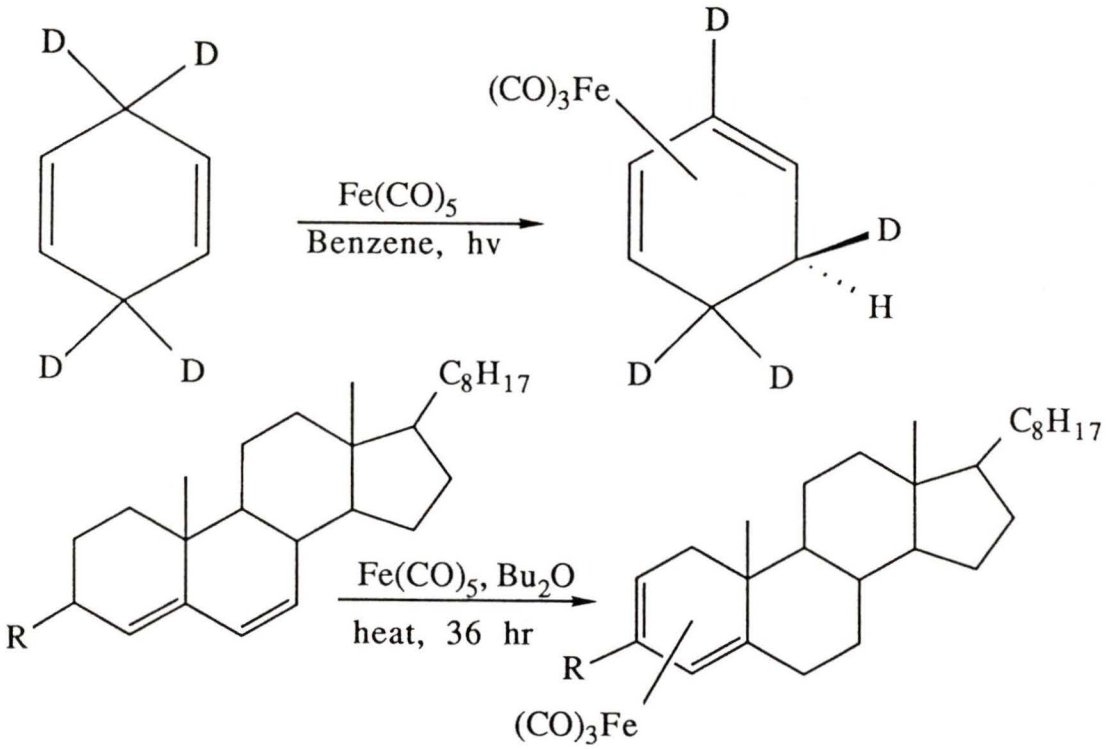


Scheme 1.5: Two reactions of cationic dienyl ligands.

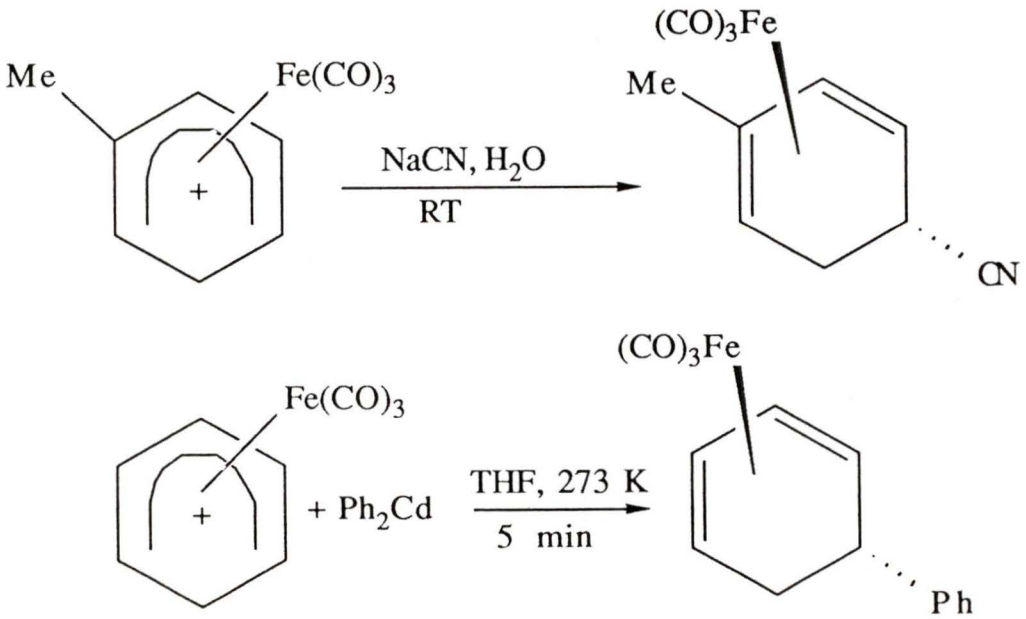

The analogous ($\eta^4$-conjugated diene)$Ru(CO)_3$ species are far less common. Treatment of a diene with a source of $Ru(CO)_3$ such as $Ru_3(CO)_{12}$ often results in formation of metal hydride species.[25] Still, ($\eta^4$-butadiene)$Ru(CO)_3$ and ($\eta^4$-cyclohexa-1,3-diene)$Ru(CO)_3$ have been isolated in good yield.[25,26]

Two fundamental steps in a range of catalytic processes are oxidative addition, and its reverse, reductive elimination.[27] Oxidative addition may occur at a single metal centre with an overall change of the electron configuration of the metal concerned from a $d^n$ to a $d^{n-1}$ or $d^{n-2}$ configuration. Vaska's complex is perhaps the best known compound which undergoes such chemistry, and two examples are shown in Scheme 1.6.[28]

Scheme 1.6: Two oxidative addition reactions of Vaska's complex.

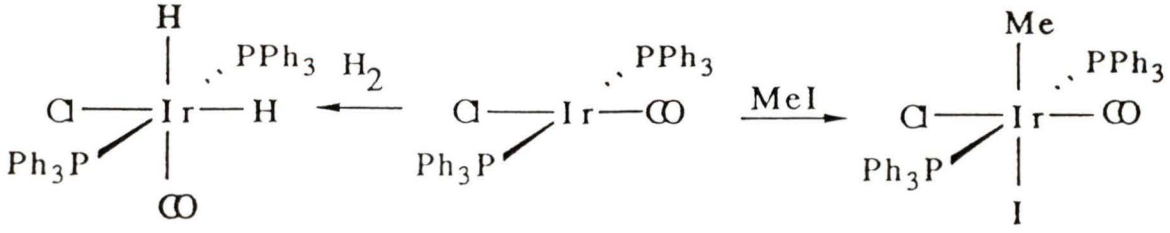

The oxidative addition process also occurs at two metal centres (usually held in close proximity by a bridging ligand)[29,30] although examples of this are less common. These systems may model some of the processes which occur in metal-mediated heterogeneous catalysis, where more than one metal centre takes part in chemical transformation. For these bimetallic systems, oxidative addition may result in (i) a two electron oxidation at one centre only and hence the formation of a mixed valency dimer; (ii) a one electron oxidation at each metal centre and the formation of a metal-metal bond; (iii) a one electron oxidation at each metal centre and the cleavage of a metal-metal bond, Fig. 1.2.[27]

A reaction of type (i) has been observed by Puddephatt et al,[30] through the addition of methyl iodide to the platinum dimer $[Me_2Pt(dmpm)]_2$, (dmpm = bis-dimethylphosphinomethane) Eqn. 1.3. The first example of a reaction of type (ii) was the addition of $X_2$ (X = Cl, Br, I) or methyl iodide to the gold dimer $[Au(CH_2)_2P(CH_3)_2]_2$, Eqn 1.4.[31] Several examples of this type have also been observed by Stobart et al[32] working with pyrazolyl bridged iridium dimers, and work in progress in this laboratory is exploring reactions of type (iii) in a similar context.[33] The systems under study are again pyrazolyl bridged rhodium dimers which possess a metal-metal bond and terminal cyclopentadienyl ligands, Eqn. 1.5.

Figure 1.2: The three modes of oxidative addition to a bimetallic system.

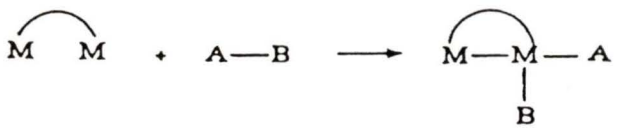


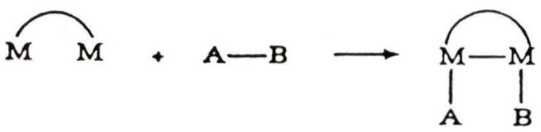


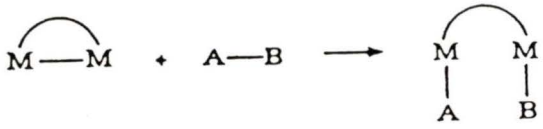

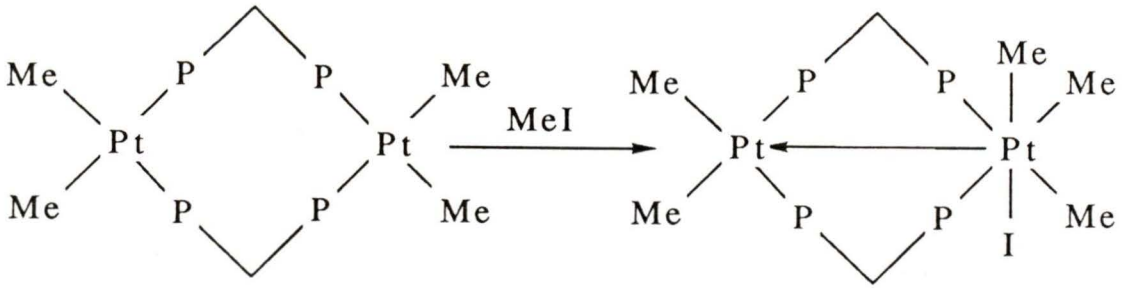


Eqn. 1.3.

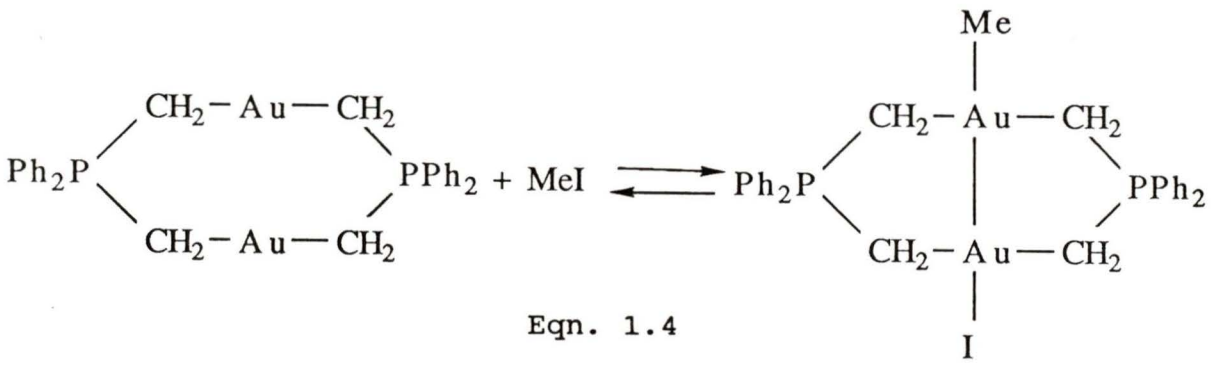


Eqn. 1.4

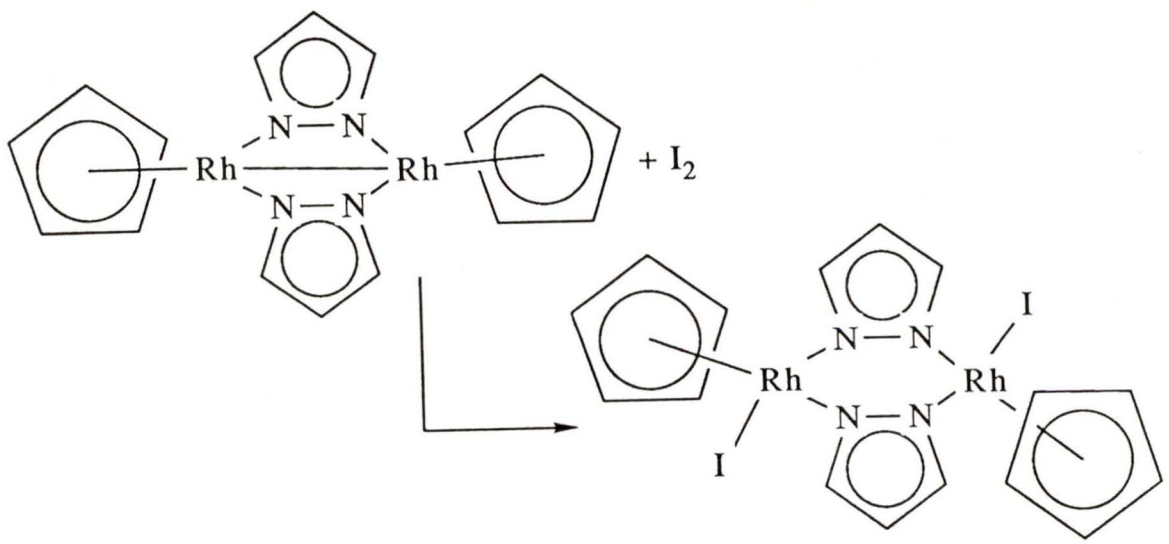


Eqn. 1.5.

The work undertaken by Stobart and co-workers has highlighted the flexibility of the pyrazolyl anion as a bridging ligand. The μ-pyrazolyl anion can accommodate a wide range of metal-metal separations, which often arise within a binuclear system when it is subjected to redox changes.[32] It is resistant to bridge cleavage, can bind to a metal in a variety of oxidation states and is unreactive to many reagents which add to the metal centres.

The number of pyrazolate ruthenium complexes is far fewer than such complexes of rhodium and iridium. The first pyrazolyl bridged ruthenium dimers were recently synthesised by Oro et al in 1987,[34] e.g. (1.IV).

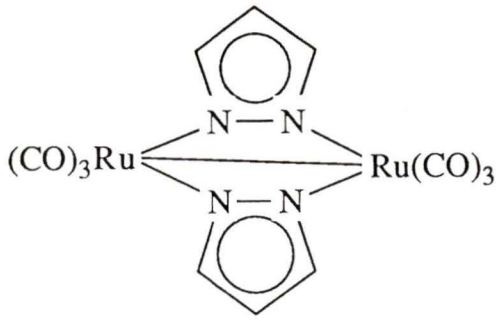


(1.IV).

These systems are also the first pyrazolate ruthenium (I) species of any kind. For the substituted pyrazolyl species, incorporating 3,5-dimethylpyrazolyl bridging ligands, a crystal structure has been obtained[34] which

shows a Ru-Ru separation of 2.705(2) Å. This is consistent with a metal-metal bond. The potential exists for such systems to undergo one electron oxidation of each centre, with cleavage of the metal-metal bond maintaining an 18 electron count for both metals.

On the basis of the foregoing discussion, it can be seen that the chemistry of transition-metal $\eta^6$-arene complexes, the relationship of the latter to $\eta^4$-diene complexes, and the properties of binuclear species are well established areas that are continuing to develop. The research described in Part 2 of this thesis has as its focus the behaviour of a π-bonding ligand, in the form of the non-conjugated tetraene 1,4,5,8,9,10-hexahydroanthracene (HHA), towards iron or ruthenium; the potential of the ruthenium complexes so formed in strategy for synthesis of pyrazolyl bridged binuclear products has also been explored.

Iron pentacarbonyl reacts with cyclohexa-1,4-diene or cyclohexa-1,3-diene to yield cyclohexa-1,3-diene iron tricarbonyl, Eqn. 1.6.[23] This reaction has been extended to a wide range of substituted cyclohexa-1,4-dienes, which are themselves formed by the metal-ammonia reduction of aromatic compounds.[35] The photochemical reaction between HHA and $Fe(CO)_5$ has been reported by Birch et al[23] to give the mononuclear 1,3-diene adduct, Eqn. 1.7, obtained as

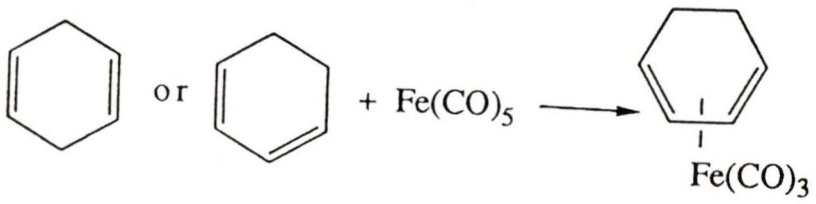


Eqn.1.6.

an orange oil. The rings in HHA have been labelled A, B, C (with A ≡ C in the uncomplexed hydrocarbon) for convenience in further discussion.

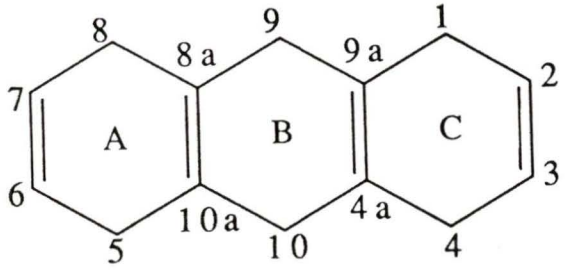


HHA.

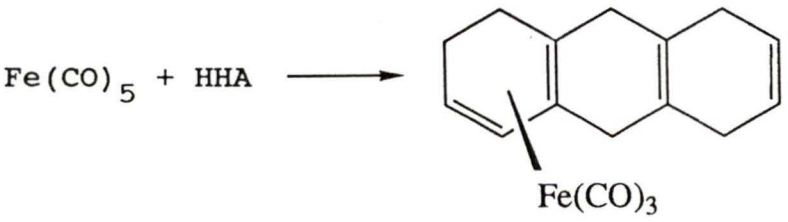


Eqn. 1.7.

An irradiation time of 16 hours and a yield of 52% were reported. Our interest in this reaction comes from the observation that a non coordinated cyclohexa-1,4-diene fragment is present in the mononuclear product; hence,

variation of reaction conditions might allow the formation of a bimetallic product.

The reaction of ruthenium dodecacarbonyl with 1,3- and 1,4-dienes has yet to be extended to polycyclic hydrocarbons with several potential coordination sites. Thus, the reactions of iron pentacarbonyl and ruthenium dodecacarbonyl with HHA are described.

Similarly, the reaction of ruthenium trichloride with cyclic 1,3- and 1,4-dienes has predominantly been concerned with monocyclic hydrocarbons. Hence, work was again initiated to study the effect of having several potential metal coordination sites on a single polycyclic hydrocarbon, a feature hitherto unexplored, and to study the effect of coordination of a bulky arene fragment on the reactivity of a ruthenium centre.

Monomeric transition metal pyrazole complexes have been extensively covered and reviewed in the literature,[36,37] with a number of these complexes shown to undergo site exchange of the nitrogen donor atom of the pyrazole ligand at the metal centre, Eqn. 1.8.[38]


Eqn. 1.8.

The $^{1}H$ NMR spectra of these species show one signal for the H(3) and H(5) protons. In contrast, some mononuclear pyrazole adducts of rhodium do not undergo this exchange process, and the $^{1}H$ NMR of these species show two distinct signals for the H(3) and H(5) protons. To expand the studies on mononuclear pyrazole systems, the synthesis of pyrazole adducts of chloro bridged ruthenium arenes was attempted to determine which type of behaviour these complexes would exhibit, i.e. dynamic or static.

Pyrazolyl bridged dimers of the type $[(\eta^{5}\text{-}C_5R_5)Rh(\mu\text{-}pz)Cl]_2$ (R = H, Me) have been synthesised in this laboratory from the corresponding chloro bridged dimers.[39] Reduction of these Rh(III)-Rh(III) species has been achieved using either zinc dust (R = H) or zinc dust/copper metal in a ratio of 1:1 (R = Me). The Rh(II)-Rh(II) species formed are at present being studied with regard to their oxidative addition properties. Therefore the synthesis of ruthenium pyrazolyl bridged dimers from $[(\eta^{6}\text{-arene})Ru(\mu\text{-}Cl)Cl]_2$ (arene = $C_{14}H_{14}$, $C_6H_6$ and $C_{10}H_{14}$) was attempted to try to establish an entry into related di-ruthenium chemistry.

# PART 2

## RESULTS AND DISCUSSION

A solution of $Fe(CO)_5$ and HHA in benzene as solvent was irradiated for 40 hours (as compared with the irradiation time of 16 hours by Birch et al); this resulted in the formation of the mononuclear adduct (compound I) of HHA, as reported by Birch,[23] isolated as an orange oil, and a yellow solid (compound II) obtained in crystalline form. The elemental analysis data (C,H) for this solid were consistent with an iron:HHA ratio of 2:1, suggesting that this product arises from coordination of a second $Fe(CO)_3$ fragment to compound I.

The $^{13}C$ NMR spectrum of compound II contains a total of eight signals (one of which appears as a shoulder in the solvent signal, Fig. 2.1, Table 2.1), with the signal at $\delta$ = 212.2 ppm assigned to the carbonyl carbons and the remaining seven signals assigned to the fourteen carbon atoms of the HHA ligand, thus indicating $C_i$ or $C_2$ symmetry in the molecule. The yellow hexagonal crystals of compound II were suitable for X-ray analysis and the resulting single crystal X-ray diffraction study confirmed that compound II was a di-iron derivative of compound I with the $Fe(CO)_3$ fragments arranged in a trans configuration. This geometry, shown in Fig. 2.2, possesses $C_i$ symmetry

Fig 2.1: The $^{13}C$ NMR spectrum of compound II.

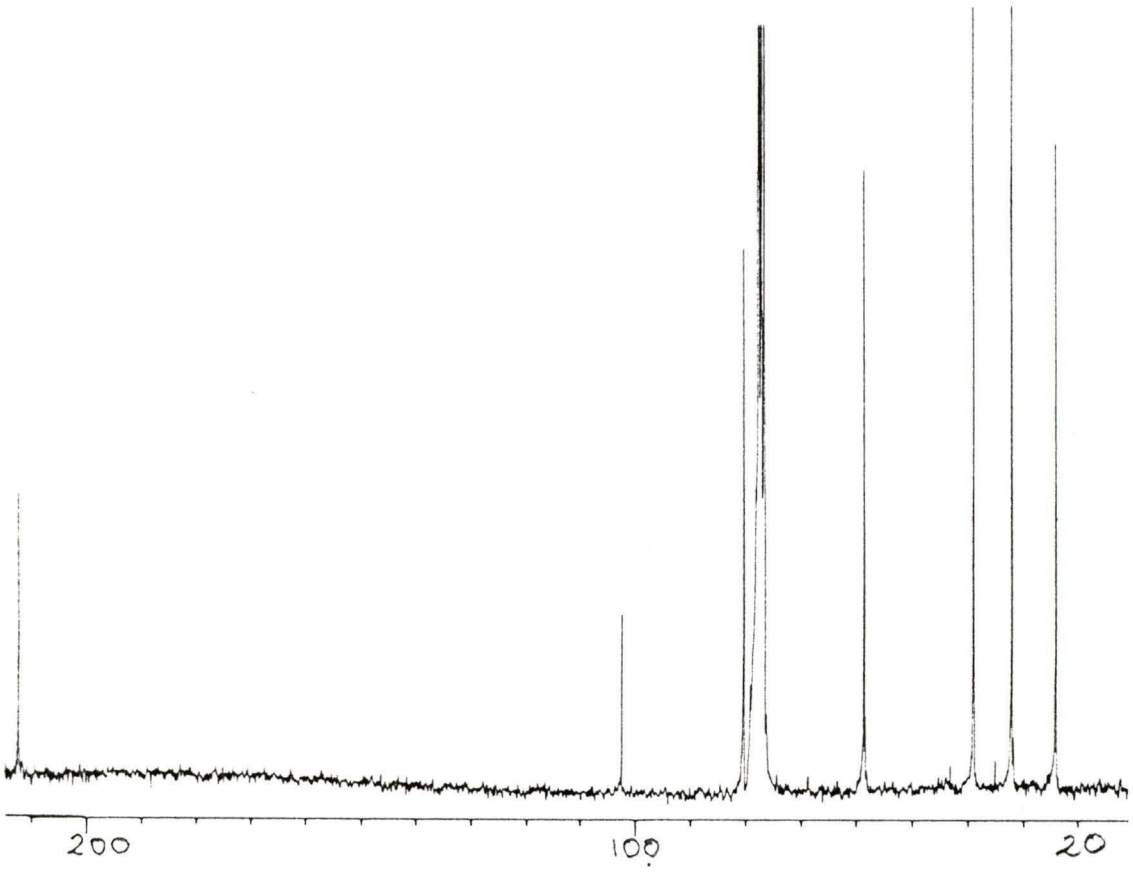


Table 2.1: The $^{13}C$ NMR data[a] for compound II.

| Carbon atom | Chemical shift/ppm |
|---|---|
| carbonyl | 212.22 |
| 1,5 | 77.00 |
| 2,6 | 58.47 |
| 3,4,7,8,9,10 | 38.89,31.98,23.86 |
| 4a,8a | 80.22 |
| 9a,10a | 102.26 |

[a]Spectrum run in $CDCl_3$ at ambient temperature.

Fig. 2.2: The molecular structure of
[($\eta^4$,$\eta^4$-HHA*)di-iron hexacarbonyl].
HHA* = 3,4,7,8,9,10-hexahydroanthracene.

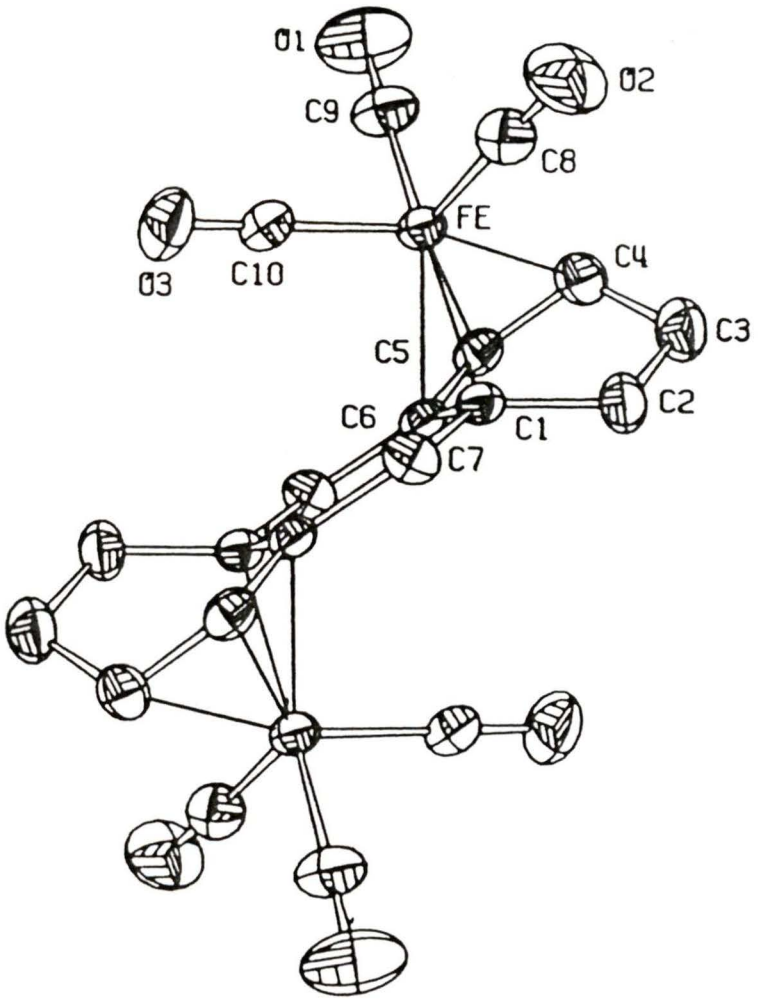

Table 2.2: Selected bond lengths for compound II.

| Atoms | Length (Å) | Atoms | Length (Å) |
|---|---|---|---|
| Fe...C(1) | 2.140(4) | Fe...C(4) | 2.106(4) |
| Fe...C(5) | 2.039(4) | Fe...C(6) | 2.075(3) |
| Fe...C(8) | 1.782(5) | C(8)...O(2) | 1.137(6) |
| C(1)...C(2) | 1.502(5) | C(2)...C(3) | 1.546(5) |
| C(3)...C(4) | 1.494(6) | C(4)...C(5) | 1.427(6) |
| C(5)...C(6) | 1.403(5) | C(6)...C(1) | 1.426(5) |
| C(1)...C(7) | 1.546(5) | | |

Estimated standard deviations are given in parentheses.

Table 2.3: Selected bond angles for compound II.

| Atoms | Angle (°) | Atoms | Angle (°) |
|---|---|---|---|
| Fe..C(8)..O(2) | 177.3(4) | C(1)..Fe..C(4) | 76.4(1) |
| C(1)..C(2)..C(3) | 111.6(3) | C(2)..C(3)..C(4) | 110.6(3) |
| C(3)..C(4)..C(5) | 119.5(4) | C(4)..C(5)..C(6) | 116.3(4) |
| C(5)..C(6)..C(1) | 114.4(3) | C(6)..C(1)..C(2) | 119.9(3) |
| C(6)..C(1)..C(7) | 119.0(3) | C(2)..C(1)..C(7) | 113.4(3) |
| C(1)..C(7)..C(6') | 114.6(4) | H(7)..C(7)..H(7') | 96(2) |

Estimated standard deviations are given in parentheses.

with an inversion centre at the centre of the middle ring (ring B) of the HHA* ligand. The numbering of the atoms of the hydrocarbon in the molecular structure is not standard. Selected bond lengths and angles are shown in Table 2.2 and Table 2.3 respectively. The $C_5$-$C_6$, $C_1$-$C_6$ and $C_4$-$C_5$ distances of 1.403 Å, 1.426 Å and 1.427 Å respectively, are consistent with an average carbon-carbon bond order of ca. 1.5. The iron-carbon bond distances for these four carbon atoms in ring A are in the range 2.039 Å to 2.140 Å; the second iron centre is bound to the four equivalent carbon atoms in ring C. Double bond rearrangement has occurred on coordination of the iron centres, i.e HHA contains four non-conjugated double bonds (1,4-diene relationship) whereas compound II contains two 1,3-dienes which are delocalised. The expected bond order for the three bonds $C_5$-$C_6$, $C_1$-$C_6$ and $C_4$-$C_5$ is 1.67; the actual lengths indicate a lower bond order which likely results from backbonding between filled d orbitals in the iron atoms and the $\phi_3$ molecular orbital of the buta-1,3-diene fragments. Back donation into the $\phi_3$ molecular orbital (LUMO) magnifies the $C_5$-$C_6$ bonding interaction and the $C_1$-$C_6$ and $C_4$-$C_5$ antibonding interactions, thus explaining the shorter $C_5$-$C_6$ bond length with respect to the two other coordinating bonds.

There is a high degree of planarity in the central ring (ring B) of the HHA* ligand; hence although the $C_7$

atom is $sp^3$ hybridised ($C_1$-$C_7$ length = 1.546 Å), the $C_1$-$C_7$-$C_6$, angle is 114.6(4)° which is midway between the angle expected for $sp^3$ and $sp^2$ hybridised carbon atoms. The molecular structure was crucial to the interpretation of the $^1H$ NMR spectrum of compound II (Fig. 2.3, Table 2.4), in the sense that the large coupling constant for the geminal hydrogens in ring B (an AB spin system with $^2J_{AB}$ = 18.8 Hz) correlates with the $H_7$-$C_7$-$H_7$, angle of 96(2)°.[40]

Compound II was further characterised by mass spectroscopy, a molecular ion $M^+$ = 464 a.m.u was observed with fragment ions corresponding to successive loss of the six carbonyl ligands. The IR spectrum (in dichloromethane solution) of compound II shows two CO stretches at 2040 $cm^{-1}$ (sharp) and 1970 $cm^{-1}$ (broad). The nujol mull spectrum of a single crystal showed six peaks in the range 2040 $cm^{-1}$ to 1935 $cm^{-1}$. Quantitative analysis of compound II by UV/visible spectroscopy gave a value of $\epsilon$ = 4.89 x $10^3$ litres $mol^{-1}$ $cm^{-1}$ at $lambda_{max}$ = 300 nm.

Further attempts to isolate compound II were unsuccessful and instead a yellow powder was obtained, which was shown to be a mixture of compound II and a second component (compound III). The elemental analysis data of this powder were identical to that obtained for compound II, suggesting that compound III is an isomer of compound II. Separation of these compounds by fractional

Fig 2.3: The $^{1}H$ NMR spectrum of compound II.

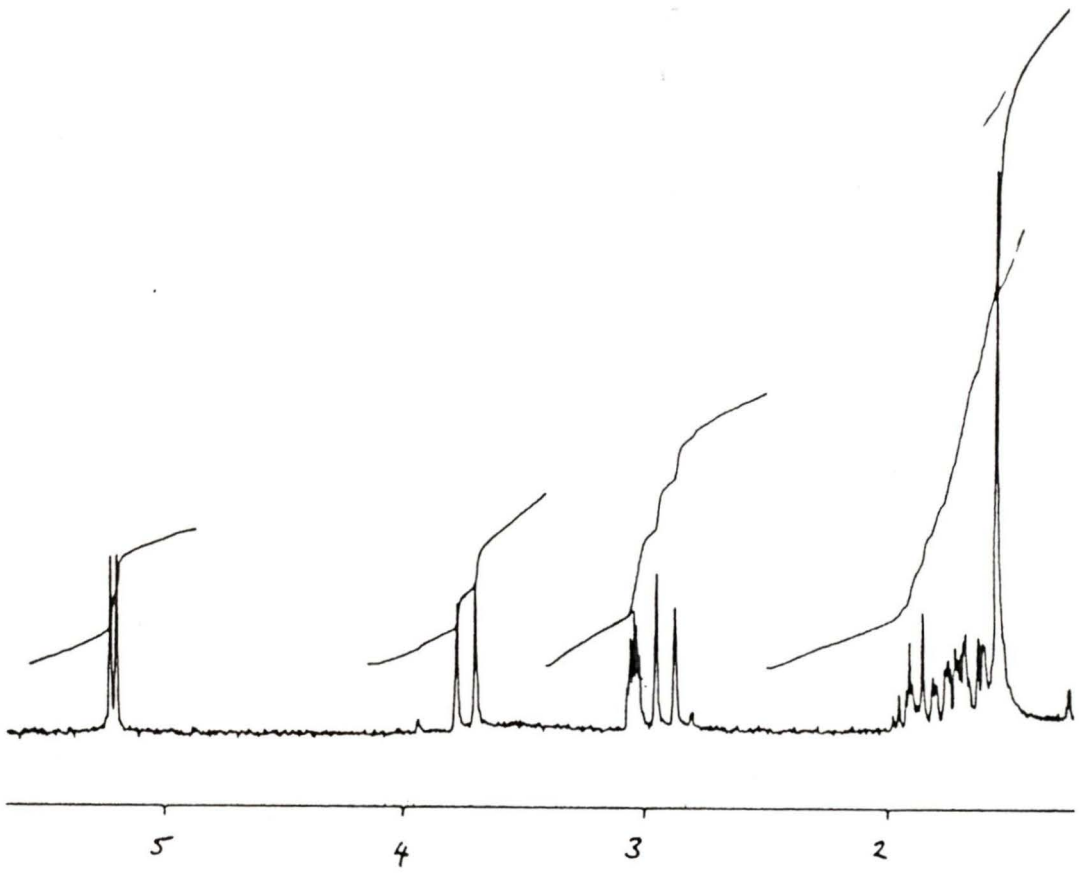


Table 2.4: The $^{1}H$ NMR data[a] for compound II.

| Proton | Chemical shift/ppm | J(H-H)/Hz |
|---|---|---|
| 1,5 | 5.20(d) | 6.3 |
| 2,6 | 3.03(m) | - |
| 9,9',10,10' | 3.73(d),2.91(d) | 18.8 |
| other | 1.97 to 1.60 | - |

[a]Spectrum run in $CDCl_3$ as solvent at ambient temperature

Multiplicity of signals denoted in brackets.

crystallisation and thin layer chromatography was not successful.

The $^{13}C$ NMR spectrum of the mixture (Fig 2.4) contains fifteen peaks, seven of which are assignable to the hydrocarbon fragment in compound III, thus indicating this second species possesses $C_i$ or $C_2$ symmetry; the latter has been assigned since compound II possesses $C_i$ symmetry, and a second isomeric molecule containing such symmetry is not possible. The $^1H$ NMR spectrum of the mixture (Fig 2.5) allows identification of splitting patterns, similar to those observed in compound II, due to compound III. This combination of spectral data has led to the conclusion that compound III is a cis di-iron species. In the $^1H$ NMR spectrum of the mixture, the doublet (2H) at $\delta$ = 5.21 ppm is assigned to the vinylic protons on the C(1) and C(5) atoms in compound III. Two singlets (4H) at $\delta$ = 3.92 ppm and 2.79 ppm are assigned to the geminal hydrogens in ring B of compound III with the following explanation: minimising the C(8a)-C(9)-C(9a) and C(10a)-C(10)-C(4a) angles (and hence maximising the angle between the geminal hydrogens attached to C(9) and C(10) respectively) reduces the interaction between these hydrogens and the $Fe(CO)_3$ fragments, notably the carbonyl ligands; thus this assumed large angle (ca. 120°) between the geminal hydrogens results in zero coupling.[40] Prolonged irradiation of this isomeric mixture does not

Fig. 2.4: The $^{13}C$ NMR spectrum of the isomeric mixture.

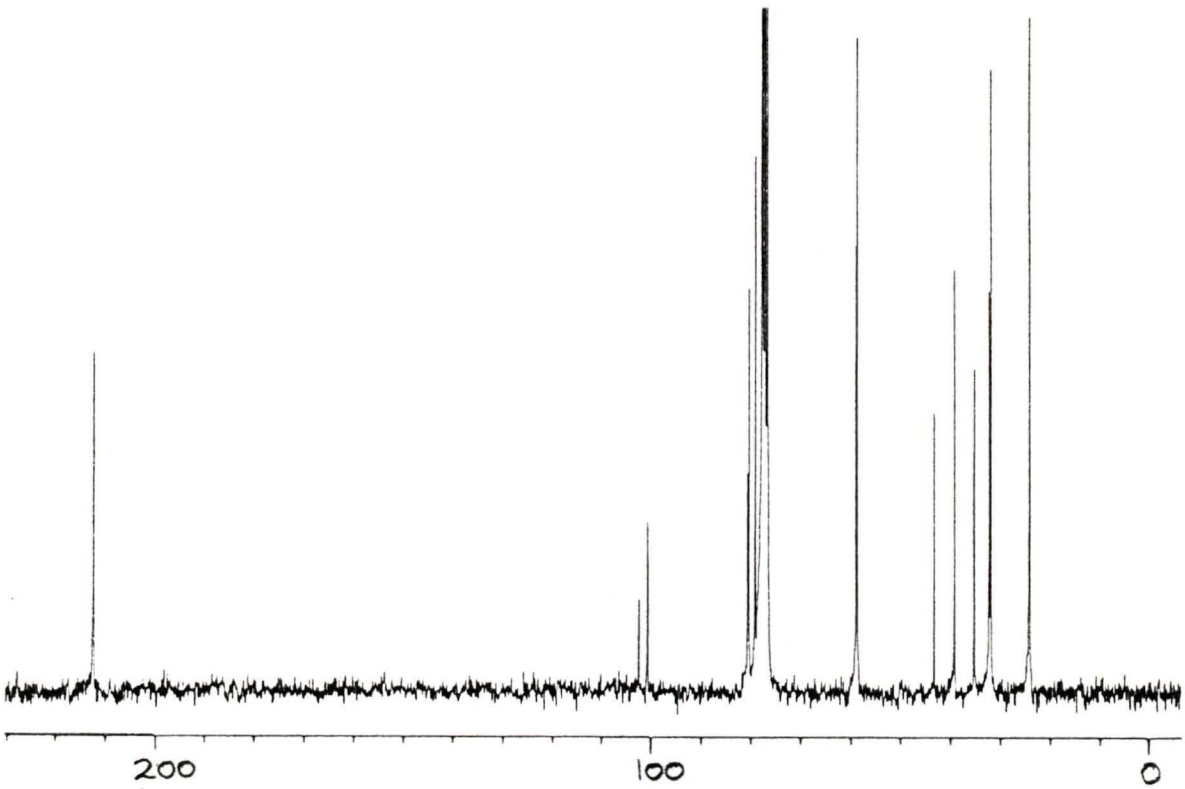


Fig. 2.5: The $^{1}H$ NMR spectrum of the isomeric mixture.

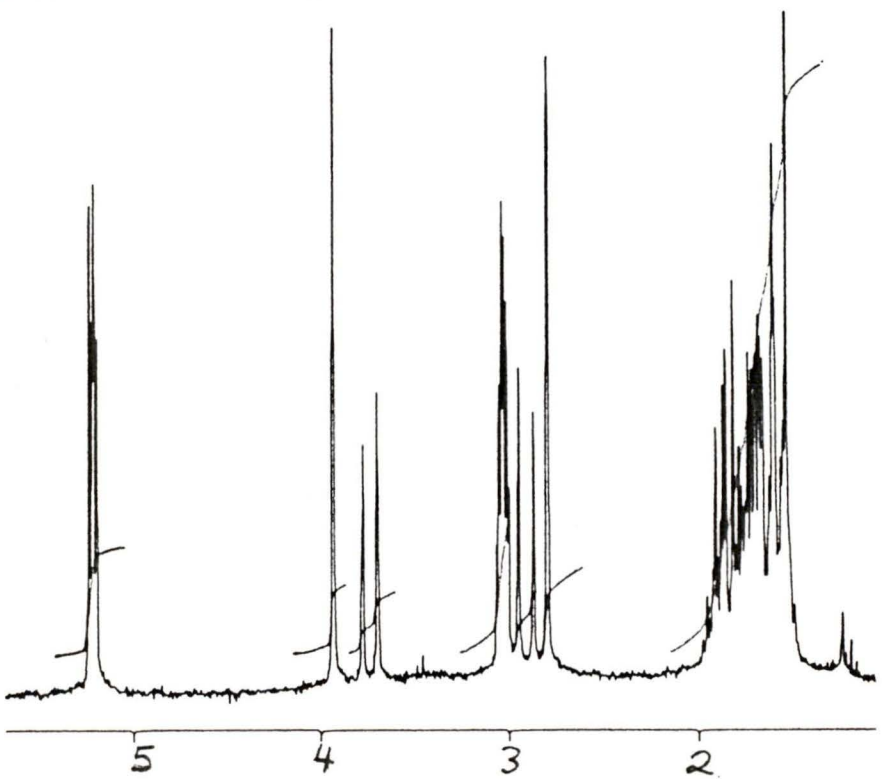

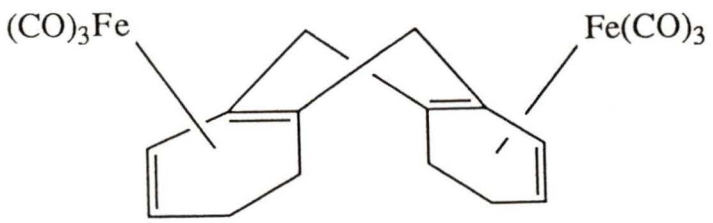


Compound III.

alter their proportions, suggesting they are formed by separate reaction pathways.

The carbonyl displacement reactions of compound II were investigated. There was no reaction with triphenylphosphine in dichloromethane; or when trimethylamine oxide was added to the same mixture. The solid state IR spectrum of compound II shows two CO stretches above 2000 $cm^{-1}$; trimethylamine oxide is expected to displace a CO group if this is the case,[41] but work up and analysis by IR spectroscopy showed no reaction had taken place. Treatment of compound II with iodine in benzene as solvent, resulted in decomposition. Reaction at the coordinated hydrocarbon was then attempted, and treatment of compound II with half an equivalent of $Ph_3CBF_4$ (a hydride abstractor) per iron centre in dichloromethane resulted in the formation of a yellow/orange solid (compound IV).

The IR spectrum of this compound shows the CO stretching peaks are in the 2100 $cm^{-1}$ to 1975 $cm^{-1}$ region, as compared to 2040 $cm^{-1}$ to 1935 $cm^{-1}$ in compound II, suggesting it is a cationic complex, resulting from hydride abstraction from the HHA* ligand in compound II. This change in wavenumber is expected for a cationic complex[27] as electron density has been removed from the iron centre and hence the amount of back donation from this centre to the CO $\pi^*$ antibonding orbitals will decrease, thereby increasing the bond order and strength of the CO bonds. Assuming compound IV results from abstraction of a single hydride from compound II, then there are three possible isomeric structures for this compound, which are shown below.

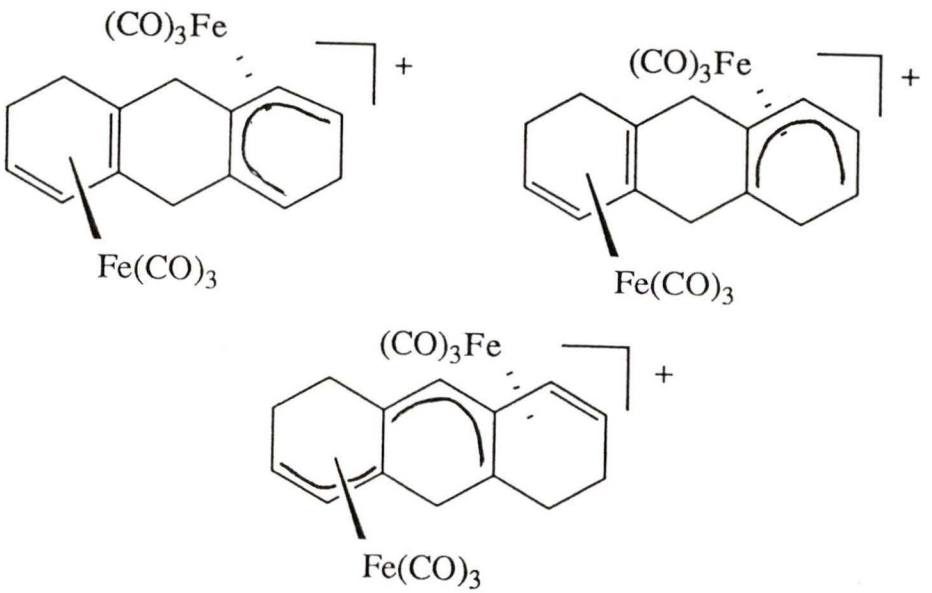

The reaction of $Ru_3(CO)_{12}$ with HHA was investigated to see if complexes similar to compounds I to III would be produced. The analogous preparation to that incorporated by Stone et al to form [($\eta^4$-cyclobuta-1,3-diene)$Ru(CO)_3$] from $Ru_3(CO)_{12}$ and the diene was utilised.[42] Hence, refluxing a mixture of $Ru_3(CO)_{12}$ with an excess of HHA in cyclohexane as solvent resulted in the isolation of a brown oil, the IR spectrum of which contained two carbonyl stretches at 2040 $cm^{-1}$ and 1968 $cm^{-1}$, i.e. similar to the carbonyl stretches observed for the carbonyl ligands in compounds I and II. The $^1H$ NMR spectrum of this oil indicated the oil contained more than one hydrocarbon complex and showed no unchanged HHA to be present. Neither the IR data nor the $^1H$ NMR data indicated that a metal-hydride containing species was present. Isolation of the components of the mixture by fractional crystallisation was not successful, but sublimation under reduced pressure led to the recovery of a white solid and the decomposition of the brown oil. This solid was analysed by gas liquid chromatography, which showed it was composed of five major components (greater than 90% of the mixture which was comprised of a total of ten species).

The solid was further analysed by gas liquid chromatography/mass spectroscopy, $^{13}C$ and $^1H$ NMR spectroscopy, and IR spectroscopy. The IR spectrum showed no carbonyl stretches. The gas liquid chromatography/mass

spectroscopy data indicated the molecular weights of the five major components were 180, 182, 184, 184 and 186 a.m.u respectively. By comparing the $^{13}C$ and $^{1}H$ NMR data for this mixture with the spectra of known polycyclic compounds derived by the selective hydogenation of anthracene,[43] the five major compounds (V to IX) were identified ,the relative yields of which are given in Table 2.5.

Thermochemical studies on the products obtained from the liquefaction of coal[44] have produced data for the heats of formation of a wide range of hydrogenated anthracene derivatives. These data support the formation of compounds V to IX on the grounds of their thermodynamic stability, i.e for dihydro-anthracenes (molecular weight 180 a.m.u), compound V is the most stable isomer by 42 KJ/mol; for tetrahydro-anthracenes (molecular weight 182 a.m.u), compound VI is the most stable isomer by 85 KJ/mol. For hexahydro-anthracenes (molecular weight 184 a.m.u) the most stable isomer is 1,2,3,4,4a,10-hexahydroanthracene, but the $^{13}C$ NMR data discounted the formation of this, suggesting the next two most stable isomers (compounds VII and VIII) have been formed. The thermodynamic stabilities of these compounds are just 6 and 8.5 KJ/mol less respectively than the most stable isomer. For octahydro-anthracenes (molecular weight 186 a.m.u) compound IX is marginally more stable than the

Table 2.5: The relative yields of compounds V to IX.

| Compound | | Yield |
|---|---|---|
| 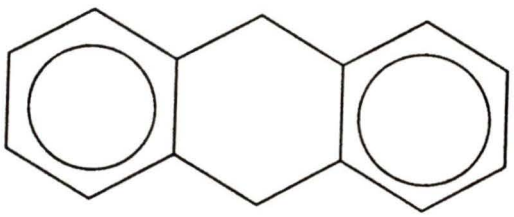 | (V). | 8% |
| 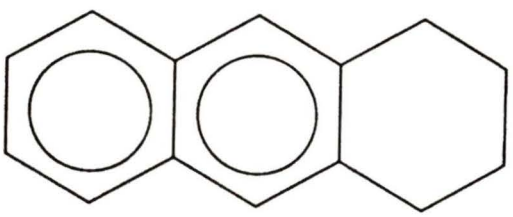 | (VI). | 34% |
| 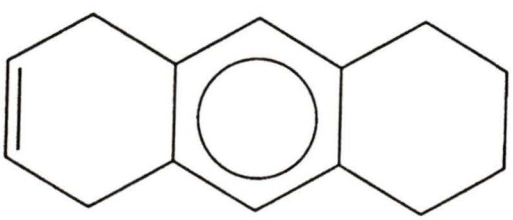 | (VII). | combined 23% |
| 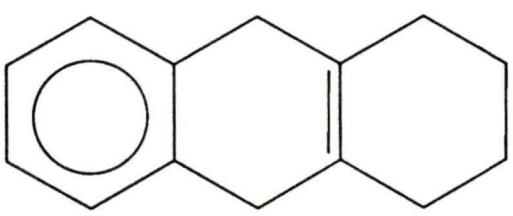 | (VIII). | |
| 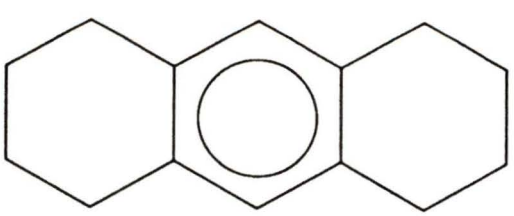 | (IX) | 35% |

isomer with the aromatised end ring whose formation is again discounted by the $^{13}C$ NMR data.

In the course of the reaction between $Ru_3(CO)_{12}$ and HHA, a small amount of decomposition occurred, with a fine black powder being deposited on the bottom of the reaction flask. This decomposition product was isolated and was subsequently used in place of $Ru_3(CO)_{12}$ under otherwise identical reaction conditions. This time no reaction with or conversion of HHA was observed, establishing that this decomposition product (likely ruthenium metal) is not acting as a heterogeneous catalyst for the conversion of HHA. Thus, the reaction of $Ru_3(CO)_{12}$ with an excess of HHA is catalytic. Indeed, assuming a stoichiometry of one ruthenium centre per HHA ligand, addition of at least a ten fold excess of HHA results in conversion of all of the latter to the five major components. The product distribution shows a slight loss of hydrogen from the system. Hydrogen transfer has resulted in double bond isomerisation and disproportionation. There are many reports of such behaviour by group eight metals in the literature,[45,46] with examples including the $Ru_3(CO)_{12}$ catalysed isomerisation of 1-pentene to cis-2-pentene and trans-2-pentene;[47] the Vaska's complex catalysed disproportionation of cyclohexa-1,4-diene to benzene and cyclohexene.[48]

In the catalytic isomerisation of cyclohexa-1,4-diene

to cyclohexa-1,3-diene by $RuCl_2(PPh_3)_3$ reported by J.E. Lyons,[48] a co-catalyst is employed which is a source of CO acquired by the ruthenium centre to form an active carbonyl complex. The mechanism proposed for this isomerisation reaction involves oxidative addition of the diene (forming a metal hydride), isomerisation of the coordinated hydrocarbon and finally reductive elimination of the isomeric diene. Steric reasons are given for the fact that only isomerisation occurs, i.e. a second hydrocarbon is unable to undergo migratory insertion into the ruthenium hydrogen bond which is a necessary step for disproportionation. Thus when the coordinatively unsaturated complex $IrCl(CO)(PPh_3)_2$ (Vaska's complex) is employed as catalyst, 60% of the products are cyclohexene and benzene which arise through disproportionation.

Whitesides and Budnik[49] report that $[(\eta^4\text{-cyclohexa-1,3-diene})Ru(CO)_3]$ is a catalyst for the disproportionation of cyclohexa-1,3-diene to benzene and cyclohexene. A similar type of ruthenium compound may be formed in the $Ru_3(CO)_{12}$-HHA system which could be responsible for the disproportionation observed. The diversity of the products obtained in the $Ru_3(CO)_{12}$-HHA system reflects the variety of ruthenium carbonyl fragments which coordinate to dienes. For example, the reaction of $Ru_3(CO)_{12}$ with 2,3-dimethylbuta-1,3-diene reported by Valle et al[50] gives $[(\eta^4\text{-}C_6H_{10})Ru(CO)_3]$,

$[(C_6H_{10})Ru_2(CO)_6]$ and $[(C_6H_{10})Ru_3(CO)_8]$ as products. In the catalytic isomerisation of pentenes by $Ru_3(CO)_{12}$ reported by Valle et al,[47] a trinuclear species is believed to be responsible for the conversions.

The reaction of $Ru_3(CO)_{12}$ with HHA is significant in that it catalyses isomerisation and disproportionation within a single polycyclic framework. Separate hydrogenation and dehydrogenation steps may also occur in addition to these processes. Comments on the mechanism are hazardous, still it seems likely that cleavage of Ru-CO bonds and ruthenium hydride formation would be likely steps in the overall reaction scheme. Characterisation of any ruthenium containing species in the $Ru_3(CO)_{12}$ system has not been achieved.

The reaction of $RuCl_3 \cdot 3H_2O$ with HHA was investigated to see if a complex, similar to those obtained when $RuCl_3 \cdot 3H_2O$ is reacted with monocyclic dienes, would be formed. The production of dinuclear species, as observed with $Fe(CO)_5$ and HHA, was a possible outcome of such a reaction.

Refluxing a mixture of $RuCl_3 \cdot 3H_2O$ and HHA in ethanol as solvent resulted in the formation of a yellow/brown solid (compound X). The elemental analysis data (C,H,N,Cl) obtained for the product were consistent with an arene:ruthenium ratio of 1:1, ruling out the coordination of two ruthenium centres to a single hydrocarbon, although this possibility exists since a cyclohexa-1,4-diene fragment can remain in a mono metallated $C_{14}$ system. Compound X shows minimal solubility in a wide range of non-coordinating solvents; however, it is soluble in coordinating solvents such as DMSO and acetonitrile. The $^1H$ NMR spectrum in $d^6$-DMSO showed an AA'BB' spin system (4H) which suggested that coordination had occurred at one of the end rings. A singlet at 5.71 ppm (2H) was assigned to the two vinylic protons in the non-coordinated ring (ring A) of the organic fragment by comparison with the chemical shift of the vinylic protons in HHA. This gave further evidence for ruthenium coordination at just ring C of the organic fragment and suggested that compound X is as shown Eqn. 2.1.

Red crystals suitable for X-ray analysis were obtained by the slow diffusion of ether into a DMSO solution of compound X. The resulting single crystal X-ray diffraction study showed that a new species (compound XI) had been formed, Eqn. 2.2, a monomeric DMSO adduct as shown in Fig. 2.6. This product is formed as the result of cleavage of

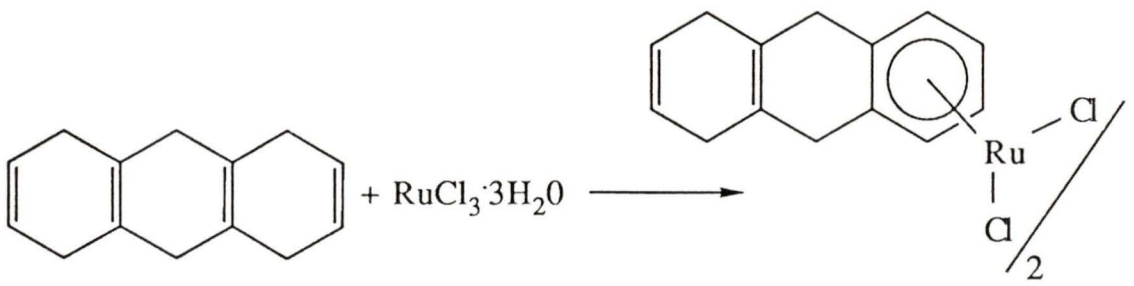


Eqn. 2.1.

the chloro bridges in compound X by DMSO, in a manner analogous to the formation of the monomeric compound [(benzene)$RuCl_2$DMSO] by the dissolution of the chloro bridged species [(benzene)Ru(μ-Cl)Cl]$_2$ in DMSO.[12] The numbering of the hydrocarbon atoms in the molecular structure is not standard. Selected bond angles and lengths are listed in Table 2.6 and Table 2.7 respectively.

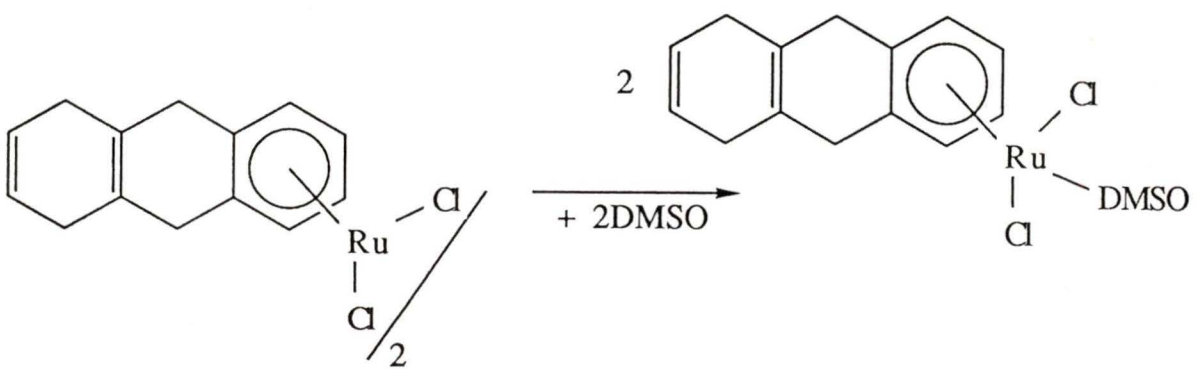


Eqn. 2.2

The six carbon atoms of the coordinated ring were all found to be within bonding distance of the ruthenium centre (2.16-2.20 A), consistent with $\eta^6$-coordination. This ring was refined as a regular hexagon to give bond

Fig. 2.6: The molecular structure of [($\eta^6$-THA)ruthenium(dimethyl-$\eta^1$sulphoxide)dichloride]. THA = 1,4,9,10-tetrahydroanthracene.

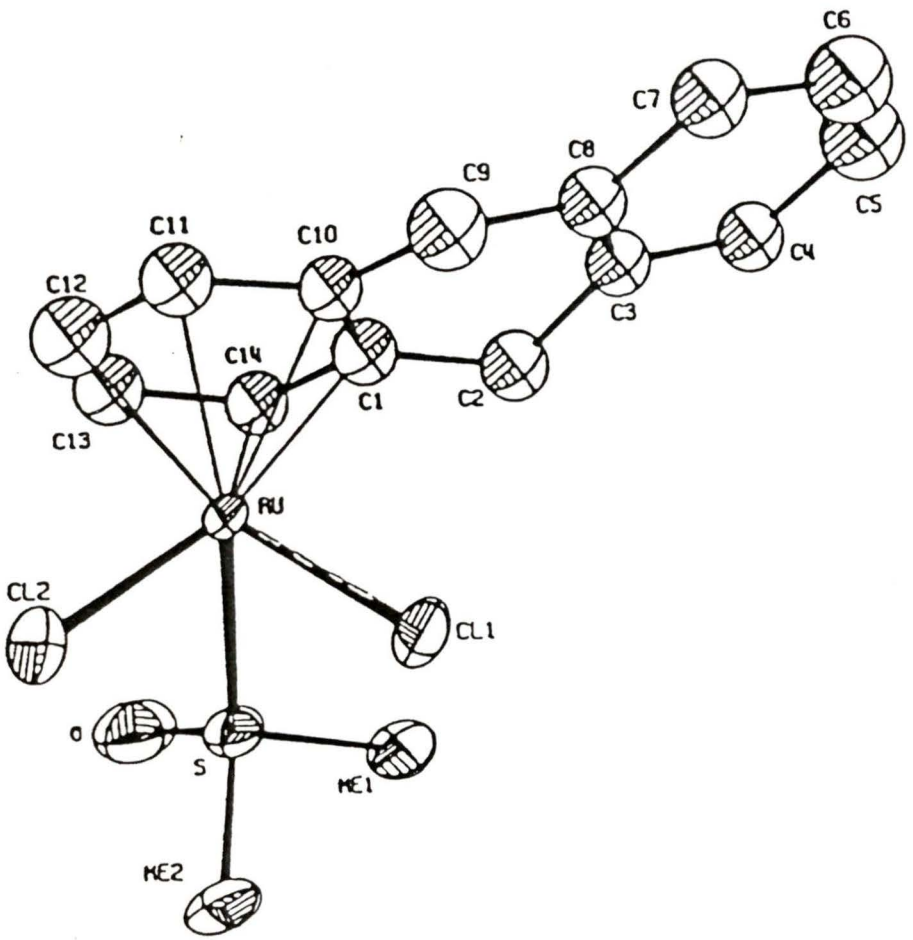

Table 2.6: Selected bond lengths for compound XI.

| Atoms | Length (Å) | Atoms | Length (Å) |
|---|---|---|---|
| Cl(1)...Ru | 2.391(5) | Cl(2)...Ru | 2.401(6) |
| S....Ru | 2.333(5) | S...O | 1.48(2) |
| Me(1)...S | 1.78(2) | Me(2)...S | 1.80(2) |
| C(1)...Ru | 2.196(2) | C(10)...Ru | 2.202(1) |
| C(11)...Ru | 2.187(1) | C(12)...Ru | 2.167(1) |
| C(1)...C(2) | 1.56(2) | C(2)...C(3) | 1.53(3) |
| C(3)...C(4) | 1.51(3) | C(4)...C(5) | 1.52(3) |
| C(5)...C(6) | 1.28(3) | C(3)...C(8) | 1.26(3) |
| C(13)...Ru | 2.161(2) | C(14)...Ru | 2.176(2) |

Estimated standard deviations are given in parentheses.

Table 2.7: Selected bond angles for compound XI.

| Atoms | Angle (°) | Atoms | Angle (°) |
|---|---|---|---|
| Cl(1)..Ru..Cl(2) | 89.1(2) | S..Ru..Cl(1) | 85.4(2) |
| S..Ru..Cl(2) | 86.4(2) | O..S..Ru | 114.7(6) |
| Me(1)..S..Ru | 108.8(7) | Me(2)..S..Ru | 114.2(8) |
| Me(1)..S..O | 108.5(11) | Me(2)..S..O | 109.9(10) |
| C(1)..Ru..C(10) | 37.0 | C(10)..Ru..C(11) | 37.1 |
| C(1)..C(10)..C(11) | 120.0 | C(10)..C(11)..C(12) | 120.0 |
| C(1)..C(2)..C(3) | 114.2(15) | C(2)..C(3)..C(4) | 112(2) |
| C(2)..C(3)..C(8) | 123(2) | C(3)..C(4)..C(5) | 111(2) |
| C(4)..C(5)..C(6) | 124(2) | C(5)..C(6)..C(7) | 127(2) |
| C(6)..C(7)..C(8) | 108(2) | C(7)..C(8)..C(9) | 109(2) |
| C(8)..C(9)..C(10) | 108.9(15) | C(9)..C(10)..C(1) | 125.6(8) |

Estimated standard deviations are given in parentheses.

lengths of 1.395 Å. The $C_5$-$C_6$ and $C_3$-$C_8$ distances of 1.28(3) Å and 1.26(3) Å respectively identify double bond character between these carbon atoms. All the remaining C-C distances were between 1.50 Å and 1.56 Å and represent single bonds between these carbon atoms. These data are entirely consistent with the $^1$H NMR spectrum of this compound, illustrated in Fig. 2.7, which shows the resonance of the methyl protons of the DMSO ligand has shifted 0.7 ppm downfield with respect to the free ligand. This is a typical coordination shift for these protons when the DMSO ligand is coordinated to a group VIII metal through the sulphur atom[51,52] (for oxygen coordinated DMSO, the maximum coordination shift to have been observed is ca. 0.5 ppm).[53] DMSO would be expected to coordinate to ruthenium (considered to be a soft metal)[53] through the soft sulphur atom, as opposed to the harder oxygen atom. However, there are cases of sulphoxides coordinating to soft metals via oxygen,[53] and a ruthenium species containing two DMSO ligands coordinated in opposing modes (one oxygen coordinated, one sulphur coordinated) has been reported by Mercer and Trotter.[54]

The crystal structure showed that the DMSO molecule was coordinated to the ruthenium centre through the sulphur atom with a Ru-S distance of 2.333(5) Å. The S-O distance of 1.48(2) Å indicates a slight shortening of this bond, relative to its value of 1.53 Å in uncomplexed

Fig. 2.7: The $^{1}H$ NMR spectrum of compound XI.

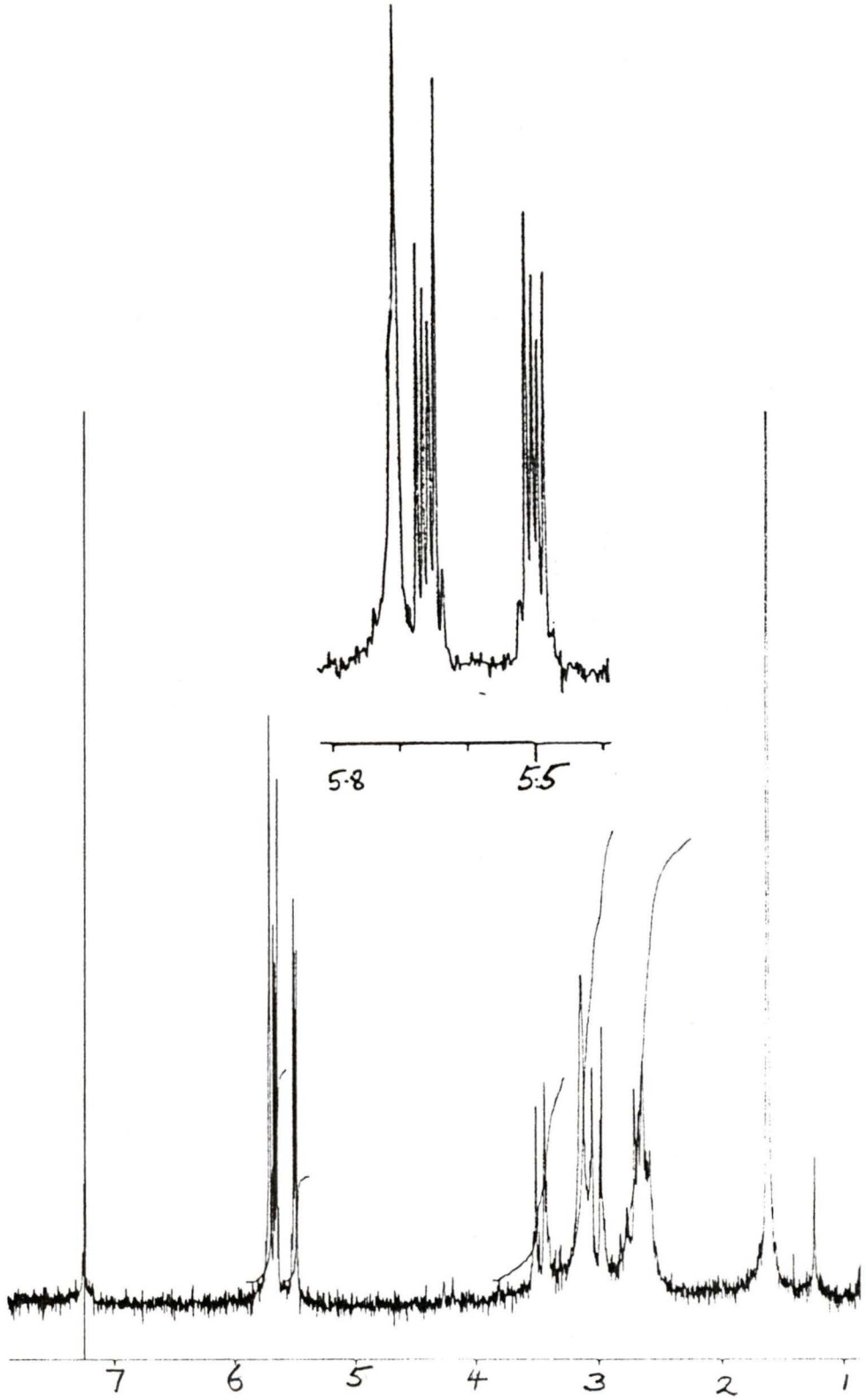

DMSO.[55] This arises from an increase in π bonding between the sulphur and oxygen atoms through a pπ-dπ interaction, with electron density being transferred from the oxygen to the sulphur atom.

Isolation of other derivatives of compound X by reactions like that of Eqn. 2.2 proved difficult, due partly to its poor solubility properties and possibly related to steric hindrance by the coordinated arene fragment of the approach of potential donor ligands to the rather crowded dimeric species . Hence no reaction is observed between compound X and triphenylphosphine. Treatment of compound X with trimethylphosphite in stoichiometries varying from one to three phosphite ligands per ruthenium centre has not yielded pure compounds: mixtures containing mono-, di- and tri-substituted compounds along with unreacted starting material were obtained, suggesting the existence of a complex series of equilibria.

Substitution reactions of the mononuclear DMSO adduct (compound XI) with phosphorus donor ligands proved to be far more successful. Purification of compound XI via soxhlet extraction with dichloromethane allows the isolation of a pure material with much improved solubility properties relative to those of the dimer (compound X). Hence it is possible to get a reasonable concentration of compound XI into solution (approximately 80 mg in 15 mL of

dichloromethane in a typical experiment) before addition of a donor ligand is effected. Addition of one equivalent of triethylphosphite to compound XI leads to almost quantitative formation of a further mono substituted adduct (compound XII). Addition of two equivalents of triphenylphosphine again leads only to the formation of a mono adduct (compound XIII) (see Eqn. 2.3), suggesting that the coordination of the first triphenylphosphine ligand hinders the approach of a second ligand to the ruthenium centre. These products were fully characterised by microanalysis, $^{31}P$ NMR and $^{1}H$ NMR.

Compounds XII and XIII exhibit interesting NMR properties. The $^{1}H$ NMR spectra in the range $\delta$ = 4.3 ppm to 5.7 ppm are illustrated in Fig. 2.8. In both spectra shown, the signal at 5.7 ppm is assigned to the two vinylic protons in the end ring (ring A). In each case, signals attributable to the four coordinated arene protons

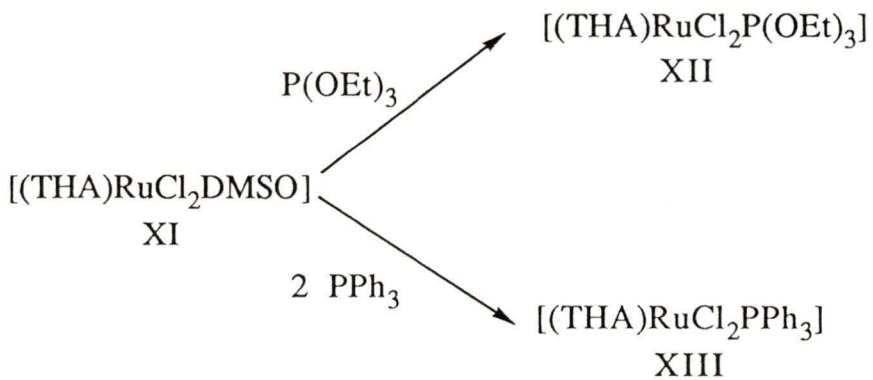


Eqn. 2.3.

Fig. 2.8: The $^{1}H$ NMR spectra of compounds XII and XIII in the range $\delta$ = 4.3 ppm to 5.7 ppm.

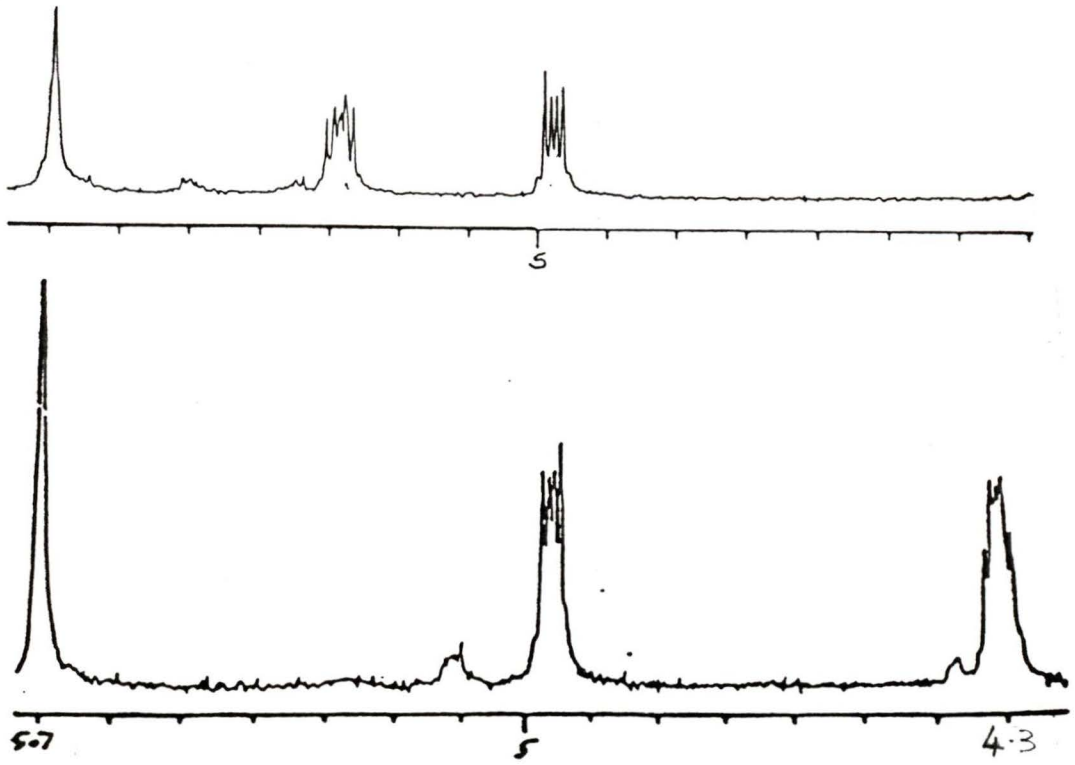


Fig. 2.9: The AA'MM'X spin system in compounds XII and XIII.

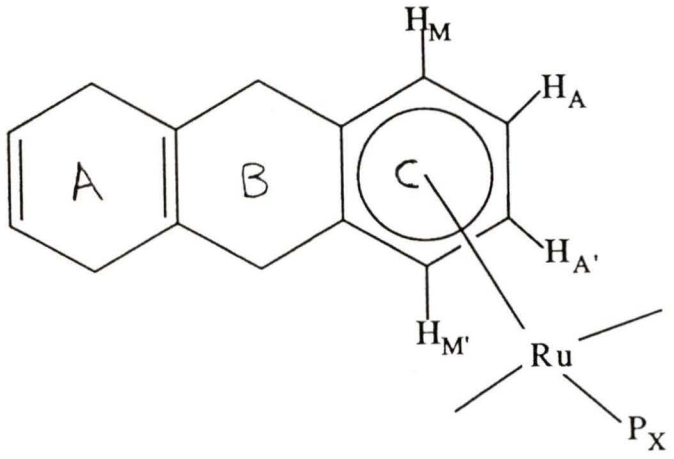

give splitting patterns consistent with that expected for an AA'MM'X spin system, see Fig. 2.9; however, homo-nuclear decoupling experiments show coupling of the X nucleus (i.e. phosphorus) to only the A and A' nuclei. Thus for compound XII, decoupling by irradiation of the proton resonance at 5.3 ppm (due to the A protons) led to the collapse (Fig. 2.10) of the complex multiplet at 4.95 ppm (due to the M protons) to a singlet, with no observable effect on the rest of the spectrum. In contrast, decoupling by irradiation of the proton resonance at 4.95 ppm (due to the M protons) resulted in collapse (also Fig. 2.10) of the complex multiplet at 5.3 ppm (due to the A protons) to a doublet. The latter must be due to coupling to $^{31}P$ ($I=\frac{1}{2}$, 100%) since resolvable proton-proton coupling of the A nuclei occurs only to the M nuclei as shown previously, hence $^{3}J(P\text{-}H_A) = 3.0$ Hz.

Homo-nuclear decoupling experiments were also performed on the alkyl proton resonances of the coordinated triethylphosphite ligand in compound XII. Decoupling by irradiation of the proton resonance at 4.11 ppm (due to the $C\underline{H}_2$ protons) led to the collapse of the triplet at 1.25 ppm (due to the $C\underline{H}_3$ protons) to a singlet, with no observable effect on the remainder of the spectrum. By contrast, decoupling by irradiation of the proton resonance at 1.25 ppm (due to the $C\underline{H}_3$ protons)

Fig. 2.10: Decoupling of the arene proton resonances of the coordinated THA ligand.

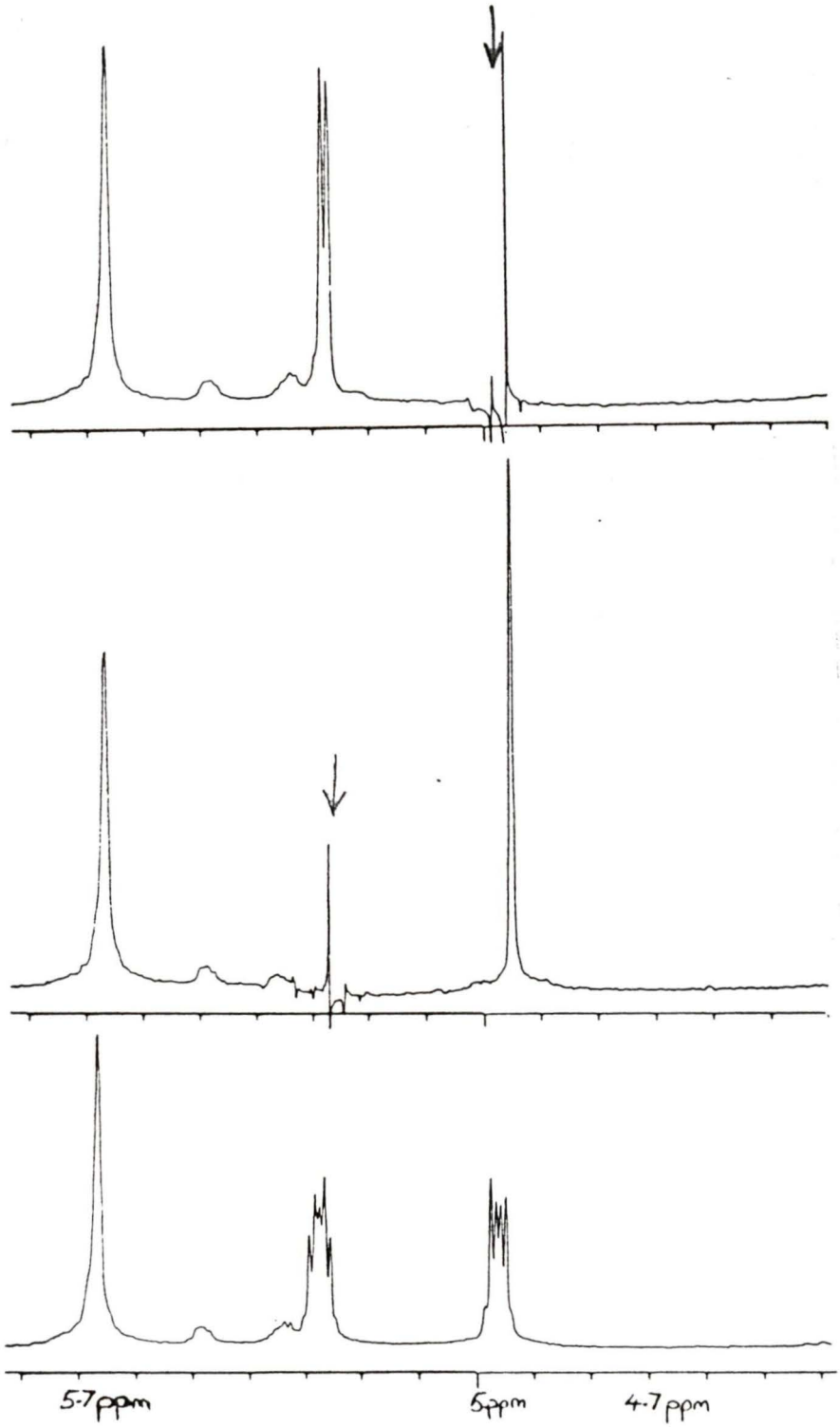

led to the collapse of the complex multiplet at 4.11 ppm (due to the $C\underline{H}_2$ protons) to a doublet, $^3J(P-H)$ = 7.0 Hz.

Similar results were obtained for the analogous homonuclear decoupling experiment performed on the coordinated arene protons ($H_A$ and $H_M$) of the triphenylphosphine adduct (compound XIII), $^3J(P-H_A)$ = 3.0 Hz. A computer simulation of the $^1H$ NMR spectrum of this compound was carried out to further verify its interpretation. The arene proton resonances $H_A$ and $H_M$ were simulated using an AA'MM'X spin system shown in Fig. 2.11, along with the actual spectrum. The simulated results gave very good correlation to the real spectrum with regard to peak position and relative peak intensity allowing assignment of all the coupling values, which are listed in Table 2.8. The phosphorus-proton coupling values assigned from the decoupling experiments are supported by these data.

Decoupling of the phenyl protons in the triphenylphosphine ligand was investigated: irradiation of the proton resonance at 7.72 ppm altered (Fig. 2.12), but did not simplify, the signal centred at 7.35 ppm. Irradiation of the resonance at 7.35 ppm led to the collapse (also Fig. 2.12) of the multiplet signal at 7.72 ppm to a doublet, revealing a $^3J_{P-H}$ (coupling of the ortho protons to $^{31}P$) = 10.7 Hz.

Fig. 2.11: $^{1}H$ NMR spectrum of compound XIII in the region $\delta$ = 5.5 ppm to 4.0 ppm.

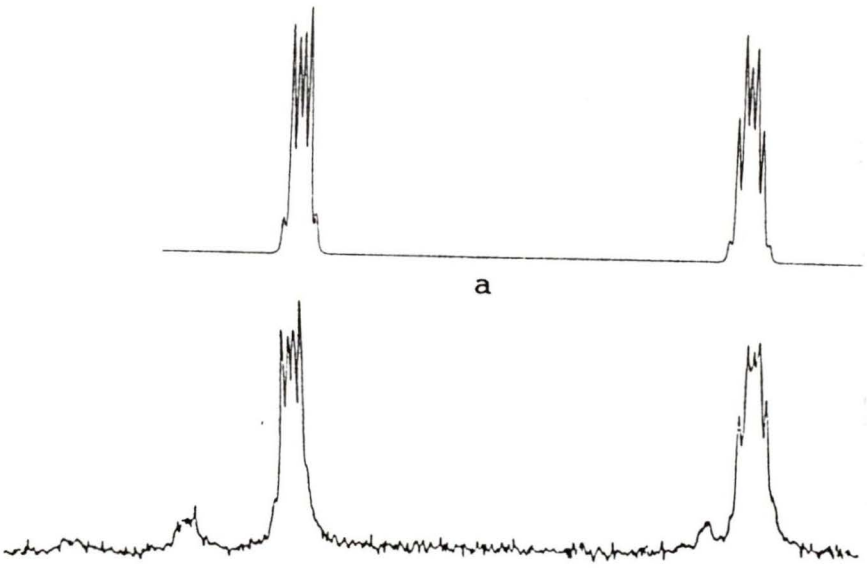


a: Simulated spectrum using AA'MM'X spin system.

b: Actual spectrum.

Table 2.8: Simulated $^{1}H$ NMR spectral data for the AA'MM'X spin system in compound V.

| Chemical shift/Hz. | | Calculated coupling constant/Hz. | |
|---|---|---|---|
| Calculated | Observed | | |
| 1071.63 | 1071.54 | $J_{AA'}$ | 4.990 |
| 1074.28 | 1074.09 | | |
| 1076.78 | 1076.95 | $J_{AM}$ | 5.607 |
| 1078.56 | 1078.53 | | |
| 1079.18 | 1079.21 | $J_{AM'}$ | 0.795 |
| 1081.10 | 1080.78 | | |
| 1083.42 | 1083.62 | $J_{AX}$ | 2.558 |
| 1086.11 | 1086.22 | | |
| | | $J_{MM'}$ | -0.026 |
| 1236.61 | 1236.95 | | |
| 1239.39 | 1239.29 | $J_{MX}$ | 0.0 |
| 1241.60 | 1241.23 | | |
| 1243.54 | 1243.58 | | |
| 1245.78 | 1245.92 | | |
| 1248.52 | ---- | | |

Fig. 2.12: Decoupling of the phenyl proton resonances of the coordinated triphenylphosphine ligand.

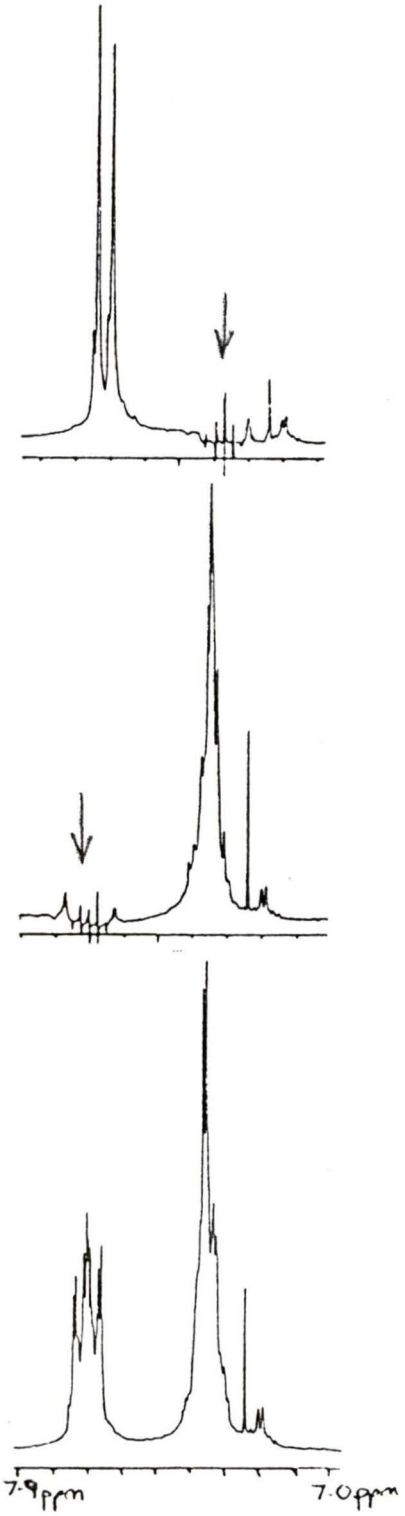

The chemical shift of the A protons in the coordinated arene ring (ring C) of the triphenylphosphine adduct (compound XIII) is significantly different from that observed for the analogous protons of the triethylphosphite adduct (compound XII) (4.30 ppm vs 5.30 ppm). A possible explanation for this marked chemical shift difference might be anisotropic shielding effects arising from the ring currents in the phenyl groups in the triphenylphosphine ligand;[56] this idea was pursued through synthesis of the corresponding methyldiphenylphosphine and the tricyclohexylphosphine adducts. In each case, slightly greater than one equivalent of the phosphine per ruthenium centre was added to compound XI in dichloromethane as solvent, yielding only the monophosphine adducts, compounds XIV and XV respectively. The products were characterised by microanalysis, $^{31}P$ NMR and the $^{1}H$ NMR spectroscopic results discussed below. The chemical shifts of the coordinated arene protons ($H_A$ and $H_M$) in compounds XII-XV and their $^{31}P$ data are compared in Table 2.9.

The chemical shift of the A protons in compound XIII is again significantly different from that observed in compound XV. As the tricyclohexylphosphine and triphenylphosphine ligands are comparable in steric properties, the upfield chemical shift of the A protons in compound XIII (with respect to their position in compounds XII and XV) cannot be due to a steric interaction between

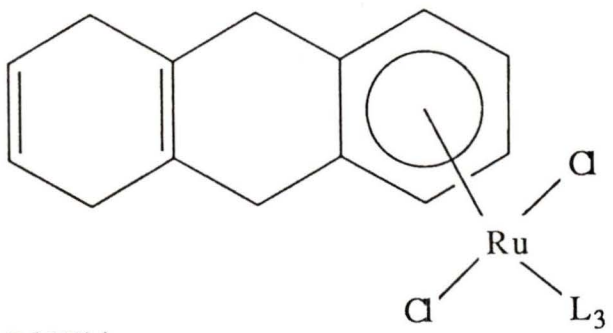


Compound XII, L = $P(OEt)_3$.

Compound XIII, L = $PPh_3$.

Compound XIV, L = $PPh_2Me$.

Compound XV, L = $PCy_3$.

Table 2.9: The chemical shifts of the $H_A$ and $H_M$ protons and the $^{31}P$ NMR data of compounds XII to XV[a].

| Compound. | $V_A$/ppm. | $V_M$/ppm. | $^{31}P$ data/ppm |
|---|---|---|---|
| XII | 5.30 | 4.95 | 118.1 (s) |
| XIII | 4.30 | 4.95 | 30.5 (s) |
| XIV | 4.55 | 4.89 | 26.6 (s) |
| XV | 5.32 | 4.83 | 35.2 (s) |

The multiplicity of the signals are denoted in brackets.

[a]Spectra recorded in $CDCl_3$ at ambient temperature.

these protons and the bulky phosphine ligands. Further evidence that this upfield chemical shift is due to phenyl ring currents is provided by the chemical shift data for compound XIV in which the coordinated phosphine is methyldiphenylphosphine. Here a similar upfield shift of the A protons is observed, but by 0.75 ppm vs 1.0 ppm in compound XIII (Table 2.9). An example of the shielding properties of the triphenylphosphine ligand has recently been reported by White et al[57] who observed that a chemical shift change of 1.27 ppm for the highest field $^{1}H$ cyclopentadienyl signal occurs in $[Ru(\eta^{5}\text{-}C_5H_4CH_2CH_2PPh_2)LCl]$ on going from L = $P(OMe)_3$ to L = $PPh_3$.

The $^{13}C$ NMR spectrum of compound XIII (Fig. 2.13, Table 2.10) shows that the three phenyl rings are magnetically equivalent and hence there must be free rotation about the ruthenium-phosphorus bond (on the NMR time scale). In assigning the peaks in the $^{13}C$ NMR spectrum of compound XIII comparison was drawn with the $^{13}C$ NMR spectrum of compound I (Fig. 2.14, Table 2.11). This suggested the peaks at 124 and 121 ppm were due to the vinylic carbon atoms (6,7 and 8a,10a) which are also present in HHA and chemical shifts of which do not change greatly upon coordination of the hydrocarbon to the metal. A DEPT $^{13}C$ NMR spectrum of compound XIII showed that the peaks at 85 and 82ppm were due to CH carbon atoms

Fig. 2.13: The $^{13}C$ NMR spectrum of compound XIII.

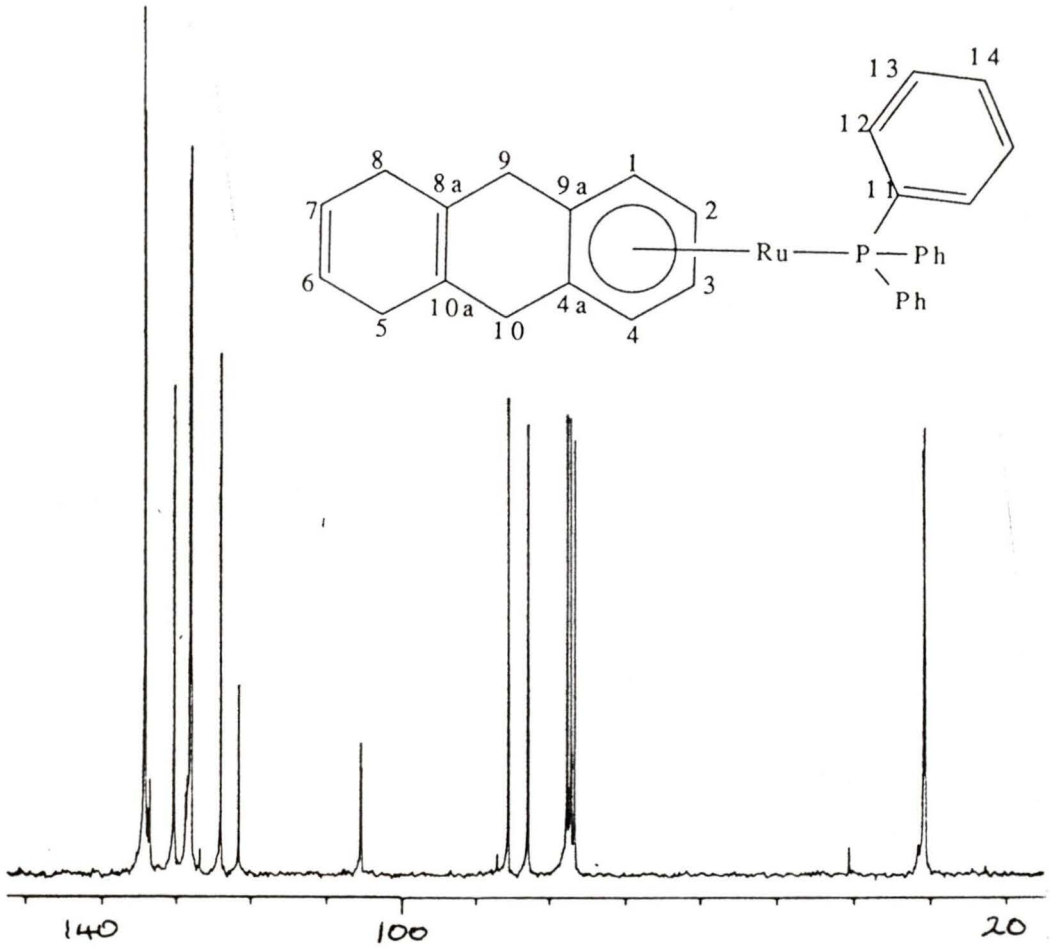


Table 2.10: $^{13}C$ NMR data[a] for compound XIII.

| Carbon atom. | Chemical shift/ppm. | J(C-P)/Hz. |
|---|---|---|
| 1,4 | 82.74 | 0 |
| 2,3 | 85.44 | 0 |
| 4a,9a | 105.32 | 9.5 |
| 5,8 | 30.49 | 0 |
| 6,7 | 123.97 | 0 |
| 8a,10a | 121.60 | 0 |
| 9,10 | 30.70 | 0 |
| 11 | 133.66 | 20.2 |
| 12,13 | 134.18, 127.98 | 9.3,10.3 |
| 14 | 130.25 | 0 |

[a]Spectrum recorded in $CDCl_3$ at ambient temperature. Two Chlorine atoms have been omitted for clarity.

Fig. 2.14: The $^{13}C$ NMR spectrum of HHA.

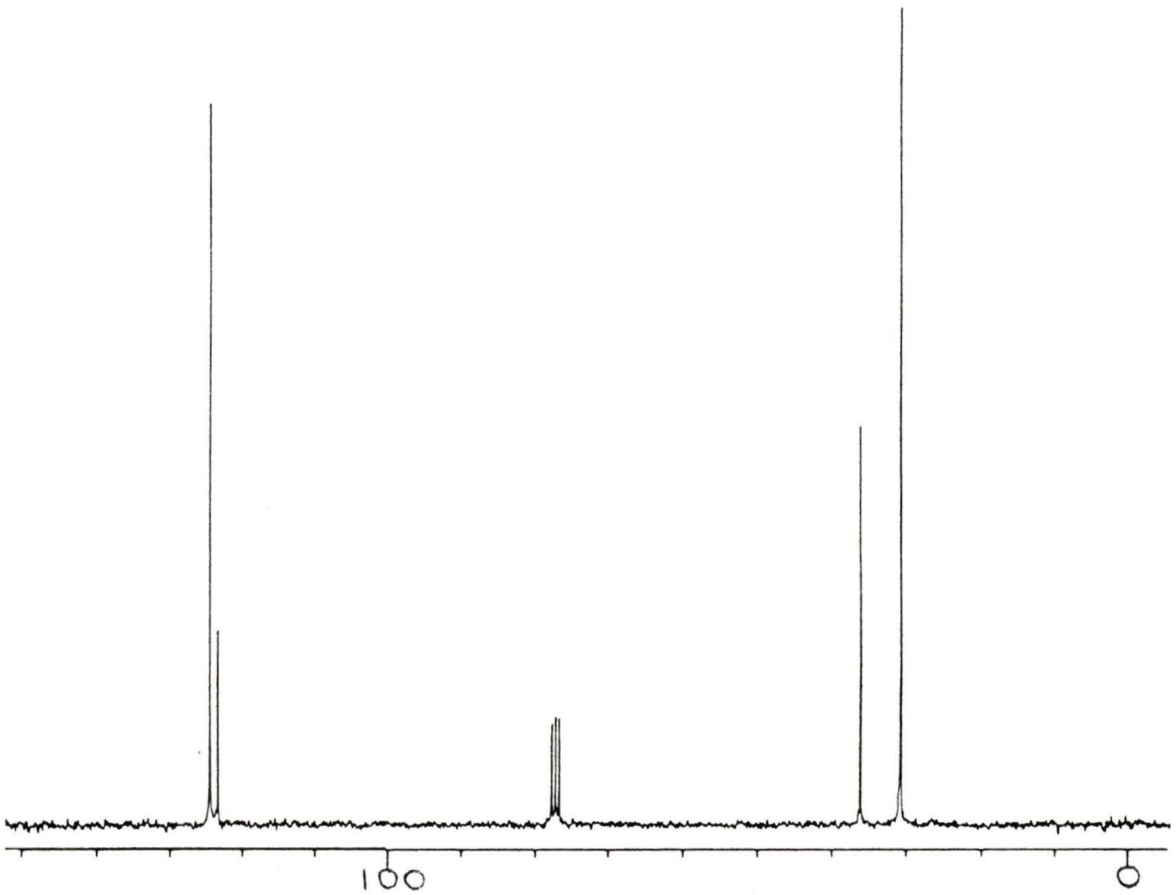


Table 2.11: $^{13}C$ NMR data[a] for HHA.

| Carbon atom. | Chemical shift/ppm. | Intensity. |
|---|---|---|
| 2,3,6,7 | 124.43 | 15.1 |
| 4a,8a,9a,10a | 123.32 | 4.3 |
| 9,10 | 35.88 | 8.4 |
| 1,4,5,8 | 30.49 | 17.1 |

[a]Spectrum recorded in $CDCl_3$ at ambient temperature.

(2,3 and 1,4) and the two peaks at 30 ppm were due to $\underline{C}H_2$ atoms (9,10 and 5,8). The doublet at 105 ppm was assigned to the quaternary aromatic carbons (4a,9a), $^2J(P-C) = 8.4$ Hz. The phosphorus nucleus is selectively coupling to these latter carbon nuclei, suggesting it is trans to these two atoms. The carbon nuclei to which the $H_A$ and $H_{A'}$ protons are attached do not couple to the phosphorus nuclei, although their attached protons do, $^3J(P-H) = 3.0$ Hz. It seems likely that this coupling arises from a "through space interaction".

These results show the reaction between $RuCl_3 \cdot 3H_2O$ and HHA leads to the formation of the dimeric species $[(\eta^6\text{-THA})Ru(\mu\text{-}Cl)Cl]_2$ (X). Dissolution of this species in DMSO cleaves the chloro bridges to form the mononuclear species $[(\eta^6\text{-THA})RuCl_2DMSO]$ (XI). The set of compounds $[(\eta^6\text{-THA})RuCl_2L]$ (L = $P(OEt)_3$ (XII), $PPh_3$ (XIII), L = $PPh_2Me$ (XIV) and L = $PCy_3$) have been formed. These compounds show selective coupling between the phosphorus nucleus and two of the four protons on the arene ring of the coordinated THA ligand. In compounds XIII and XIV, an upfield shift of these two protons is observed, relative to their position in compounds XII and XV. This has been attributed to an interaction of the protons with the phenyl ring currents in the coordinated phosphine ligands.

In order to explore further the cleavage reactions of compound X and the substitution reactions of compound XI, the reactions of these compounds with pyrazole (pzH) and 3,5-dimethylpyrazole ($Me_2$pzH) were attempted. Addition of one equivalent of pyrazole per ruthenium centre to compound X in dichloromethane as solvent, gave the bis pyrazole mononuclear cation (XVI) and unreacted starting material only. It seems likely that any mono pyrazole species formed is converted to the bis pyrazole mononuclear cation by the free pyrazole in the system. Hence addition of two equivalents of pyrazole per ruthenium centre to compound X resulted in the formation of compound XVI in good yield (80%). The $^1$H NMR data for the pyrazole resonances are shown in Table 2.12.

Four resonances are observed for the pyrazole protons in compound XVI indicating that the species is non-fluxional on the NMR timescale and contains a two-fold symmetry element which relates the two pyrazole ligands and makes them chemically equivalent. A doublet-triplet-doublet splitting pattern is observed for the H(3), H(4) and H(5) protons in compound XVI suggesting that the coupling constant value for J[H(1)-H(X)] (X = 3,4,5) is approximately zero (within experimental error). A triplet-quartet-triplet splitting pattern is observed in related rhodium-containing species where this is not the case.[58] The signal corresponding to the H(1) proton is

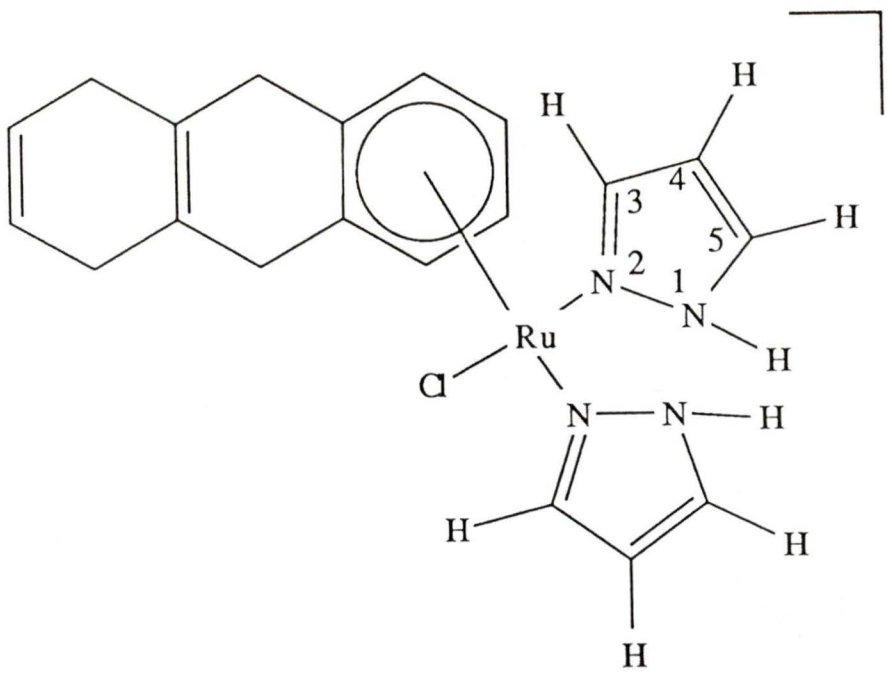


Compound XVI.

Table 2.12: The $^{1}H$ NMR data[a] for the pyrazole protons in compounds XVI and XVII.

| Proton | Chemical shift/ppm | |
|---|---|---|
| | Compound XVI | Compound XVII |
| H(1) | 14.49(s) | 10.80(s) |
| H(3), H(5) | 7.93, 7.71(d) | 2.49, 2.17(s) |
| Me(3), Me(5) | -- | 2.49, 2.17(s) |
| H(4) | 6.24(t) | 5.92(d) |

Multiplicity of the signals denoted in brackets.

[a]Spectrum recorded in $CDCl_3$ at ambient temperature.

significantly broader than the signals for the other pyrazole protons and is a result of quadrupolar broadening of the H(1) resonance, due to the proximity of the $^{14}N$ nucleus (I = 1) to which it is bonded.[40] Analogous results were obtained when pyrazole was added to the mononuclear DMSO adduct (compound X) with the bis pyrazole adduct (compound XVI) being the only pyrazole containing metal species isolated.

Addition of one equivalent of 3,5-dimethylpyrazole to compound IX in dichloromethane as solvent formed the mononuclear mono 3,5-dimethylpyrazole derivative (compound XVII) of compound IX, but in low yield (30%). The $^{1}H$ NMR data for the 3,5-dimethylpyrazole resonances in compound IX are also shown in Table 2.12. Decoupling by irradiation of the signal at 10.80 ppm (assigned to the H(1) proton) led to the collapse of the doublet at 5.92 ppm (assigned to the H(4) proton) to a singlet, with no observable effect on the remainder of the spectrum, showing selective

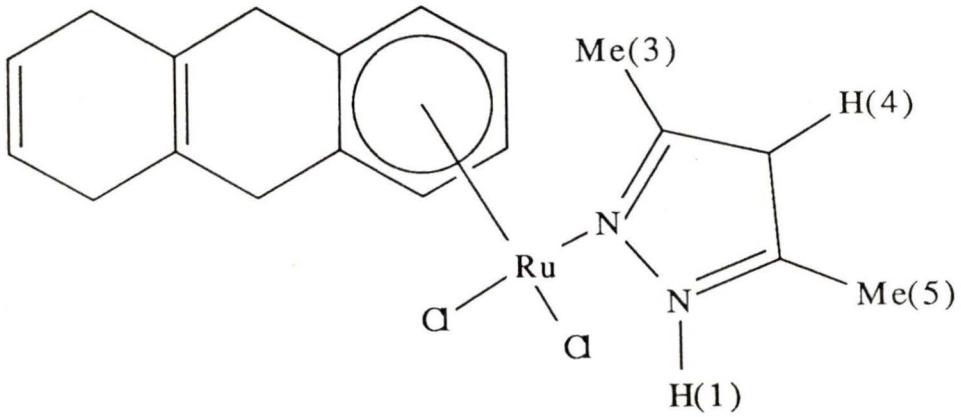


Compound XVII.

coupling between the H(1) and H(4) protons, $^{4}J[H(1)-H(4)]$ = 2.3 Hz.

Similarly, addition of one equivalent or excess (ca. 20 fold) of 3,5-dimethylpyrazole to compound XI in dichloromethane as solvent resulted in the formation of compound XVII only, and in higher yield (80%). This substitution of DMSO by 3,5-dimethylpyrazole is of mechanistic interest, as it could occur by an associative or dissociative mechanism or by a mechanism intermediate between the two ($I_A$ or $I_D$). The pathways for the two limiting mechanisms (associative or dissociative) are shown in Schemes 2.1 and 2.2. For the associative pathway shown, a $\eta^6$ to $\eta^4$ to $\eta^6$ ring slippage of the coordinated arene ring would be required to maintain an 18 electron count at the ruthenium centre. Examples of such slippages are rare in the context of ruthenium arenes,[59] and are confined to pre-equilibrium steps in arene displacement reactions of the type shown in Scheme 2.3. There are more examples of ring slippages occurring in the substitution reactions of metal carbonyl fragments,[60] such as the $Rh(CO)_3$ group coordinated to $\eta^5$-cyclopentadienyl, where the analogous associative pathway for ligand displacement of carbonyl occurs via a $\eta^5$ to $\eta^3$ to $\eta^5$ ring slippage of the cyclopentadienyl ring: an example of this type of reaction, studied by Basolo et al, is shown in Scheme 2.4.[61]

Scheme 2.1: The associative pathway for the substitution of DMSO by 3,5-dimethylpyrazole to yield compound XVII.

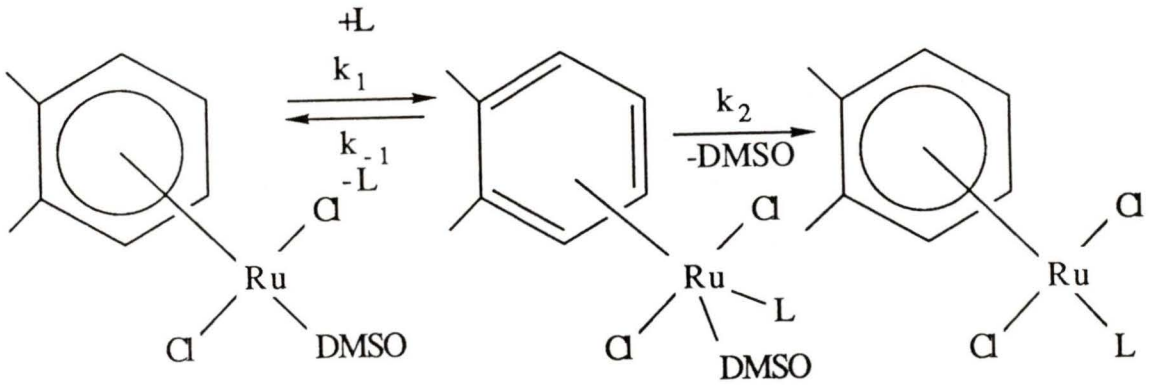


Scheme 2.2: The dissociative pathway for the substitution of DMSO by 3,5-dimethylpyrazole to yield compound XVII.

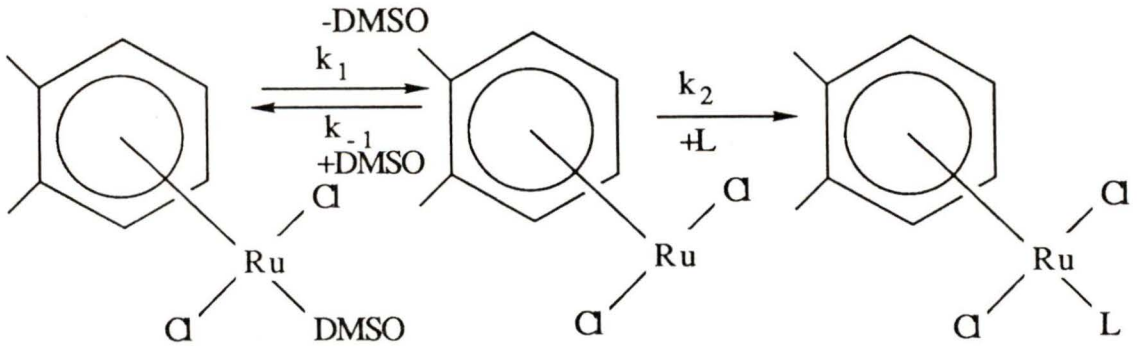

Scheme 2.3: $\eta^6$ to $\eta^4$ preequilibrium mechanism for displacement of anthracene in $[(\eta^5\text{-Cp}^*)\text{Ru(anthracene)}]^+$. by acetonitrile.

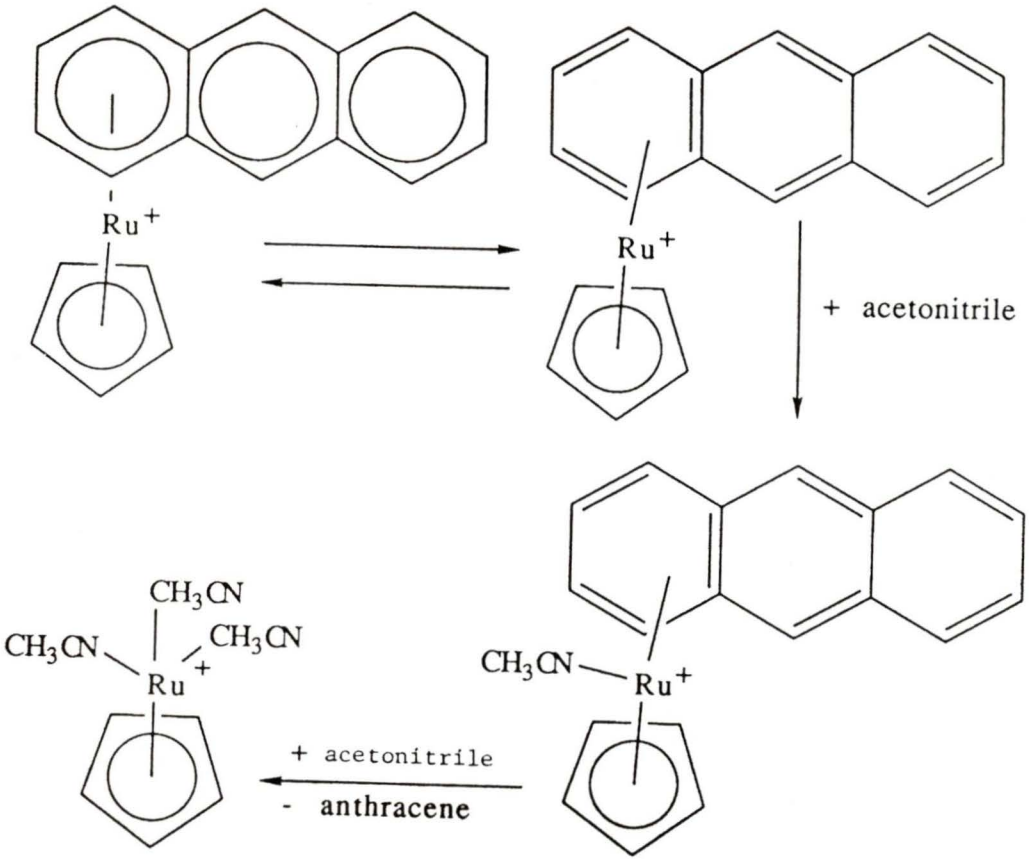


Scheme 2.4: $\eta^5$ to $\eta^3$ to $\eta^5$ ring slippage in the nucleophilic substitution reactions of $[(\eta^5\text{-Cp})\text{Rh(CO)}_2]$.

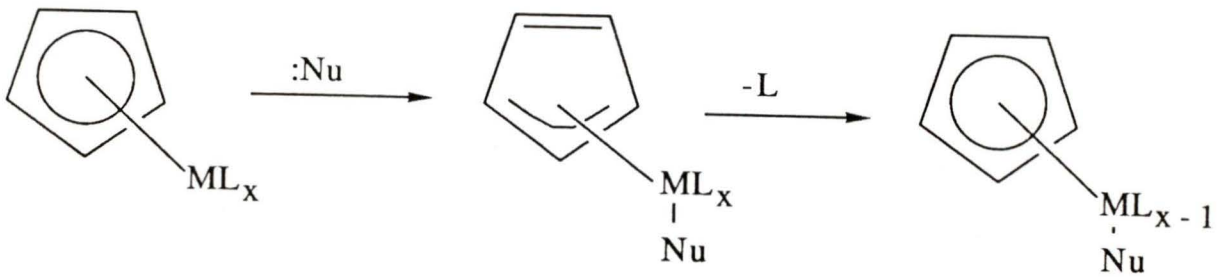

The first experimental systems to be studied were as follows: [XI] was held constant at 1 x $10^{-3}$ M with [3,5-dimethylpyrazole] ([L]) having values of 20,30,40,50 and 80 equivalents respectively, and in each case no DMSO was added to the system. The UV/visible spectra of compounds XI and XVII, in the range lambda = 300 nm to 600 nm, are shown in Fig. 2.15. The wavelength chosen for study of the systems was 380 nm, where the change in absorbance on going from compound XI to compound XVII is greatest. In addition, the change in absorbance with wavelength for the individual species is slight in this region of the spectrum, hence reducing error in absorbance measurements between systems. A plot of absorbance versus time of reaction, at this wavelength, for the addition of 20 equivalents of 3,5-dimethylpyrazole (L) to compound XI is shown in Fig. 2.16.

The reactions effectively went to completion in five minutes. The observed pseudo first order rate constants $k_{obs}$ ([L] was always large with respect to [XI] and effectively remained constant during the reaction) were then calculated by plotting $\ln(A_t - A_\infty)$ vs time of reaction (usually up to 60 seconds after the initial reading of absorbance) and taking the slope of the line obtained. The value of $k_{obs}$ obtained for each system is shown in Table 2.13 and the plot of $k_{obs}$ versus [L], shown in Fig. 2.17, follows a Michaelis-Menten type curve; a plot of $1/k_{obs}$

Fig. 2.15: The UV/visible spectra of compounds XI and XVII in the range lambda = 300 nm to 600 nm.

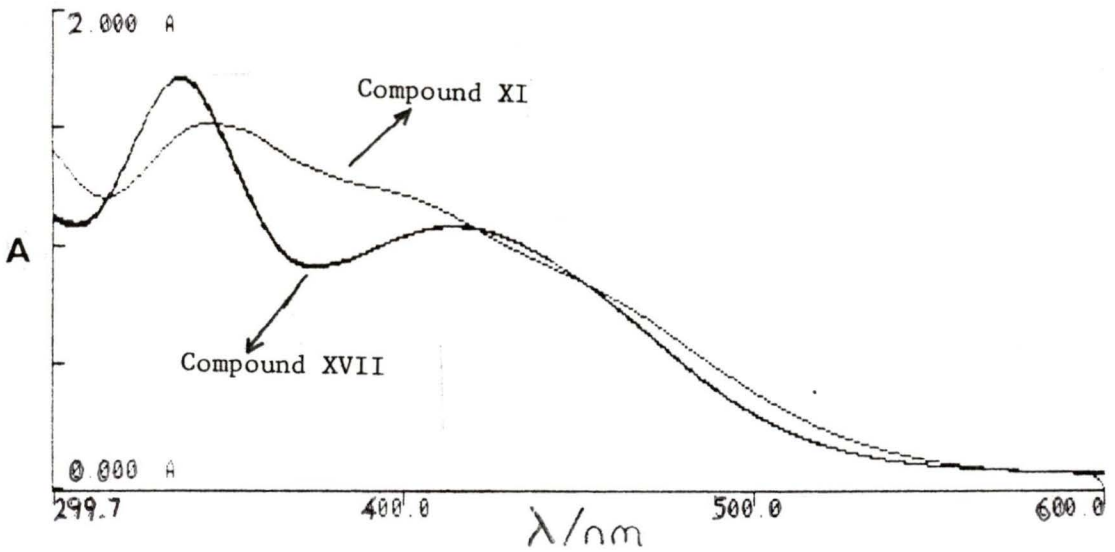


Fig. 2.16: Plot of absorbance vs time for the addition of 20 equivalents of L to compound XI.

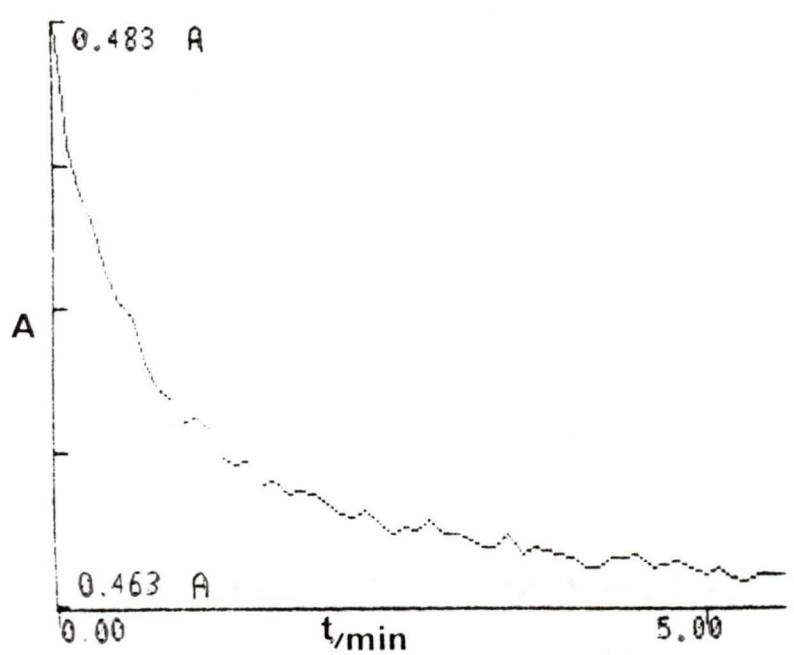

Table 2.13: $k_{obs}$ as a function of [L].

| [L]/equiv. | 20 | 30 | 40 | 50 | 80 | 200 |
|---|---|---|---|---|---|---|
| $k_{obs} \times 10^3/s^{-1}$ | 20.89 | 31.29 | 36.17 | 43.87 | 58.37 | 85.43 |

Fig. 2.17: Plot of $k_{obs}$ vs [L].

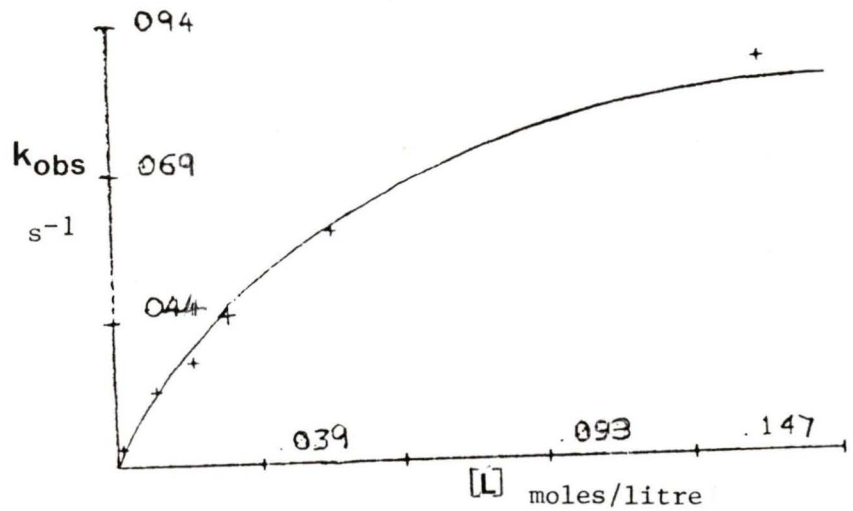


Fig. 2.18: Plot of $1/k_{obs}$ vs 1/[L].

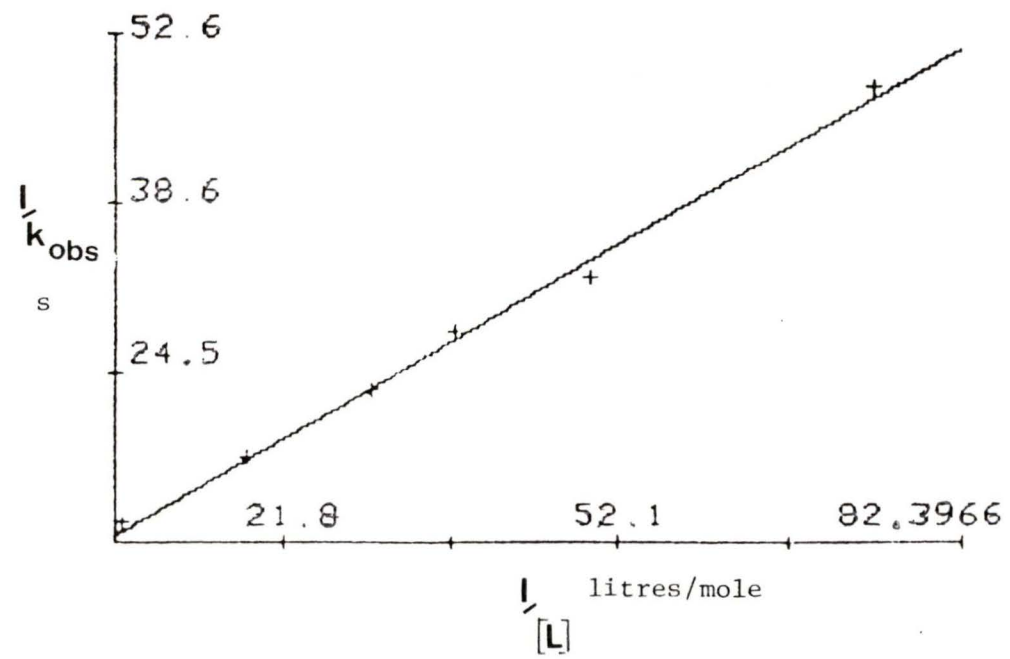

versus 1/[L] yielded the graph shown in Fig. 2.18

The Michaelis-Menten plot obtained indicates the reaction is first order with respect to [L] at low [L], and trancends to zero order with respect to [L] at high [L]. The following reaction rate expressions for the two limiting pathways are consistent with this data, and are derived using the rate constants $k_1$, $k_{-1}$ and $k_2$ of Schemes 2.1 and 2.2.

Associative.

$$\text{Rate} = \frac{k_2 K[L][XI]}{1 + K[L]}$$

Dissociative.

$$\text{Rate} = \frac{k_1 k_2 [XI][L]}{k_{-1}[DMSO] + k_2[L]}$$

K = equilibrium constant for the first step of the associative pathway.

XI = [($\eta^6$-THA)$RuCl_2$DMSO].

L = 3,5-dimethylpyrazole.

To gain more information about the reaction mechanism, the effect of adding DMSO to the system was studied. As can be seen from the rate law expressions given, addition of DMSO should lower the rate of reaction if the dissociative pathway is followed, but should not effect the rate of reaction if the associative pathway ensues. The following experimental systems were employed for this purpose: [XI] was held constant at $1 \times 10^{-3}$M with [L] having a value of 10 equivalents and added [DMSO] having

values of 0,1,10,100 and 1000 equivalents respectively. The reaction was again monitored by following the changes in light absorption at 380 nm, which were used to calculate $k_{obs}$ as done previously. These values are shown in Table 2.14. The results show $k_{obs}$ and hence the reaction rate increasing with added [DMSO], with a thousand fold increase in the amount of DMSO added to the system effectively doubling the value of $k_{obs}$. This observation is in sharp contrast to the results obtained for the kinetic study of the substitution of coordinated DMSO by triphenylphosphine in $[(\eta^6\text{-}C_6H_6)RuCl_2DMSO]$,[62] (Scheme 2.5), which has been studied by Kane-Maguire et al. A dissociative pathway is proposed for this reaction, because when followed in dichloromethane as solvent, a 700 fold increase in the amount of DMSO added to the system is accompanied by a decrease in the reaction rate of a factor of 750, as is expected from the form of the dissociative rate law expression (page 66). This is plainly not the case for the ruthenium-THA system (see Table 2.14).

The Michaelis-Menten type plot obtained for the plot of reaction rate versus [L] also suggests the reaction does not proceed via a concerted reaction mechanism ($I_A$ or $I_D$) which would be expected to give a linear plot for $k_{obs}$ vs [L]. In practical terms, 1000 equivalents of DMSO occupies a volume of 0.13 mL in a total solvent volume of 3 mL (the rest of the solvent volume is dichloromethane).

Table 2.14: $k_{obs}$ as a function of [DMSO].

| [DMSO]/equiv. | 0 | 1 | 10 | 100 | 1000 |
|---|---|---|---|---|---|
| $k_{obs} \times 10^3/s^{-1}$ | 8.95 | 8.82 | 10.58 | 12.20 | 21.63 |

Scheme 2.5: Reaction mechanism for the substitution of DMSO by triphenylphosphine in $[(\eta^6\text{-}C_6H_6)RuCl_2DMSO]$.

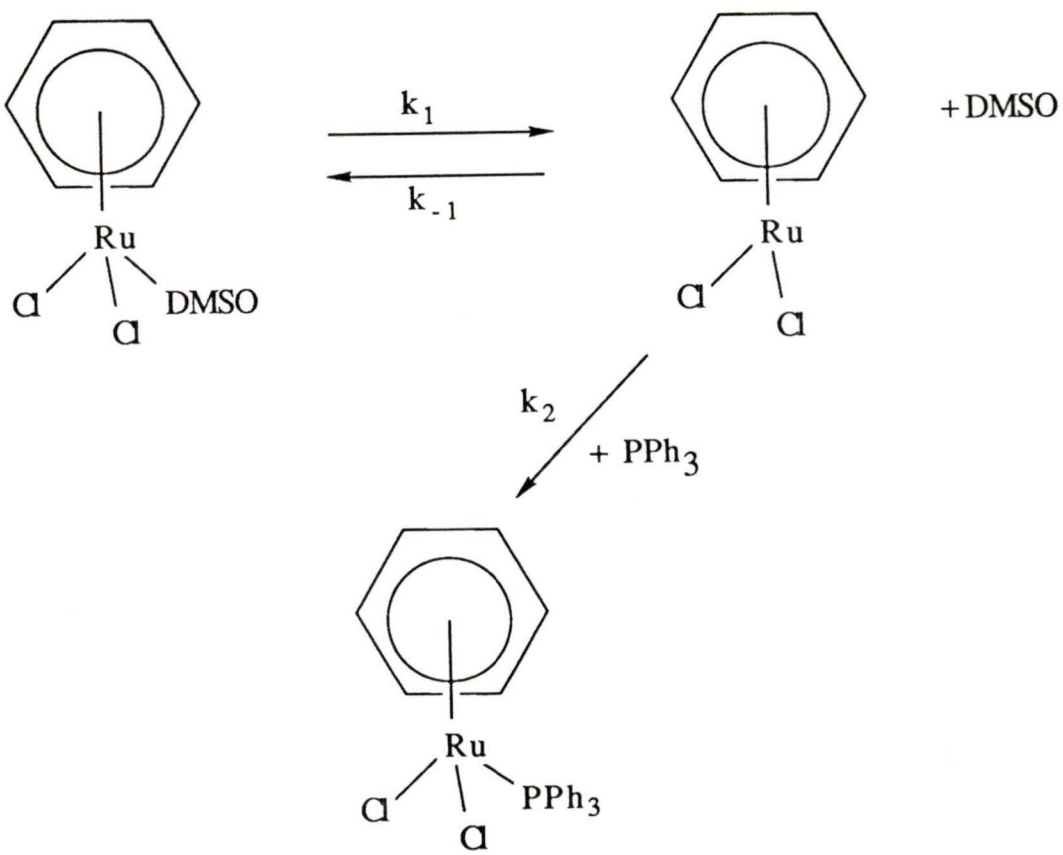

Hence, solvent effects may alter the reaction rate as more DMSO is added to the system and are a possible explanation for the minor rate increase with increased [DMSO] to the ruthenium-THA system.

The important conclusion of this work is that the kinetic data obtained for the reaction of 3,5-dimethylpyrazole with compound XI are consistent with a substitution reaction which follows an associative pathway; the most likely mechanism for this involves an $\eta^6$-$\eta^4$ ring slippage at the coordinated arene, thus preserving an 18 electron count at the metal centre.

To extend the series of mononuclear ruthenium pyrazole systems, the cleavage of the chloro bridges in $[(\eta^6\text{-arene})Ru(\mu\text{-}Cl)Cl]_2$ (arene = $C_6H_6$, $C_{10}H_{14}$) by pyrazole was attempted. Addition of one equivalent of pyrazole per ruthenium centre to $[(\eta^6\text{-}C_6H_6)Ru(\mu\text{-}Cl)Cl]_2$ in either dichloromethane or methanol as solvent yielded a mixture of the mono pyrazole adduct (compound XVIII), the bis pyrazole cation (compound XIX) and unreacted starting material. The ratio of compound XIX:compound XVIII was of the order of 6:5. Addition of two equivalents of pyrazole per ruthenium centre to $[(\eta^6\text{-}C_6H_6)Ru(\mu\text{-}Cl)Cl]_2$ yielded compound XIX only in good yield (80%).

Likewise, addition of one equivalent of pyrazole per ruthenium centre to $[(\eta^6\text{-}C_{10}H_{14})Ru(\mu\text{-}Cl)Cl]_2$ in dichloromethane as solvent yielded a mixture of the mono

pyrazole adduct (compound XX), the bis pyrazole cation (compound XXI) and unreacted starting material. The ratio of compound XXI:compound XX was 7:3. Hence, addition of 1.3 equivalents of pyrazole per ruthenium centre to $[(\eta^6\text{-p-cymene})Ru(\mu\text{-Cl})Cl]_2$ yielded compound XX and compound XXI only, in the same proportion and addition of two equivalents of pyrazole per ruthenium centre yielded compound XXI only, in good yield (85%). For both mixtures (compounds XVIII and XIX; compounds XX and XXI), fractional crystallisation and thin layer chromatography were unsuccessful in the isolation of the mononuclear species.

The $^1$H NMR data for the pyrazole protons of compounds XVIII to XXI are shown in Table 2.15; the $^1$H NMR spectrum of a mixture of compounds XVIII and XIX is shown in Fig. 2.19. For all the compounds, four resonances are observed for the pyrazole protons, and with the exception of compound XIX, the resonances for the H(3), H(4) and H(5) pyrazole protons appear as a triplet-quartet-triplet splitting pattern, suggesting these protons couple significantly to the H(1) proton as in related rhodium species,[58] and indicating these species are non-fluxional on the NMR timescale at ambient temperature (as is the case for all the ruthenium pyrazole monomers encountered in this research; furthermore, the bis pyrazole cations compounds XIX and XXI must contain a two-fold symmetry

element, relating the two pyrazole ligands, making them chemically equivalent.

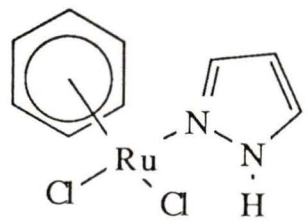


XVIII

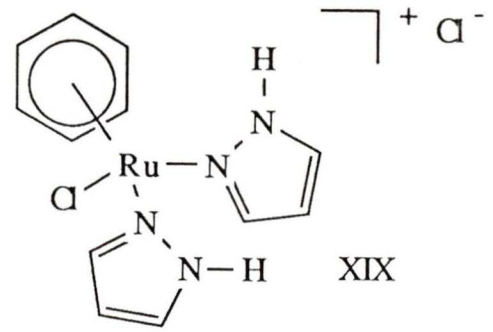


XIX

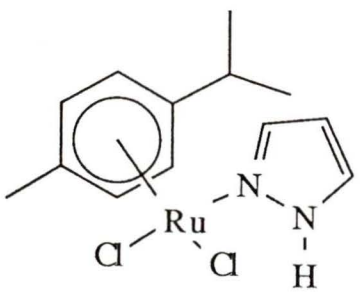


XX

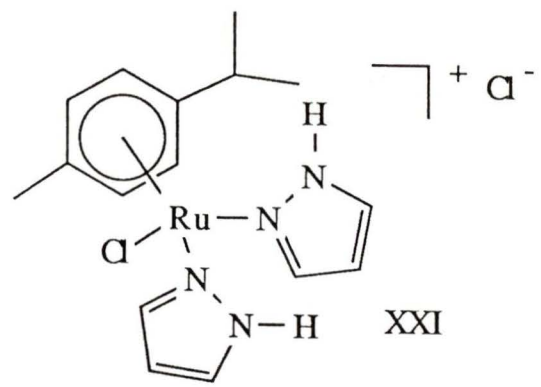


XXI

Table 2.15: The $^{1}H$ NMR data for the pyrazole protons in compounds XVIII to XXI.

| | Chemical shift/ppm. | | |
|---|---|---|---|
| Compound | H(1) | H(3), H(5) | H(4). |
| XVIII[a] | 11.50 (b) | 8.13, 7.69 (t) | 6.52 (q) |
| XIX[a] | 13.88 (b) | 8.02, 7.80 (d) | 6.39 (t) |
| XX[c] | 11.74 (b) | 7.87, 7.47 (t) | 6.35 (q) |
| XXI[c] | 14.26 (b) | 7.98, 7.71 (t) | 6.24 (q) |

The multiplicity of the signals are denoted in brackets.

[a]Spectra recorded in $CD_3NO_2$ at ambient temperature.

[c]Spectra recorded in $CDCl_3$ at ambient temperature.

Fig. 2.19: The $^{1}H$ NMR spectrum of a mixture of compounds XVIII and XIX.

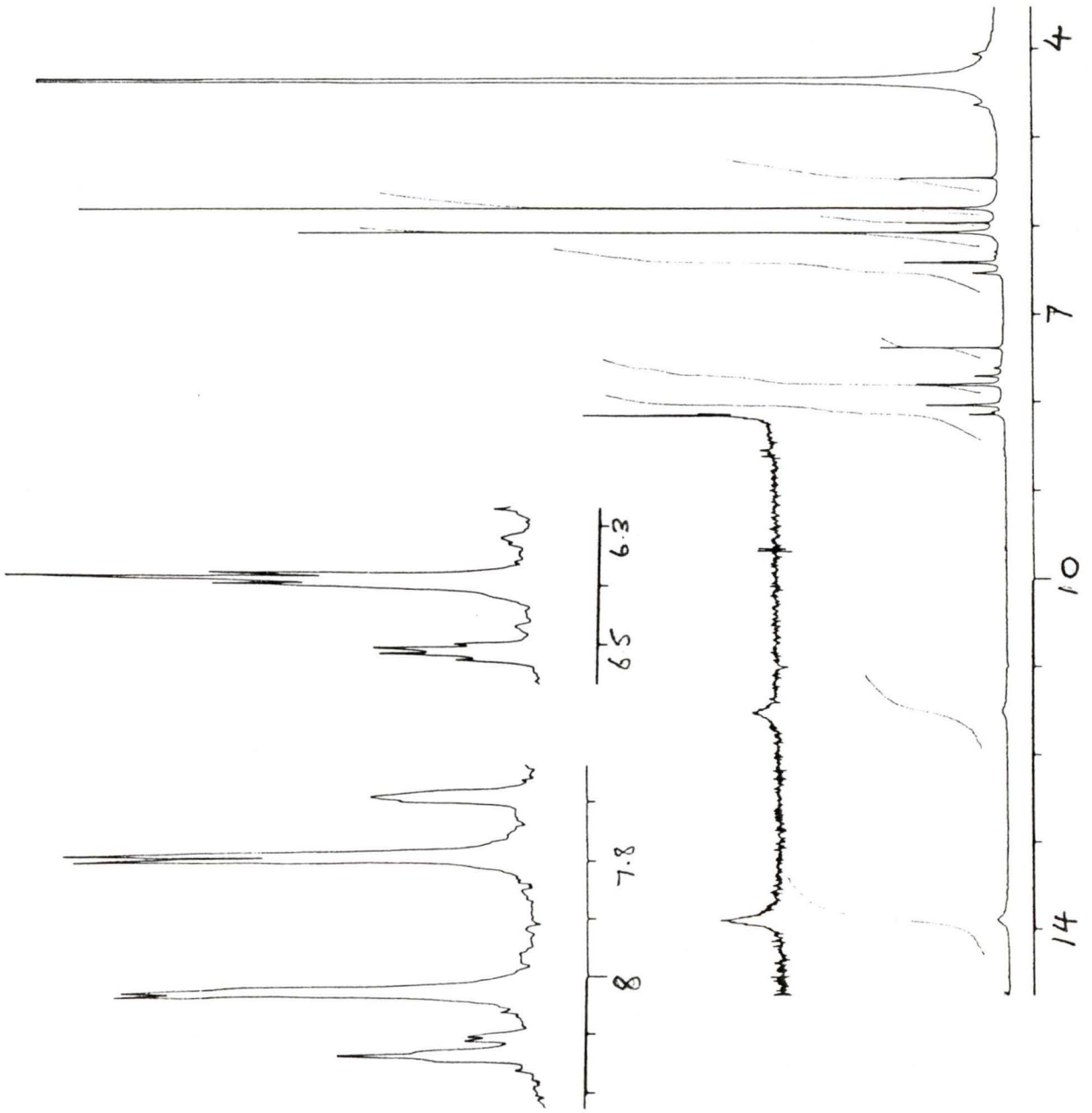

Attempts to form the pyrazolyl bridged dimeric derivatives of compound X (arene = THA) shown in Table 2.16 proved unsuccessful. Addition of triethylamine to the reaction mixture obtained by adding one equivalent of pyrazole per ruthenium centre to compound X failed to facilitate dimerisation and decomposition of the metal complex occurred. The presence of triethylamine hydrochloride in the reaction mixture, identified by $^{1}H$ NMR, suggested triethylamine was successful in the abstraction of the H(1) proton in the bis pyrazole cation (compound XVI), but decomposition rather than the expected dimerisation ensued.[63] Similar observations were made when triethylamine was added to the analogous reaction mixture originating from the addition of pyrazole to the mononuclear DMSO adduct (compound XI). Likewise, attempts to form the 3,5-dimethylpyrazolyl bridged dimeric derivative of compound X proved unsuccessful. Addition of triethylamine to the mono 3,5-dimethylpyrazole ruthenium species (compound XVII) in dichloromethane resulted in decomposition, although triethylamine hydrochloride was again present in the reaction mixture. The large size of the coordinated arene ligand may inhibit the process of dimerisation. So, the synthesis of pyrazolyl bridged ruthenium dimers from the monocyclic arene dimers $[(\eta^{6}\text{-arene})Ru(\mu\text{-}Cl)Cl]_2$ (arene = $C_6H_6$, $C_{10}H_{14}$) was attempted.

Table 2.16: Attempted syntheses of pz bridged species.

1. Compound X + pzH/$Et_3N$ -----> Decomposition.
2. Compound XI + pzH/$Et_3N$ -----> Decomposition.
3. Compound X + $Me_2$pzH/$Et_3N$ -----> Decomposition.
4. Compound XVII + $Et_3N$ -----> Decomposition.

In the preparations starting from $[\eta^6\text{-}C_6H_6)Ru(\mu\text{-}Cl)Cl]_2$, one mole of pyrazole per ruthenium centre was added and triethylamine was generally employed as base (one preparation used sodium carbonate), while various solvents were utilised. The best results, with regard to yield and purity of a pyrazolyl bridged species (compound XXII), were obtained using triethylamine in methanol. The main by-product in all these preparations is the bis pyrazole mononuclear cation (compound XIX). Dimerisation is most successful when triethylamine is added to mono pyrazole mononuclear species. The poor solubility of the chloro bridged dimer used means that although the ratio of ruthenium:pyrazole in the system is 1:1, in solution the ratio of ruthenium:pyrazole is at least 1:2 meaning the bis pyrazole cation (compound XIX) is formed along with the mono pyrazole species, so the yield of dimer is low.

The $^1H$ NMR spectrum of compound XXII, Fig. 2.20, shows two resonances for the six pyrazolyl protons in a 2:1 ratio for the H(3), H(5) and H(4) positions respectively.

Fig. 2.20: The $^{1}H$ NMR spectrum of compound XXII.

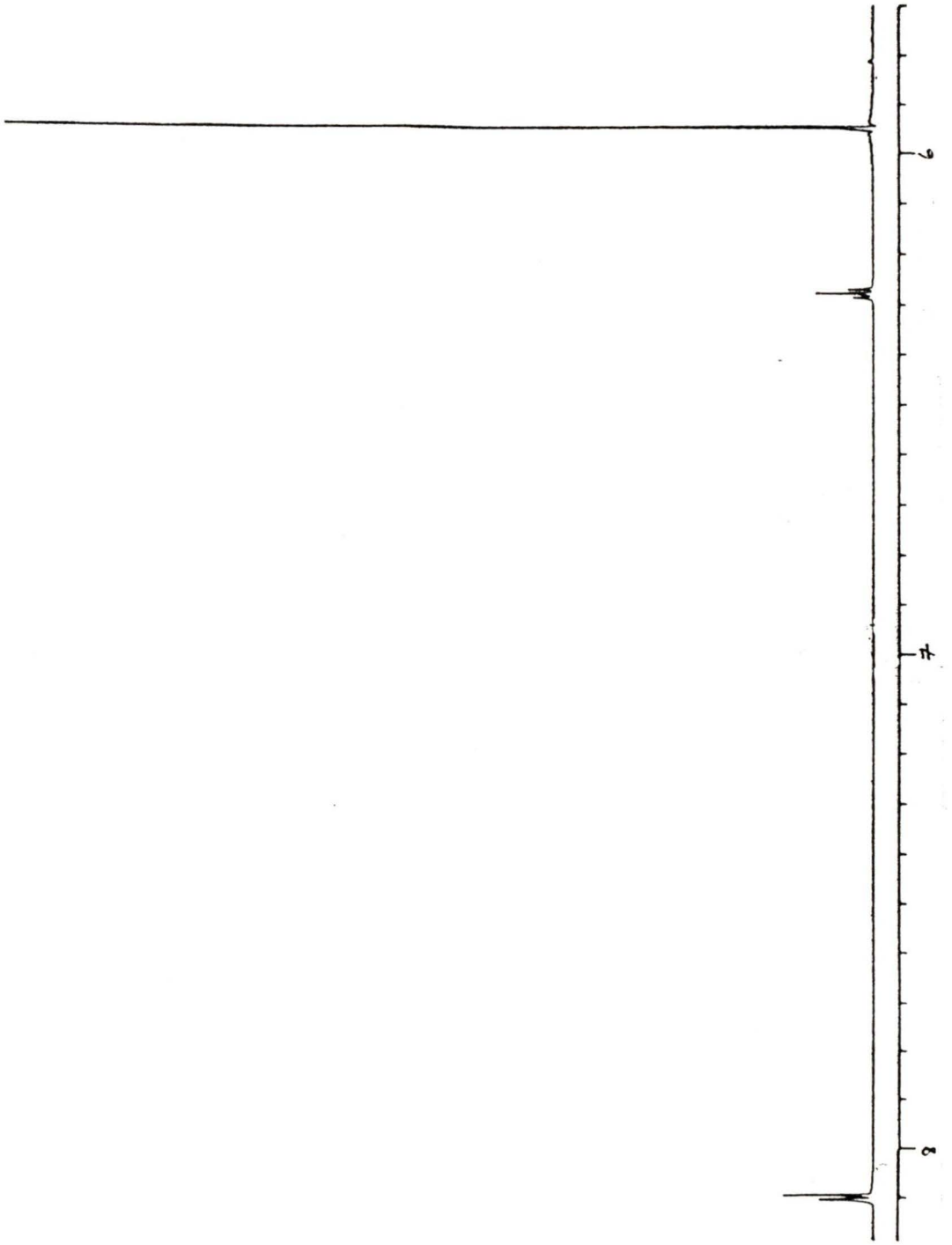

This shows that the symmetry of the molecule relates the two pyrazolyl ligands and further relates the H(3) and H(5) protons. Elemental analysis data (C,H,N) were consistent with the formation of a bridged species. There are three possible isomeric forms of compound XXII, shown in Fig. 2.21, which could exhibit such $^{1}H$ NMR properties.

Addition of silver tetrafluoroborate to $[(\eta^5\text{-}Cp^*)Rh(\mu\text{-}pz)Cl]_2$ by Stobart et al[63] results in the formation of the triply bridged bis pyrazolyl chloro species $[(\eta^5\text{-}Cp^*)Rh(\mu\text{-}pz)_2(\mu\text{-}Cl)]BF_4$, Eqn. 2.4, and the chemical shifts of the H(3) and H(5) positions in this compound shift by 0.3 ppm to lower field.[49] Similarly, addition of ammonium hexafluorophosphate to compound XXII in water results in the formation of the yellow hexafluorophosphate salt $[(\eta^6\text{-}C_6H_6)Ru_2(\mu\text{-}pz)_2(\mu\text{-}Cl)]PF_6$ (compound XXIII), Eqn. 2.5. Compound XXIII and compound XXII have identical $^{1}H$ NMR patterns and very similar (identical within experimental error) absolute chemical shift values. This strongly suggests that compound XXII is in the form of isomer 3, as this would be expected to have very similar chemical shift values to compound XXIII; as opposed to isomers 1 and 2, which although showing identical NMR splitting patterns to compound XV, would likely have significantly different chemical shift values due to the different chemical environment of the protons. The $^{1}H$ NMR data for compounds XXII and XXIII are shown

Fig. 2.21: The possible isomeric forms of compound XXII.

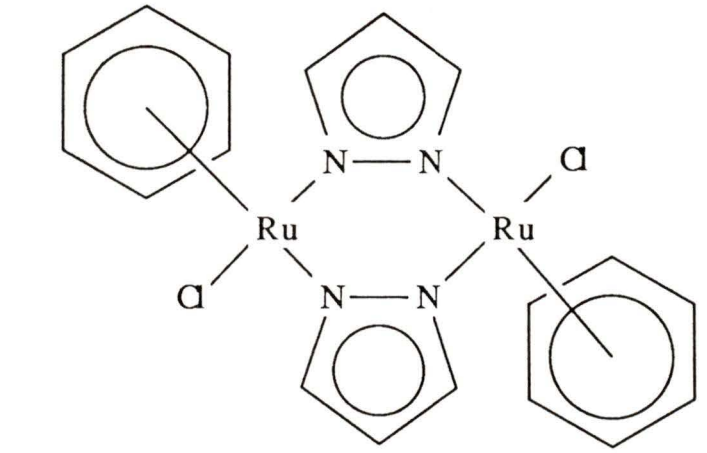


Isomer 1.

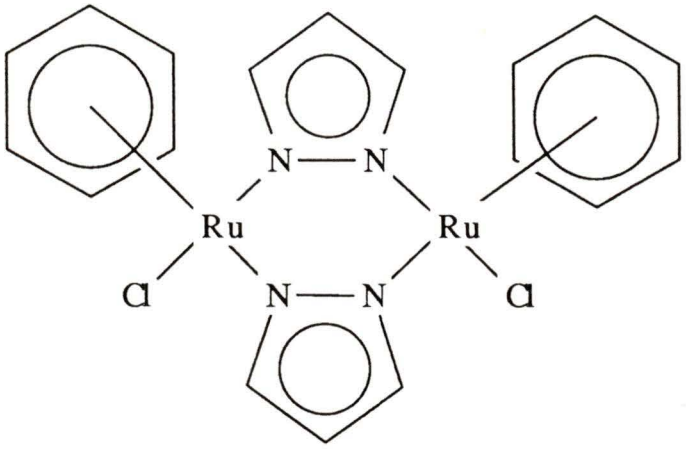


Isomer 2.

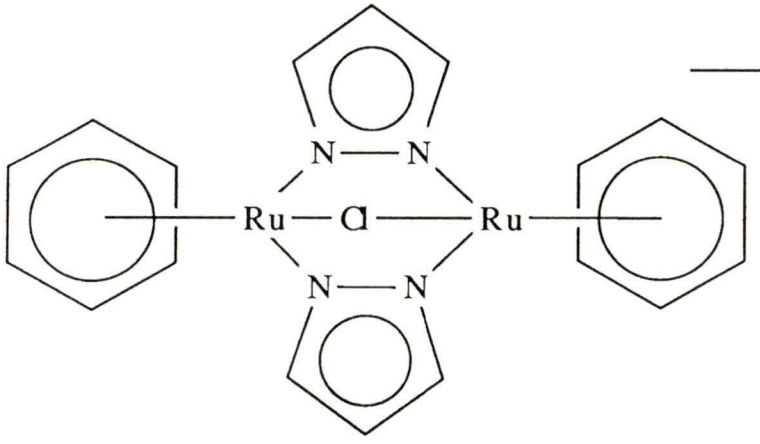


Isomer 3.

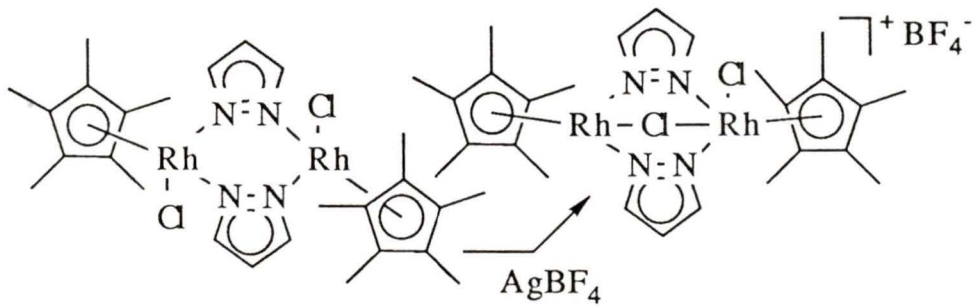


Eqn. 2.4.

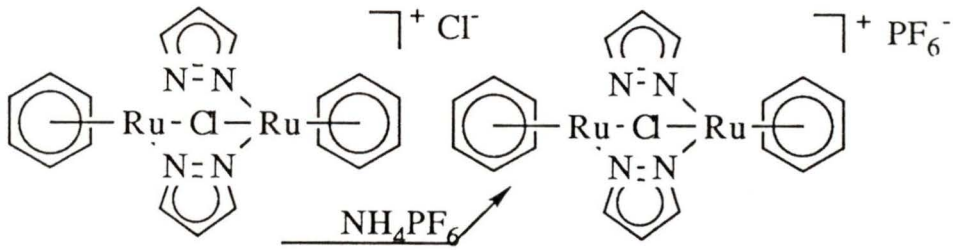


Eqn. 2.5.

Table 2.17: $^{1}$H NMR data[a] for compounds XXII and XXIII.

| Protons. | Compound XXII. Chemical shift/ppm. | Compound XXIII. Chemical shift/ppm. |
|---|---|---|
| Arene | 5.95(s) | 5.95(s) |
| H(3),H(5) | 8.10(d) | 8.10(d) |
| H(4) | 6.27(t) | 6.28(t) |

The multiplicity of the signals are denoted in brackets.

[a]Spectra recorded in $CD_3NO_2$ at ambient temperature.

in Table 2.17.

Red crystals suitable for X-ray analysis were obtained by the slow evaporation of a 1:1 methanol:dichloromethane solution of compound XXII and the molecular structure is shown in Fig. 2.22. Selected bond lengths and angles are shown in Table 2.18 and Table 2.19 respectively. Noticeably, a chloride ion occupies a bridging position, there are two pyrazolyl bridges, and a second chloride acts as the counter ion; this was inferred from the $^{1}H$ NMR data and synthetic results. The two ruthenium atoms are present in a distorted 'piano stool' environment: The N-Ru-Cl and N-Ru-N angles are all between 83° and 84°, while the seperation between the two ruthenium atoms is 3.659(2) Å which is a non-bonding interaction.[64]

The analogous pyrazolyl dimer (compound XXIV), derived from $[(\eta^6\text{-}C_{10}H_{14})Ru(\mu\text{-}Cl)Cl]_2$ proved far simpler to prepare than compound XXII, giving a higher yield of a pyrazolyl bridged species; 80% for compound XXIV, as opposed to 25% for compound XXII. The higher solubility of $[(\eta^6\text{-}C_{10}H_{14})Ru(\mu\text{-}Cl)Cl]_2$ as compared to $[(\eta^6\text{-}C_6H_6)Ru(\mu\text{-}Cl)Cl]_2$ means a sufficient quantity of the chloro bridged dimer can be dissolved in solvent (ca. 200 mg in dichloromethane (30 mL) in a typical experiment), so the formation of the bis pyrazole mononuclear species (compound XIX) is suppressed.

Fig. 2.22: The geometry of the

[(bis(benzene)di-ruthenium bis(μ-pz)μ-chloro] cation.

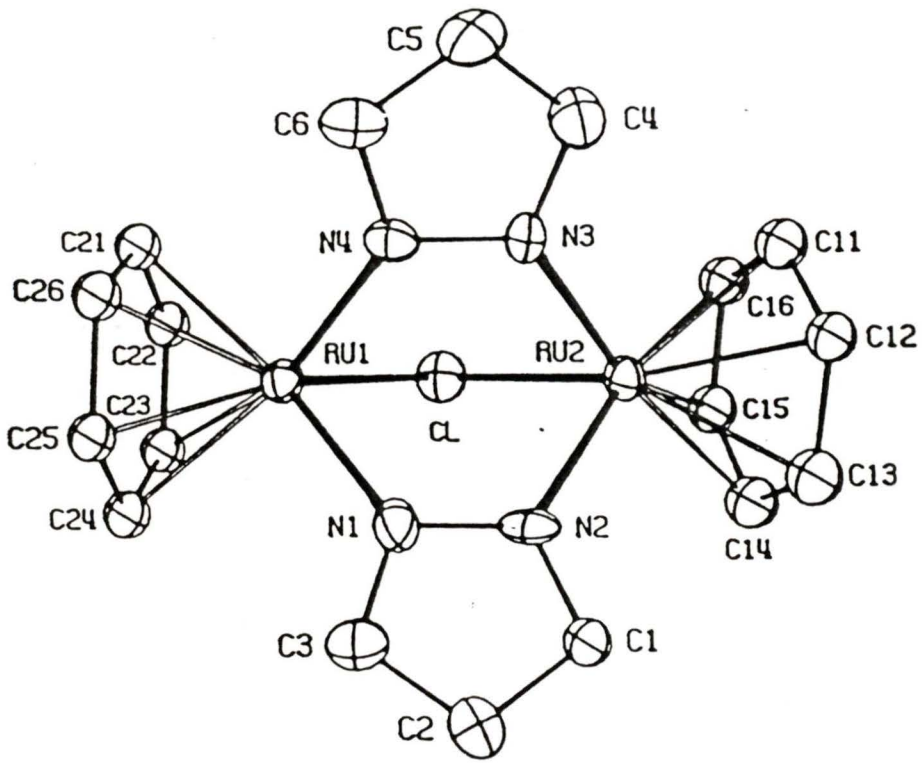

Table 2.18: Selected bond lengths for compound XXII.

| Atoms | Length (Å) | Atoms | Length (Å) |
|---|---|---|---|
| Ru(1)...Ru(2) | 3.659(2) | Ru(1)...Cl | 2.411(5) |
| Ru(1)...N(1) | 2.093(15) | Ru(1)...N(4) | 2.067(15) |
| Ru(2)...N(2) | 2.124(14) | Ru(2)...N(3) | 2.070(14) |
| Ru(1)...C(21) | 2.18(2) | Ru(2)...C(11) | 2.17(2) |
| Ru(1)...C(24) | 2.20(2) | Ru(2)...C(14) | 2.21(2) |
| N(1)...N(2) | 1.34(2) | N(3)...N(4) | 1.36(2) |
| N(1)...C(3) | 1.36(2) | N(3)...C(5) | 1.35(2) |
| C(1)...C(2) | 1.42(2) | C(2)...C(3) | 1.41(3) |
| C(4)...C(5) | 1.36(3) | C(5)...C(6) | 1.40(3) |
| C(11)...C(12) | 1.40(3) | C(21)...C(22) | 1.39(3) |

Estimated standard deviations are given in parentheses.

Table 2.19: Selected bond angles for compound XXII.

| Atoms | Angle (°) | Atoms | Angle (°) |
|---|---|---|---|
| N(1)..Ru(1)..Cl | 84.5(4) | N(2)..Ru(2)..Cl | 84.8(4) |
| N(4)..Ru(1)..Cl | 84.8(4) | N(3)..Ru(2)..Cl | 83.8(4) |
| N(1)..Ru(1)..N(4) | 83.3(6) | N(2)..Ru(2)..N(3) | 83.9(5) |
| N(1)..Ru(1)..C(24) | 94.3(7) | N(2)..Ru(2)..C(14) | 99.3(7) |
| N(4)..Ru(1)..C(21) | 95.1(7) | N(3)..Ru(2)..C(11) | 92.0(7) |
| N(1)..N(2)..Ru(2) | 122.2(11) | N(4)..N(3)..Ru(2) | 124.5(10) |
| N(1)..C(3)..C(2) | 110(2) | N(3)..C(4)..C(5) | 111(2) |
| C(1)..C(2)..C(3) | 104(2) | C(4)..C(5)..C(6) | 105(2) |
| C(11)..C(12)..C(13) | 117(2) | C(21)..C(22)..C(23) | 120(2) |

Estimated standard deviations are given in parentheses.

Compound XXIV was shown to be the triply bridged bis pyrazolyl chloro species $[(\eta^6\text{-}C_{10}H_{14})_2Ru_2(\mu\text{-}Pz)_2(\mu\text{-}Cl)]Cl$ through its conversion to the hexafluorophosphate salt (compound XXV) by the addition of ammonium hexafluorophosphate in water. The $^1H$ NMR splitting patterns for compounds XXIV and XXV are identical as are the chemical shift values. The symmetry of these binuclear cations leads to only two resonances for the six pyrazolyl protons in a 2:1 ratio for the H(3), H(5) and H(4) positions respectively. The $^1H$ NMR spectrum of compound XXIV is shown in Fig. 2.23, the $^1H$ NMR data for the pyrazolyl protons in compounds XXIV and XXV are shown in Table 2.20

As compound XXIV (arene = $C_{10}H_{14}$) proved to be the more accessible of the pyrazolyl bridged ruthenium dimers, reduction studies were predominantly undertaken using this species as a starting point. This Ru(II)-Ru(II) system can be converted to a Ru(I)-Ru(I) system using the following reducing agents: i) sodium/naphthalene; ii) sodium/mercury amalgam and iii) zinc dust with copper filings; zinc dust alone was unsuccessful as a reducing agent. Reducing agents ii and iii were preferred as the presence of naphthalene hindered the isolation of the reduced species.

Characterisation of the Ru(I)-Ru(I) species (compound XXVI) proved to be difficult, due to its high air sensitivity and reactivity. The $^1H$ NMR spectrum of

Fig. 2.23: The $^{1}H$ NMR spectrum of compound XXIV.

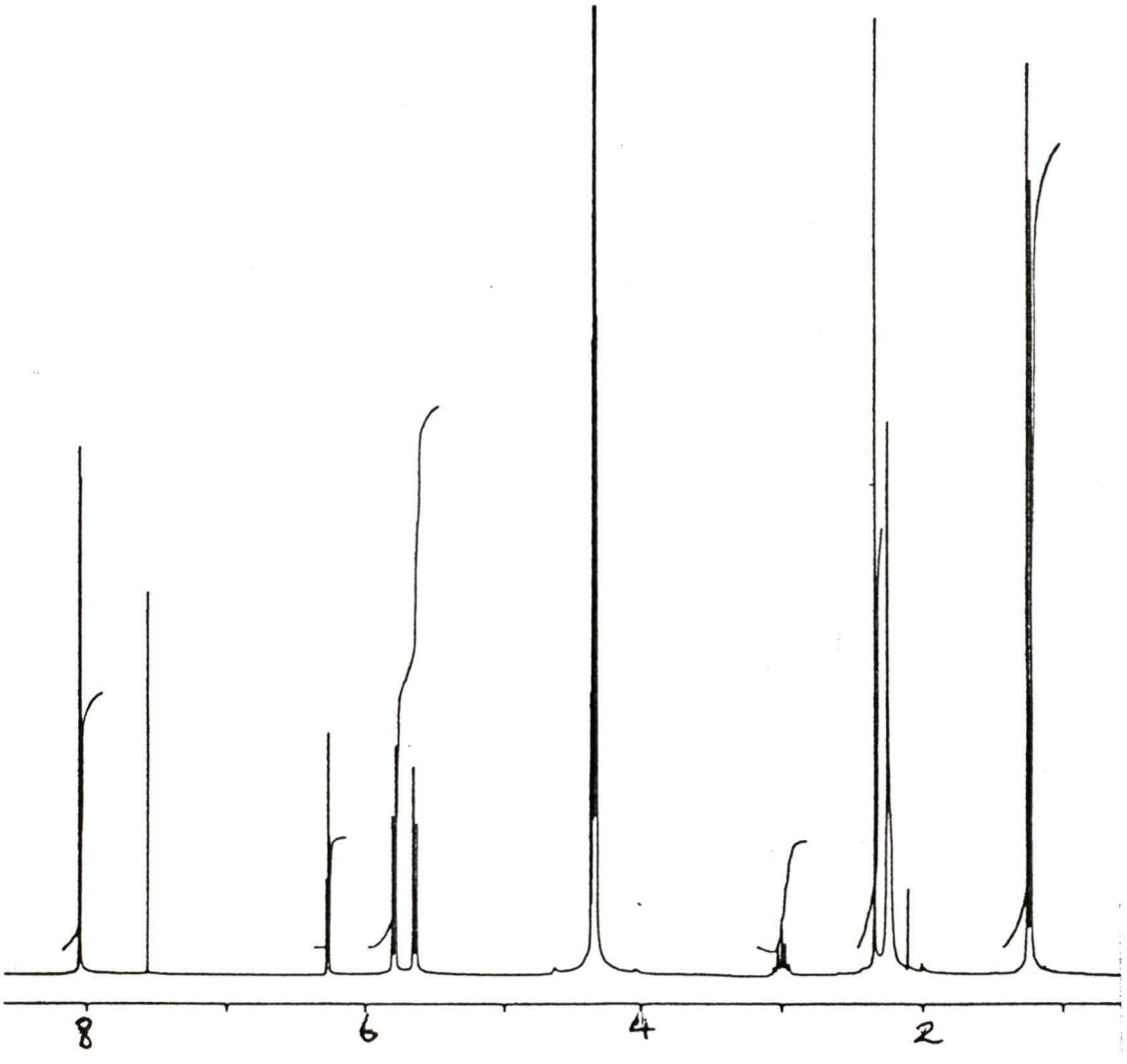


Table 2.20: The $^{1}H$ NMR data[a] for the pyrazolyl ligands in compounds XXIV and XXV.

| Protons. | Compound XXIV. Chemical shift/ppm. | Compound XXV. Chemical shift/ppm. |
|---|---|---|
| H(3),H(5) | 8.05(d) | 8.04(d) |
| H(4) | 6.27(t) | 6.27(t) |

The multiplicity of the signals are denoted in brackets.

[a]Spectra recorded in $CD_3NO_2$ at ambient temperature.

compound XXVI run in $d_3$-nitromethane as solvent shows the presence of a second species, possibly formed by the reaction of compound XXVI with water present in the NMR solvent. Observation of the $^1H$ NMR spectrum in dry $d_6$-benzene showed only the reduced species to be present and this spectrum is shown in Figure 2.24. Water was added to this sample to see if formation of the second species, present in the $d_3$-nitromethane NMR sample, would result, but decomposition ensued. The only evidence that the second species results from reaction of water with compound XXVI is the absence of a water peak in the $^1H$ NMR sample in which this species is seen. For all other $^1H$ NMR spectra run in $d_3$-nitromethane, such as for compound XXIV, a water peak is observed in the region $\delta$ = 2.1 to 2.2 ppm.

Comparison of the $^1H$ NMR spectra (run in $d_3$-nitromethane) of compound XXVI and its Ru(II)-Ru(II) precursor (compound XXIV) shows that the analogous hyrdrocarbon and pyrazolyl proton signals in the spectrum of compound XXVI are at higher field. This can be explained by the fact that reduction of the ruthenium centres results in the electron density at the metal increasing. These centres now exert a lesser electron withdrawing effect than in the corresponding Ru(II)-Ru(II) species, so the protons in compound XXVI are more shielded, and hence their signals move to higher field.

Fig. 2.24: The $^{1}H$ NMR spectrum of compound XXVI.

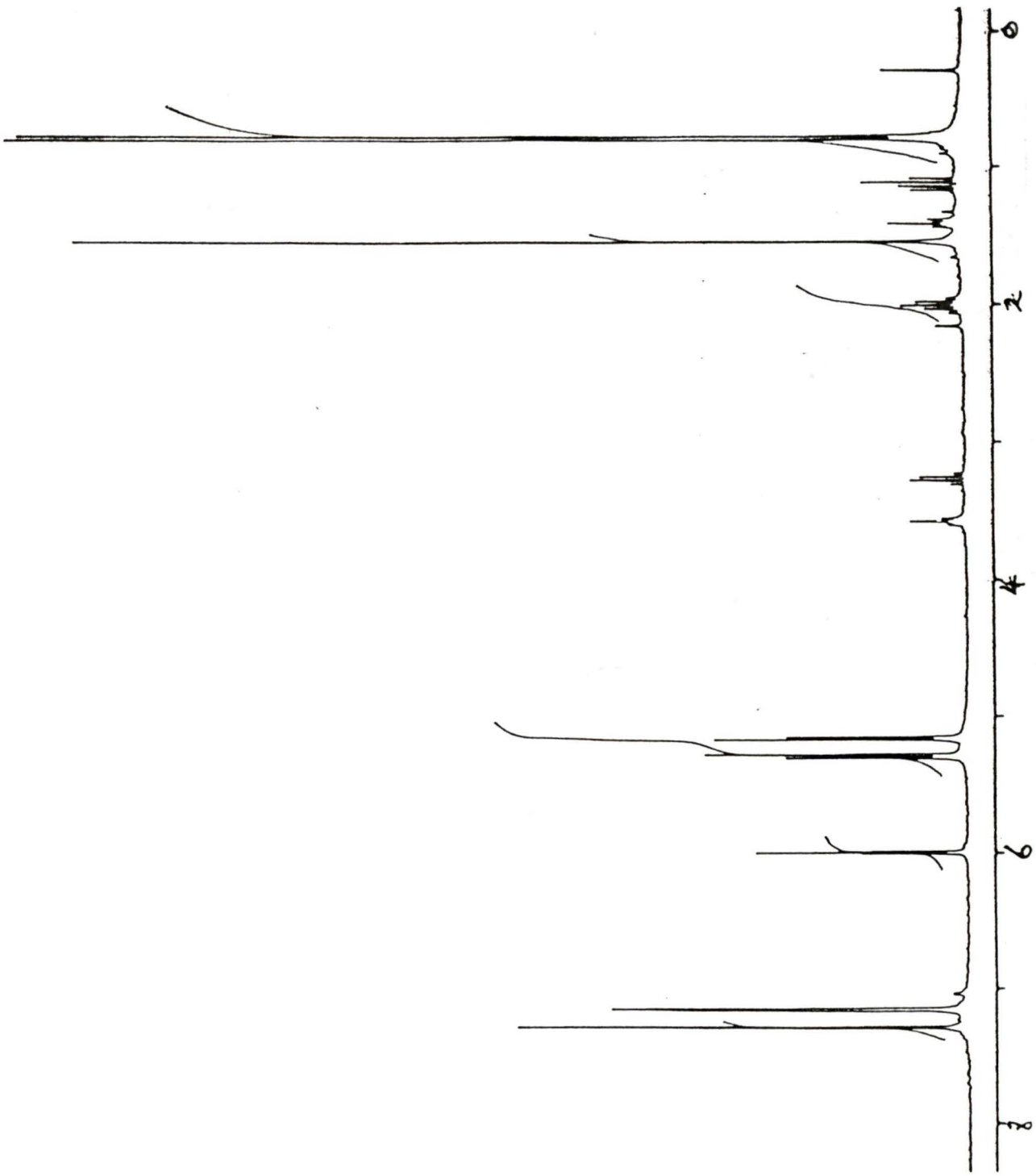

These chemical shift changes range from 0.1 ppm for the AB splitting pattern of the four coordinated arene protons, to 0.8 ppm for the H(3) and H(5) pyrazolyl protons.

In compound XXVI a metal-metal bond is implied between the two ruthenium centres so as to maintain an 18 electron count at these centres. The $^{1}H$ NMR data for compounds XXIV and XXVI are compared in Table 2.21. The chemical shift data for the pyrazolyl protons in compound XXVI compare favorably (and are similar) to those in the tricarbonyl analogue $[(CO)_3Ru(\mu\text{-}Pz)]_2$[34] where they are in a similar electronic environment.

A number of oxidative addition reactions were attempted on compound XXVI, the results of which are summarised in Table 2.22.

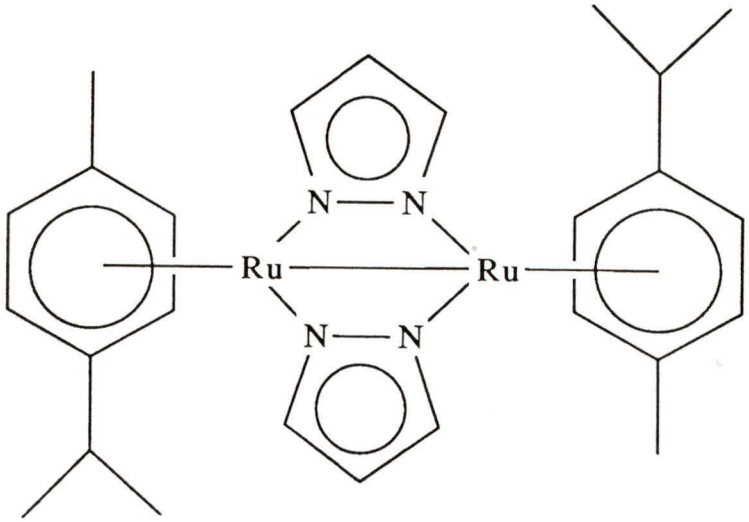


Compound XXVI.

Table 2.21: The $^{1}H$ NMR data[a] for compounds XXVI and XXIV.

| Protons. | Compound XXVI. Chemical shift/ppm. | Compound XXIV. Chemical shift/ppm. |
|---|---|---|
| H(3,5) | 7.24(d) | 8.05(d) |
| H(4) | 5.76(t) | 6.27(t) |
| H(7,8,10,11) | 5.69,5.77,5.52,5.49 | 5.80,5.77,5.65,5.62 |
| H(12) | -- | 2.99(qn) |
| $CH_3$(13,14) | 0.81(d) | 1.24(d) |
| $CH_3$(15) | 1.64(s) | 2.34(s) |

The multiplicity of the signals are denoted in brackets.

[a]Spectra recorded in $CD_3NO_2$ at ambient temperature.

Table 2.22: Reactions of compound XXVI.

XXVI + $I_2$ -----> $[(\eta^6\text{-}C_{10}H_{14})Ru_2(\mu\text{-}pz)_2\mu\text{-}I]I$

XXVI + MeI -----> $[(\eta^6\text{-}C_{10}H_{14})Ru_2(\mu\text{-}pz)_2\mu\text{-}I]I$

XXVI + $I_2CHCH_3$ -----> No reaction.

XXVI + $NOBF_4$ -----> Decomposition.

XXVI + PhCCPh -----> No reaction.

XXVI + DMAD -----> Unseparable mixture.

Addition of iodine or methyl iodide to compound XXVI results in the formation of a yellow/brown solid (compound XXVII), the elemental analysis data for which are consistent with a ruthenium to iodine ratio of 1:1. The $^{1}H$ NMR spectrum of this compound is identical to compound XXIV which contains one bridging chloride ion and a chloride counter anion, strongly suggesting that compound XXVII is the iodo analogue of compound XXIV. The $^{1}H$ NMR spectrum of compound XXVII is shown in Figure 2.25, and the $^{1}H$ NMR data of compounds XXVII and XXIV are compared in Table 2.23.

The remaining reactions have been unsuccessful in the isolation of pure compounds. No reaction occurs between compound XXVI and either 1,1-diiodoethane or diphenylacetylene. Decomposition ensues on treatment with nitrosium tetrafloroborate, although an initial green colour (characteristic of ruthenium III species) is observed suggesting that a two electron oxidation occurs at one of the ruthenium centres prior to decomposition. Treatment of compound XXVI with an excess of the electron deficient alkyne dimethyl acetylenedicarboxylate results in the formation of a brown solid, shown to be a mixture of compounds which have not been isolated.

Thus a new class of ruthenium (II) pyrazolyl bridged species, of general formula $[(\eta^{6}\text{-arene})Ru_{2}(\mu\text{-pz})_{2}\mu\text{-Cl}]Cl$ (arene = $C_{6}H_{6}$ (XXII), $C_{10}H_{14}$ (XXIV)) has been formed. For

Fig. 2.25: The $^{1}H$ NMR spectrum of compound XXVII.

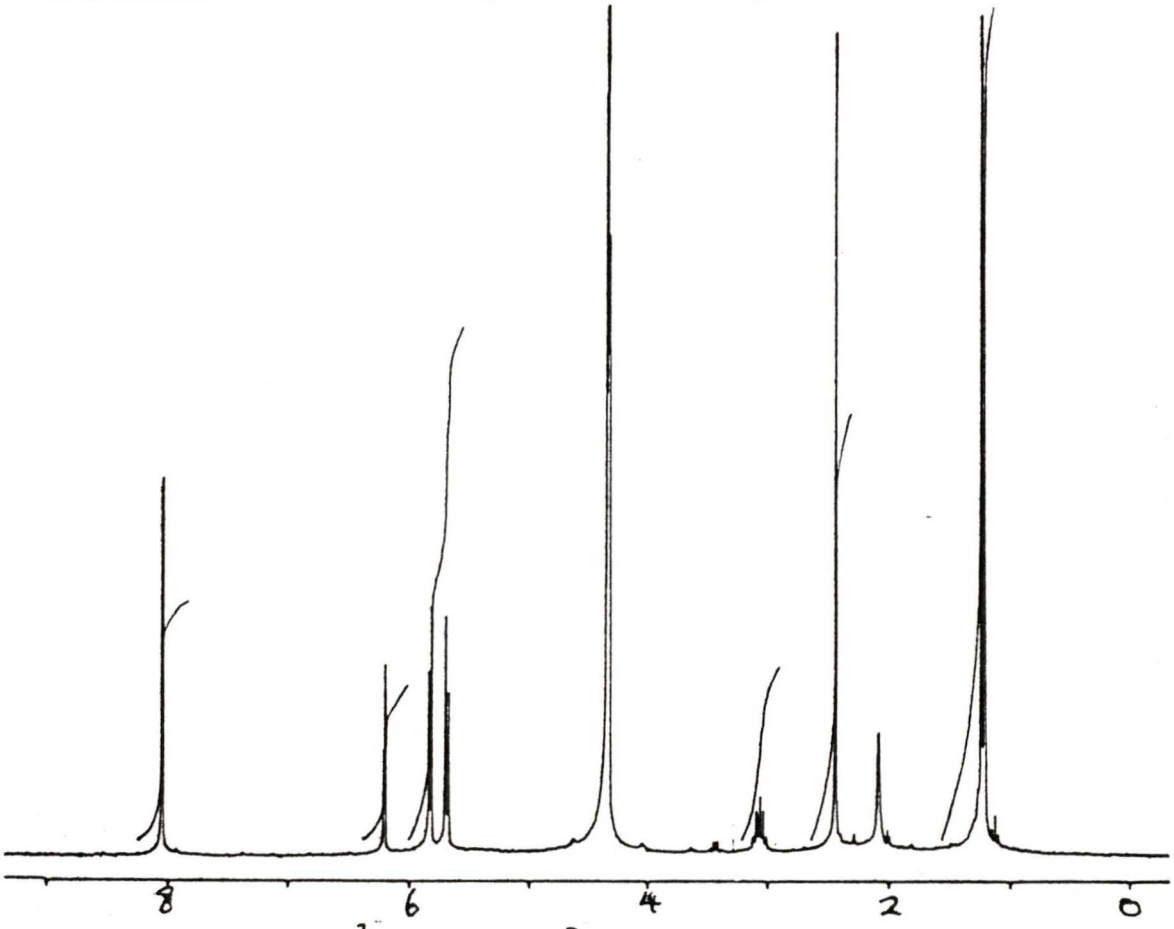


Table 2.23: The $^{1}H$ NMR data[a] for compounds XXVII and XXIV.

| Protons. | Compound XXVII. Chemical shift/ppm. | Compound XXIV. Chemical shift/ppm. |
|---|---|---|
| H(3,5) | 8.05(d) | 8.05(d) |
| H(4) | 6.18(t) | 6.27(t) |
| H(7,8,10,11) | 5.84,5.81,5.69,5.66 | 5.80,5.77,5.65,5.62 |
| H(12) | -- | 2.99(qn) |
| $CH_3$(13,14) | 1.21(d) | 1.24(d) |
| $CH_3$(15) | 2.43(s) | 2.34(s) |

The multiplicity of the signals are denoted in brackets.

[a]Spectra recorded in $CD_3NO_2$ at ambient temperature.

the case where arene = $C_{14}H_{14}$, synthesis has not been achieved. Compound XXIV has been reduced to the Ru(I)-Ru(I) pyrazolyl bridged species $[(\eta^6\text{-}C_{10}H_{14})Ru(\mu\text{-}pz)]_2$ (XXVI), which is highly air and moisture sensitive: this is the first example of a ruthenium(I) arene. On going from Ru(II) to Ru(I), the valence shell configuration of the ruthenium centre changes from $d^6$ to $d^7$ as an electron is placed in the $e^*_g$ orbitals (in an octahedral species). In the binuclear species, one electron from each metal contributes to formation of a metal-metal bond, preserving diamagnetism of the bimetallic molecule. The cleavage of this bond by oxidising substrates in a two centre addition reaction should be favored; this would regenerate a $d^6$-$d^6$ configuration and the corresponding crystal field stabilisation energy. A number of oxidative addition reactions have been attempted with compound XXVI, suggesting it is indeed reactive, although characterisation of some of the reaction products has not yet been achieved. Further investigation of the chemistry of compound XXVI is anticipated.

# PART 3

## EXPERIMENTAL

All experimental manipulations were carried out under an atmosphere of nitrogen using standard Schlenk techniques. Chemicals used were supplied by Aldrich Chemicals company and used as received unless otherwise stated or synthesised by methods in the literature.[13,65] Solvents were dried over type 4A molecular sieves and freshly distilled (with the exception of DMSO) prior to use. Dichloromethane was distilled over calcium dihydride. Hexanes were distilled over lithium aluminum hydride. Methanol was distilled over magnesium sulphate. Anhydrous diethyl ether, benzene and tetrahydrofuran were distilled over sodium/benzophenone. Reagent grade DMSO was used without further purification.

Table 3.1 lists the spectrometers used in the course of this research. Gas chromatography data were acquired on a Varian model 3700 gas chromatograph. Elemental Analyses were performed by Canadian Microanalytical Services Ltd., New Westminster. For the kinetic runs, all reagents were thermostatted in a water bath at 20°C prior to mixing and insertion into the spectrometer with the temperature control unit also set at 20°C. $^{1}H$ and $^{13}C$ NMR spectra were measured relative to tetramethylsilane, $^{31}P$ NMR

Table 3.1: Spectrometers used in research.

| Technique | Spectrometer |
|---|---|
| Infra-red | Perkin-Elmer 283. |
| UV/visible | Perkin-Elmer Lambda 4B with Haake D8 temperature control unit. |
| $^{1}H$ NMR | Bruker WM250 (250 MHz) |
| | Perkin-Elmer R32 (90 MHz) |
| | Perkin-Elmer R12B (60 MHz) |
| $^{13}C$ NMR | Bruker WM250 (62.8 MHz) |
| $^{31}P$ NMR | Bruker WM250 (24.3 MHz) |
| Mass | Finnigan 3300 |
| | VG 70E |

spectra relative to 85% phosphoric acid.
$[(\eta^6\text{-}C_6H_6)Ru(\mu\text{-}Cl)Cl]_2$ and $[(\eta^6\text{-}C_{10}H_{14})Ru(\mu\text{-}Cl)Cl]_2$ were synthesised using preparations in the literature.[13,65]

Note: with regard to the molar quantities quoted for the ruthenium arene chloro bridged dimers the values shown are calculated with respect to the mononuclear fragment RuCl(u-Cl)arene.

**Preparation of $(C_{14}H_{16})Fe(CO)_3$ (I) and $(C_{14}H_{16})Fe_2(CO)_6$ (II)**

$Fe(CO)_5$ (1g, 5 mmol) and HHA (0.92g, 5 mmol) were combined in benzene (35 mL) in a quartz tube. The solution was then photolysed for 40 hours. The resulting suspension was then stripped of solvent under vacuum. The resulting orange/brown solid was extracted with methanol (3 x 20 mL) giving an orange solution which was separated from a yellow/brown methanol insoluble residue. The orange solution was then stripped of solvent under vacuum to give an orange oil (compound I, 1 g, 3.1 mmol). Yield 60%. Soxhlet extraction with $CH_2Cl_2$ of the methanol insoluble residue gave a yellow solution , which upon cooling yielded yellow crystals (compound II, 0.35g, 0.75 mmol). Yield 30%.

Analysis for $C_{17}H_{16}FeO_3$.

Calculated: C, 62.97; H, 4.97.

Found: C, 62.64; H, 4.89.

Analysis for $C_{20}H_{16}Fe_2O_6$.

Calculated: C, 51.77; H, 3.45.

Found: C, 51.59; H, 3.45.

Note: A single crystal X-ray diffraction study showed these yellow crystals to be a trans di-iron species. Subsequent preparations however, have obtained a yellow powder, following the soxhlet extraction procedure with $CH_2Cl_2$, which is composed of the trans di-iron isomer and

a cis di-iron isomer (compound III). Fractional crystallisation and thin layer chromatography have been unsuccessful in the separation of these species.
Elemental Analysis of mixture: C, 51.82; H, 3.55.

**Treatment of compound II with $PPh_3$.**

Compound II (50 mg, 0.11 mmol) and $PPh_3$ (29 mg, 0.11 mmol) were combined in $CH_2Cl_2$ (10 mL) and the yellow solution was stirred for 24 hours with no observable change occurring. Work up and analysis by IR spectroscopy indicated that no reaction had taken place.
Note: Similar results were obtained when $Me_3NO$ (10 mg, 0.11 mmol) was added to an identical mixture employing the same parameters.

**Treatment of compound II with $I_2$.**

$I_2$ (14 mg, 0.11 mmol) dissolved in benzene (5 ml) was added to a suspension of compound II (50 mg, 0.11 mmol) in benzene (10 mL) with stirring for 10 min, which resulted in decomposition.

**Reaction of compound II with $Ph_3CBF_4$.**

Compound II (50 mg, 0.11 mmol) was dissolved in $CH_2Cl_2$ (15 mL). $Ph_3CBF_4$ (36 mg, 0.11 mmol), dissolved in $CH_2Cl_2$ (10 mL), was added dropwise over two hours to this stirred pale yellow solution. The solution was stirred

for an additional two hours which resulted in the formation of an orange solution. This solution was reduced to 1/10 th of its initial volume and then precipitated with diethyl ether to give an orange solid (compound IV).

**Reaction of the mixture of compound II and compound III with $Ph_3CBF_4/Na_2CO_3/CH_3OH$.**

A mixture of compounds II and III (100 mg, 0.22 mmol) was dissolved in dichloromethane (20 mL). $Ph_3CBF_4$ (72 mg, 0.22 mmol), dissolved in $CH_2Cl_2$ (10 mL) was added dropwise over two hours to this stirred pale yellow solution. This solution was stirred for an additional two hours resulting in the formation of an orange solution which was stripped of solvent under vacuum to give an orange solid which on dissolution in methanol (10 mL) gave a purple solution. Addition of an excess (ca 50 fold) of $Na_2CO_3$ to this stirred solution resulted in the immediate formation of a yellow solution which was filtered and then stripped of solvent under vacuum to give a yellow solid. Analysis by $^1H$ NMR spectroscopy of this solid showed it to be a mixture of several methoxy containing compounds. Isolation of these compounds by thin layer chromatography was unsuccessful.

**Reaction of $Ru_3(CO)_{12}$ with HHA.**

$Ru_3(CO)_{12}$ (100 mg, 0.16 mmol) and an excess of HHA (230 mg, 1.26 mmol) were dissolved in cyclohexane (100 mL) and the resulting orange solution was refluxed for 48 hours. The resultant pale orange solution was separated from a small amount of decomposition product, and stripped of solvent under vacuum to yield a brown oil. Analysis by $^1H$ NMR spectroscopy of this oil indicated more than one species was present. Work up and chromatography were unsuccessful in the isolation of the components of this mixture. Sublimation under reduced pressure led to the isolation of a white solid which was shown (by $^{13}C$ NMR spectroscopy and gas chromatography/mass spectroscopy) to consist of five major organic compounds (compounds V to IX). Sublimation resulted in the decomposition of the brown oil.
Note: Identical results were obtained when a 10 fold and 30 fold excess of HHA were employed. When $Ru_3(CO)_{12}$ was substituted by the black decomposition product and otherwise identical reaction parameters were employed, no reaction with HHA was observed.

**Preparation of $[(\eta^6\text{-}C_{14}H_{14})RuCl(\mu\text{-}Cl)]_2$ (X).**

$RuCl_3 \cdot 3H_2O$ (0.5 g, 1.9 mmol) and HHA (0.7g, 3.8 mmol) were combined in ethanol (50 mL). The solution was stirred under reflux for 18 hours. Filtration of the warm

reaction mixture followed by washing with diethyl ether (3 x 20 mL) led to the isolation of a yellow/brown solid (0.54 g, 1.5 mmol). Yield 80%.

Analysis for $C_{14}H_{14}Cl_2Ru$.

Calculated: C, 47.47; H, 3.98; Cl, 20.02.

Found: C, 45.89; H, 3.80; Cl, 20.42.

**Preparation of [($\eta^6$-$C_{14}H_{14}$)$RuCl_2$DMSO] (XI).**

Compound X (100 mg, 0.28 mmol) was dissolved in a minimum volume of dimethylsulphoxide (5 mL). The deep red solution was then precipitated with diethyl ether (20 mL). The resulting red precipitate was further washed with diethyl ether (3 x 20 mL) and then air dried to give a red solid (80 mg, 0.19 mmol). Yield 65%.

Analysis for $C_{16}H_{20}Cl_2ORuS$.

Calculated: C, 44.42; H, 4.67; Cl, 16.41.

Found: C, 44.12; H, 4.58; Cl, 16.54.

**Treatment of compound X with triphenylphosphine.**

Compound X (80 mg, 0.22 mmol) and $PPh_3$ (59 mg, 0.22 mool) were combined in THF (30 mL) and the resulting brown suspension was stirred for 10 hours, in which time there was no observable change. Work up of the brown suspension followed by analysis by $^1H$ NMR spectroscopy indicated that no reaction had occurred.

**Synthesis of $[(\eta^6\text{-}C_{14}H_{14})RuCl_2(P(OCH_3)_3)]$**

Compound X (50 mg, 0.14 mmol) was suspended in THF (10 mL), to which was added a solution of $P(OCH_3)_3$ (17 mg, 0.14 mmol) in THF (0.34 mL). The suspension was refluxed for 20 hours. On cooling, a red solution was isolated from unreacted starting material by filtration. Slow diffusion of hexane (20 mL) into the solution led to the formation of a brown solid, assumed to be a mixture of $[(\eta^6\text{-}C_{14}H_{14})RuCl_2(P(OCH_3)_3]$ and the bis- and tri-phosphite derivatives.

**Preparation of $[(\eta^6\text{-}C_{14}H_{14})RuCl_2(P(OC_2H_5)_3)]$ (XII).**

Compound XI (80 mg, 0.18 mmol) was dissolved in $CH_2Cl_2$ (10 mL), to which was added a solution of $P(OEt)_3$ (31 mg, 0.18 mmol) in $CH_2Cl_2$ (1 mL). The orange solution was stirred for 5 minutes and the resulting deep orange solution was reduced to one fifth initial volume and precipitated with hexane (15 mL) to give a salmon pink solid (86 mg, 0.16 mmol). Yield 90%.

Analysis for $C_{20}H_{29}Cl_2O_3PRu$.

Calculated: C, 46.13; H, 5.61.

Found: C, 45.65; H, 5.52.

**Preparation of $[(\eta^6\text{-}C_{14}H_{14})RuCl_2(PPh_3)]$ (XIII).**

Compound XI (80 mg, 0.18 mmol) was dissolved in $CH_2Cl_2$ (10 mL), to which was added $PPh_3$ (96 mg, 0.36

mmol). The orange solution was stirred for 30 minutes and the resulting deep orange solution was reduced to one fifth initial volume and precipitated with hexane (15 mL) to give a pink salmon solid (92 mg, 0.15 mmol). Yield 85%. The solid was recrystallised from $CHCl_3$ and hexane.

| Analysis for $C_{32}H_{29}Cl_2PRu$, | for $C_{32}H_{29}Cl_2PRu \cdot 1CHCl_3$. |
|---|---|
| Calculated: C, 62.33; H, 4.74. | C, 53.80; H, 4.10. |
| Found: C, 53.75; H, 4.14. | C, 53.75; H, 4.14. |

**Preparation of $[(\eta^6\text{-}C_{14}H_{14})RuCl_2(PPh_2Me)]$ (XIV).**

Compound XI (80 mg, 0.18 mmol) was dissolved in $CH_2Cl_2$ (10 mL), to which was added an excess of $PPh_2Me$ (ca. two fold). The orange solution was stirred for 30 minutes and the resulting yellow solution was stripped of solvent under vacuum. The resulting yellow solid was washed with hexane (15 mL) for 12 hours to give a sand coloured solid (78 mg, 0.14 mmol). Yield 78%. The solid was recrystallised from $CHCl_3$ and hexane.

| Analysis for $C_{27}H_{27}Cl_2PRu$, | for $C_{27}H_{27}Cl_2PRu \cdot 1CHCl_3$. |
|---|---|
| Calculated: C, 58.47; H, 4.90. | C, 49.89; H, 4.18. |
| Found: C, 50.89; H, 4.35. | C, 50.89; H, 4.35. |

**Preparation of $[(\eta^6\text{-}C_{14}H_{14})RuCl_2(PCy_3)]$ (XV).**

Compound XI (80 mg, 0.18 mmol) was dissolved in $CH_2Cl_2$ (15 mL), to which was added slightly greater than one equivalent of $PCy_3$ per ruthenium centre (65 mg, 0.23

mmol). The orange solution was stirred for 10 minutes and the resulting red solution was stripped of solvent under vacuum. The resulting orange solid was dissolved in $CHCl_3$ (2 mL), filtered and precipitated with hexane (10 mL) to give a red solid (95 mg, 0.15 mmol). Yield 85%.

Analysis for $C_{32}H_{47}Cl_2PRu$.

Calculated: C, 60.54; H, 7.47.

Found: C, 58.33; H, 7.11.

**Attempted preparation of $[(\eta^6\text{-}C_{14}H_{14})RuCl_2(pzH)]$.**

Compound X and one equivalent of pzH per ruthenium centre were combined in $CH_2Cl_2$ and stirred for 15 hours. Unreacted starting material was separated from the resulting yellow solution by filtration. The solution was then stripped of solvent under vacuum. Analysis by $^1H$ NMR spectroscopy showed that only the bis pyrazole mononuclear derivative (compound XVI) had been formed.

**Preparation of $[(\eta^6\text{-}C_{14}H_{14})RuCl(pzH)_2]Cl$ (XVI).**

Compound X (100 mg, 0.28 mmol) and pzH (40 mg, 0.56 mmol) were combined in $CH_2Cl_2$ (40 mL) and stirred for 20 hours. Unreacted starting material was separated from the resulting yellow solution by filtration. This solution was reduced to one tenth of its initial volume and then precipitated with hexane (20 mL) to give a yellow solid (110 mg, 0.22 mmol). Yield 80%.

Analysis for $C_{20}H_{22}N_4Cl_2Ru$.

Calculated: C, 48.98; H, 4.33; N, 11.43.

Found: C, 48.81; H, 4.44; N, 11.50.

**Attempted preparation of $[(\eta^6\text{-}C_{14}H_{14})RuCl(\mu\text{-}pz)]_2$.**

Method A.

Compound X and one equivalent of pzH per ruthenium centre were combined in $CH_2Cl_2$. Addition of triethylamine to the stirred suspension resulted in decomposition.

Method B.

Compound XI and one equivalent of pzH per ruthenium centre were combined in $CH_2Cl_2$ . Addition of triethylamine to the stirred orange solution resulted in decomposition. Note: With regard to the above attempted preparation, addition of triethylamine before addition of pzH did not alter the outcome of the reaction.

**Preparation of $[(\eta^6\text{-}C_{14}H_{14})RuCl_2(Me_2pzH)]$ (XVII).**

Method A.

Compound X (50 mg, 0.14 mmol) was suspended and stirred in $CH_2Cl_2$ (10 mL), to which was added a solution of $Me_2pzH$ (14 mg, 0.14 mmol) in $CH_2Cl_2$ (10 mL) over a time span of 2 hours. The resulting suspension was stirred for 14 hours. Unreacted starting material was separated from the resulting orange solution by

filtration. This solution was reduced to one fifth of its initial volume and then precipitated with hexane (20 mL) to give an orange solid (30 mg, 0.07 mmol). Yield 50%.

Method B.

Compound XI (86 mg, 0.2 mmol) and $Me_2pzH$ (20 mg, 0.2 mmol) were combined in $CH_2Cl_2$ (20 mL). The orange solution was stirred for 2 hours, then reduced to one fifth of its initial volume and precipitated with hexane (20 mL) to give an orange solid (70 mg, 0.16 mmol). Yield 80%.

Note: The use of $Me_2pzH$ in stoichiometric amounts varying from 1 (as above) to 20 equivalents per ruthenium centre did not alter the outcome of the reaction.

Analysis for $C_{19}H_{22}N_2Cl_2Ru$.

Calculated: C, 50.67; H, 4.89; N, 6.22.

Found: C, 50.42; H, 4.85; N, 6.21.

**Attempted synthesis of $[(\eta^6\text{-}C_{14}H_{14})RuCl(\mu\text{-}Me_2Pz)]_2$.**

Compound XVII and triethylamine were combined in $CH_2Cl_2$. Stirring the orange solution resulted in decomposition.

**Synthesis of $[(\eta^6\text{-}C_6H_6)RuCl_2(pzH)]$ (XVIII).**

$[(\eta^6\text{-}C_6H_6)Ru(\mu\text{-}Cl)Cl]_2$ (100 mg, 0.40 mmol) and pzH (29 mg, 0.42 mmol) were combined in $CH_2Cl_2$ (20 mL). The resulting brown suspension was stirred for 18 hours.

Unreacted starting material was separated from the resulting orange solution by filtration. This solution was reduced to one tenth of its initial volume and precipitated with hexane to give an orange solid. Analysis by $^{1}$NMR spectroscopy of this solid showed it to be a mixture of the desired mono pyrazole mononuclear adduct (compound XVIII) and the bis pyrazole mononuclear cation (compound XIX). Separation of these compounds by fractional crystallisation or by thin layer chromatography was not successful.

Note: Identical results were obtained when the reaction was carried out in methanol as solvent.

**Preparation of $[(\eta^6\text{-}C_6H_6)RuCl(pzH)_2]Cl$ (XIX).**

$[(\eta^6\text{-}C_6H_6)Ru(\mu\text{-}Cl)Cl]_2$ (100 mg, 0.40 mmol) and pzH (58 mg, 0.84 mmol) were combined in $CH_2Cl_2$ (20 mL) and the brown suspension was stirred for 6 hours. The resulting orange solution was filtered, reduced to one tenth of its initial volume and precipitated with hexane to give a yellow solid (105 mg, 0.27 mmol). Yield 67% .

Analysis for $C_{12}H_{14}N_4Cl_2Ru$.

Calculated: C, 37.32; H, 3.65; N, 14.50; Cl, 18.36.

Found: C, 37.15; H, 3.68; N, 14.74; Cl, 18.38.

**Synthesis of $[(\eta^6\text{-}C_{10}H_{14})RuCl_2(pzH)]$ (XX).**

$[(\eta^6\text{-}C_{10}H_{14})Ru(\mu\text{-}Cl)Cl]_2$ (100 mg, 0.32 mmol) and pzH (29 mg, 0.42 mmol) were combined in $CH_2Cl_2$ (15 mL). This red solution was stirred for 24 hours and the resulting orange solution was reduced to one tenth of its initial volume and precipitated with hexane to give an orange solid. Analysis by $^1H$ NMR spectroscopy of this solid showed it to be a mixture of the desired mono pyrazole mononuclear adduct (compound XX) and the bis pyrazole mononuclear cation (compound XXI). Attempted separation of these two compounds by fractional crystallisation or by thin layer chromatography was not successful.

Note: When one equivalent of pzH was added per ruthenium centre, a mixture of compounds XI and XII along with unreacted chloro bridged dimer was obtained.

**Preparation of $[(\eta^6\text{-}C_{10}H_{14})RuCl(pzH)_2]Cl$ (XXI).**

$[(\eta^6\text{-}C_{10}H_{14})Ru(\mu\text{-}Cl)Cl]_2$ (100 mg, 0.32 mmol) and pzH (44 mg, 0.64 mmol) were combined in $CH_2Cl_2$ (15 mL). This red solution was stirred for 24 hours and the resulting orange solution was reduced to one tenth of its initial volume and precipitated with hexane to give an orange solid (128 mg, 0.29 mmol). Yield 91%.

Analysis for $C_{16}H_{22}N_4Cl_2Ru$.

Calculated: C, 43.44; H, 5.02.

Found: C, 43.51; H, 5.07.

**Preparation of $[(\eta^6\text{-}C_6H_6)_2Ru_2\mu\text{-}Cl(\mu\text{-}pz)_2]Cl$ (XXII).**

$[(\eta^6\text{-}C_6H_6)_2Ru(\mu\text{-}Cl)Cl]_2$ (150 mg, 0.6 mmol), pzH (45 mg, 0.66 mmol) and triethylamine (5 drops, excess) were combined in methanol (30 mL). The suspension was stirred for 15 hours. The resulting solution was then filtered and taken down to dryness. The resulting brown solid was loaded onto an alumina column (1 $cm^2$ x 10 cm) and eluted with a solvent system of increasing polarity (commencing with a solvent system of 1:20 MeOH:$CH_2Cl_2$ and concluding with pure methanol). The red solution obtained using a 1:10 solvent ratio was reduced in volume and layered with hexane to yield red/brown crystals (60 mg, 0.107 mmol). Yield 35%.

Analysis for $C_{18}H_{18}N_4Cl_2Ru_2$.

Calculated: C, 38.37; H, 3.22; N, 9.94.

Found: C, 38.20; H, 3.28; N, 9.68.

**Preparation of $[(\eta^6\text{-}C_6H_6)_2Ru_2\mu\text{-}Cl(\mu\text{-}pz)_2]PF_6$ (XXIII).**

Compound XXII (40 mg, 0.071 mmol) was dissolved in $H_2O$ (5 mL), to which was added an excess of $NH_4PF_6$ (ca. 5 fold). Extraction of the resulting yellow precipitate into $CH_2Cl_2$ (10 mL) was unsuccessful. Therefore, the yellow precipitate was isolated by filtration, washed with $H_2O$ (3 x 10 mL) and then dissolved in MeOH (10 mL). The yellow solution was dried over anhydrous $MgSO_4$ (1.0 g). The suspension was filtered, and the yellow solution

obtained was stripped of solvent under vacuum to give a yellow solid (35 mg, 0.052 mmol). Yield 73%.

Analysis for $C_{18}H_{18}N_4ClF_6PRu_2$.

Calculated: C, 32.13; H, 2.70; N, 8.32.

Found: C, 32.09; H, 2.85; N, 8.26.

**Preparation of $[(\eta^6\text{-}C_{10}H_{14})_2Ru_2\mu\text{-}Cl(\mu\text{-}pz)_2]Cl$ (XXIV).**

$[(\eta^6\text{-}C_{10}H_{14})Ru(\mu\text{-}Cl)Cl]_2$ (300 mg, 0.96 mmol) and triethylamine (15 drops, excess) were combined in $CH_2Cl_2$ (30 mL) to which was added dropwise a solution of pzH (72 mg, 1.05 mmol) in $CH_2Cl_2$ (10 mL) over a time span of 1 hour. The red solution was stirred for 48 hours and then filtered and taken down to dryness. The resulting red/brown solid was loaded onto an alumina column (1 $cm^2$ x 10 cm) and eluted with a solvent system of increasing polarity (commencing with a solvent system of 1:20 MeOH:THF and concluding with pure methanol). The red solution obtained using a 1:10 solvent ratio was collected and taken down to dryness to give a red solid (260 mg, 0.385 mmol). Yield 80%.

Analysis for $C_{26}H_{34}N_4Cl_2Ru_2$.

Calculated: C, 46.22; H, 5.04; N, 8.30.

Found: C, 43.91; H, 5.31; N, 7.91.

**Preparation of $[\eta^6\text{-}C_{10}H_{14})_2Ru_2\mu\text{-}Cl(\mu\text{-}pz)_2]PF_6$ (XXV).**

Compound XXIV (20 mg, 0.030 mmol) was dissolved in $H_2O$ (5 mL), to which was added an excess of $NH_4PF_6$ (ca 5 fold). The resulting yellow precipitate was extracted into $CH_2Cl_2$ (3 x 15 mL) and the combined extracts were dried over anhydrous $MgSO_4$ (1.0 g). The suspension was filtered and stripped of solvent under vacuum to give a yellow solid (15 mg, 0.020 mmol). Yield 65%.

Analysis for $C_{26}H_{34}N_4ClF_6PRu_2$.

Calculated: C, 41.80; H, 4.55; N, 7.50.

Found: C, 38.95; H, 4.32; N, 6.82.

**Preparation of $[(\eta^6\text{-}C_{10}H_{14})Ru(\mu\text{-}pz)]_2$ (XXVI).**

Method A.

Freshly cut sodium metal (10 mg, 0.44 mmol) and naphthalene (23 mg, 0.15 mmol) were combined in THF (10 mL) and stirred for 10 min. The resultant deep green solution was added to a suspension of compound XXIV (100 mg, 0.15 mmol) in THF (15 mL) and stirred for 30 min, the resultant deep orange solution was then filtered from excess sodium metal. Work up was unsuccessful in the isolation of the orange species, and sublimation under reduced pressure resulted in decomposition.

Method B.

Freshly cut sodium metal (320 mg, excess) and mercury (13.68 g, excess) were combined in a Schlenk tube and an

amalgam was formed by pressing the sodium metal against the side of the tube. To this amalgam, compound XXIV (300 mg, 0.45 mmol) and THF (15 mL) were added and the resulting orange suspension was stirred for 18 hours. The resulting deep orange solution was filtered through oven dried celite and stripped of solvent under vacuum. Diethyl ether (10 mL) was added and the orange solution was separated from decomposition products, then stripped of solvent under vacuum to give a deep orange solid (190 mg, 0.31 mmol). Yield 68%.

Method C.

An excess (ca. 100 fold) of zinc powder and finely cut copper metal were combined in a 1:1 molar ratio. To this mixture, compound XXIV (200 mg, 0.30 mmol) and THF (20 mL) were added and the resulting orange suspension was stirred for 72 hours. The resulting deep orange solution was filtered through oven dried celite and stripped of solvent under vacuum. Diethyl ether (10 mL) was added and the orange solution was separated from decomposition products, then stripped of solvent under vacuum to give a deep orange solid (75 mg, 0.12 mmol). Yield 40%.

Analysis for $C_{26}H_{34}N_4Ru_2$.

Calculated: C, 51.64; H, 5.67; N, 9.26.

Found: C, 50.55; H, 5.75; N, 8.64.

**Preparation of $[(\eta^6\text{-}C_{10}H_{14})Ru_2(\mu\text{-}pz)_2\mu\text{-}I]I$ (XXVII).**

Method A.

A solution of iodine in diethyl ether was added dropwise to compound XXVI (50 mg, 0.08 mmol) dissolved in diethyl ether (5 mL) until the orange solution became colourless and no further yellow/brown solid precipitated. This solution was then removed and the precpitate was washed with diethyl ether (2 x 10 mL) and then dried to give a yellow/brown solid (60 mg, 0.07 mmol). Yield 90%.

Method B.

Compound XXVI (50 mg, 0.08 mmol) was dissolved in an excess of methyl iodide (1 mL) and the resulting orange solution was stirred for 18 hours. The resultant yellow/brown solid was separated from the remaining solvent and washed with diethyl ether (2 x 10 mL) and dried to give a yellow/brown solid (50 mg, 0.06 mmol). Yield 70%.

Analysis for $C_{26}H_{34}N_4I_2Ru_2$.

Calculated: C, 36.36; H, 3.96; N, 6.53.

Found: C, 36.00; H, 3.98; N, 6.81.

**Treatment of compound XXVI with 1,1-diiodoethane.**

Compound XXVI (20 mg, 0.03 mmol) was dissolved in an excess of $I_2CHCH_3$ (1 mL). The resulting orange solution was stirred for 48 hours, in which time there was no observable change. The continuation of these conditions

resulted in gradual decomposition.

**Reaction of compound XXVI with $NOBF_4$.**

Compound XXVI (75 mg, 0.12 mmol) was dissolved in diethyl ether (5 mL). $NOBF_4$ (12 mg, 0.10 mmol) was added to this stirred orange solution, which immediately turned green and then black in colour. Work up showed decomposition had occurred.

**Treatment of compound XXVI with PhCCPh.**

Compound XXVI (75 mg, 0.12 mmol) was dissolved in diethyl ether (5 mL). PhCCPh (43 mg, 0.24 mmol) was added to this stirred orange solution, which after 24 hours had not changed in appearance indicating no reaction had occurred. Prolonged stirring resulted in decomposition.

**Reaction of compound XXVI with DMAD.**

Compound XXVI (75 mg, 0.12 mmol) was dissolved in diethyl ether (5 mL). DMAD (0.2 mL, excess) was added to this stirred orange solution, and after 18 hours a brown precipitate had been formed. Analysis by $^1H$ NMR spectroscopy showed a number of species to be present Which have not been isolated.

**Crystallographic Parameters for compound II.**

| | |
|---|---|
| formula | $Fe_2O_6C_{20}H_{16}$ |
| fw | 471.96 |
| space group | $P2_1/c$ |
| systematic absences observed | 0k0, k = 2n + 1<br>00l, l = 2n + 1<br>h0l, l = 2n + 1 |
| a (A) | 11.0617(7) |
| b (A) | 12.239(2) |
| c (A) | 6.9928(5) |
| α (degrees) | 90 |
| β (degrees) | 105.82(6) |
| γ (degrees) | 90 |
| volume ($A^3$) | 910(1) |
| Z | 2 |
| calculated density (g $cm^{-3}$) | 1.71 |
| crystal size ($mm^3$) | 0.3 x 0.3 x 0.2 |
| F(000) | 472 |
| $\mu$ ($cm^{-1}$) | 16.14 |
| radiation (A) | 0.71069 |
| orientation reflections | 15 with 2θ > 30° |
| temperature (K) | 295 |
| scan method | w-2θ |
| data collected | +/-h, +k, +l;<br>1.0 < 2θ < 45° |
| total reflections collected | 1299 |
| unique data | 1252 |
| parameters refined | 142 |
| R | 0.0474 |
| $R_w$ | 0.0524 |
| largest shift/esd | 0.002 |

**Crystallographic Parameters for compound XI.**

| | |
|---|---|
| formula | $RuCl_2SOC_{16}H_{20}$ |
| fw | 432 |
| space group | $P2_1/n$ |
| systematic absences observed | h00, h = 2n + 1<br>0k0, k = 2n + 1<br>00l, l = 2n + 1<br>h0l, h + l = 2n + 1 |
| a (A) | 10.821(3) |
| b (A) | 12.472(4) |
| c (A) | 12.738(4) |
| α (degrees) | 90 |
| β (degrees) | 107.63(7) |
| γ (degrees) | 90 |
| volume ($A^3$) | 1638(2) |
| Z | 4 |
| calculated density ($g\ cm^{-3}$) | 1.73 |
| crystal size ($mm^3$) | 0.4 x 0.3 x 0.2 |
| $F(000)_1$(e) | 864 |
| μ ($cm^{-1}$) | 12.76 |
| radiation (A) | 0.71069 |
| orientation reflections | 15 with 2θ > 30° |
| temperature (K) | 295 |
| scan method | w-2θ |
| data collected | +/-h, +k, +l;<br>1.0 < 2θ < 45° |
| total reflections collected | 1621 |
| unique data | 1318 |
| parameters refined | 96 |
| R | 0.0773 |
| $R_w$ | 0.0864 |
| largest shift/esd | 0.002 |

**Crystallographic Parameters for compound XXII.**

| | |
|---|---|
| formula | $Ru_2Cl_2N_4C_{18}H_{18}$ |
| fw | 563.41 |
| space group | $P2_1/n$ |
| systematic absences observed | h00, h = 2n + 1<br>0k0, k = 2n + 1<br>00l, l = 2n + 1<br>h0l, h + l = 2n + 1 |
| a (A) | 12.901(2) |
| b (A) | 12.111(2) |
| c (A) | 11.657(2) |
| α (degrees) | 90 |
| β (degrees) | 91.81(2) |
| γ (degrees) | 90 |
| volume ($A^3$) | 1820.5(4) |
| Z | 4 |
| calculated density ($g\ cm^{-3}$) | 2.06 |
| crystal size ($mm^3$) | 0.3 x 0.2 x 0.2 |
| $F(000)_1$(e) | 1036 |
| μ ($cm^{-1}$) | 16.44 |
| radiation (A) | 0.71069 |
| orientation reflections | 25 with 2θ > 30° |
| temperature (K) | 295 |
| scan method | w-2θ |
| data collected | +/-h, +k, +l;<br>1.0 < 2θ < 40° |
| total reflections collected | 1858 |
| unique data | 1688 |
| parameters refined | 170 |
| R | 0.0613 |
| $R_w$ | |
| largest shift/esd | 0.002 |

Mr. Ron Brost is acknowledged for obtaining the above crystallographic information.

## References


1. H. Zeiss, P.J. Wheatley and H.J.S. Winkler, "Benzenoid-Metal Complexes", Ronald Press Company, New York, (1966).
2. M.F. Semmelhack, J. Organomet. Chem. Libr. **1**, 361, (1976).
3. K. Ofele and E.O Fischer, Angew. Chem. **69**, 715, (1957).
4. B. Nicholls and M.C. Whiting, J. Chem. Soc. 551, (1959).
5. G. Jaouen, Ann. NY. Acad. Sci. **295**, 54, (1977).
6. M.F. Semmelhack, Ann. NY. Acad. Sci. **295**, 36, (1977).
7. V. Desorby and E.P. Kundig, Helv. Chim. Acta **64**, 1288, (1981).
8. R.G. Gastinger and K.J. Klabunde, Transition Met. Chem. **4**, 1, (1979).
9. G. Winkhaus and H. Singer, J. Organometal. Chem. **7**, 487, (1967).
10. R.A. Zelonka and M.C. Baird, J. Organometal. Chem. **35**, C43, (1972).
11. M.A. Bennett, G.B. Robertson and A.K. Smith, J. Organometal. Chem. **43**, C41, (1972).
12. M.A. Bennett and A.K. Smith, J. Chem. Soc. Dalton Trans. 233, (1974).
13. R.A. Zelonka and M.C. Baird, Can. J. Chem. **50**, 3063, (1972).
14. D.R. Robertson and T.A. Stephenson, J. Organometal. Chem. **116**, C29, (1976).
15. I. Ogata, R. Iwaka and Y. Ikeda, Tetrahedron Lett. 3011, (1970).

16. P.S. Hallman, B.R. McGarvey and G. Wilkinson, J. Chem. Soc. A 3143, (1968).

17. Rheilen, Gruhl, Hessling and Pfengle, Annalen **482**, 161, (1930).

18. B.F. Hallam and P.L. Pauson, J. Chem. Soc. 642, (1958).

19. G.F. Emerson, L. Watts and R. Pettit, J. Am. Chem. Soc. **87**, 131, (1965).

20. J.C. Barborak, L. Watts and R. Pettit, J. Am. Chem. Soc. **88**, 1328, (1966).

21. H. Alper, P.C. LePort and S. Wolfe, J. Am. Chem. Soc. **91**, 7553, (1969).

22. H. Alper and J.T. Edward, J. Organometal. Chem. **14**, 411, (1968).

23. A.J. Birch, P.E. Cross, J. Lewis, D.A. White and S.B. Wild, J. Chem. Soc. 332, (1968).

24. A.J. Birch and A.J. Pearson, Tetrahedron Lett. 2379, (1975).

25. B.F.G. Johnson, R.D. Johnson, P.L. Josty, J. Lewis and I.G. Williams, Nature **213**, 901, (1967).

26. O. Gambino, M. Valle, S. Aime and G.A. Vaglio, Inorg. Chim. Acta **8**, 71, (1974).

27. J.P. Collman and L.S. Hegadus, "Principles and Applications of Organotransition Metal Chemistry", University Science Books: Mill Valley, CA, (1980).

28. L. Vaska, Accts. Chem. Res. **1**, 335, (1968).

29. A.W. Coleman, D.T. Eadie, S.R. Stobart, M.J. Zaworotko

and J.L Attwood, J. Am. Chem. Soc. **104**, 922, (1982).

30. S.S.M. Ling, I.R. Jobe, L. Manojlovic-Muir, K.W. Muir and R.J. Puddephatt, Organometallics **4**, 1198, (1985).
31. H. Schmidbaur and R. Franke, Inorg. Chim. Acta **13**, 85, (1975).
32. K.A. Beveridge, G.W. Bushnell, K.R. Dixon, D.T. Eadie, S.R. Stobart, J.L Attwood and M. Zaworotko, J. Am. Chem. Soc. **104**, 920, (1982).
33. J.A. Bailey, S.L. Grundy and S.R. Stobart, Personal Communication.
34. J.A. Cabeza, C. Landazuri, L.A. Oro, A. Tripicchio and M. Tiripicchio-Camellini, J. Organometal. Chem. **322**, C16, (1987).
35. A.J. Pearson, Acc. Chem. Res. **13**, 463, (1980).
36. S. Trofimenko, Chem. Rev. **72**, 497, (1972).
37. S. Trofimenko, Prog. Inorg. Chem. **34**, 115, (1986).
38. G.W. Bushnell, K.R. Dixon, D.T. Eadie and S.R. Stobart, Inorg. Chem. **20**, 1545, (1981).
39 J.A. Bailey, S.L. Grundy and S.R. Stobart, Personal Communication.
40. D.L. Pavia, G.M. Lampman and G.S. Kriz,Jr, "Introduction to spectroscopy", Saunders College Publishing, (1979).
41. T. Luh, Coord. Chem. Rev. **60**, 255, (1984).
42. B.A. Sosinsky, S.A.R. Knox and F.G.A. Stone, J. Chem. Soc. Dalton Trans. 1633, (1975).
43. K. Hayamizu and O. Yamamoto, "$^{13}$C NMR Spectra of

Polycyclic Aromatic Compounds", Japan Industrial Technology Association, Tokyo, (1982).

44. R. Shaw, D.M. Golden and S.W. Benson, J. Phys. Chem. **81**, 1716, (1977).

45. R. Wilczynski, W.A. Fordyce and J. Halpern, J. Am. Chem. Soc. **105**, 2066, (1983).

46. M.A. Bennett, T. Huang and T.W. Turney, J. Chem. Soc. Chem. Comm. 312, (1979).

47. M. Castiglioni, L. Milone, D. Osella, G.A. Vaglio and M. Valle, Inorg. Chem. **15**, 394, (1976.).

48. J.E. Lyons, J. Catal. **28**, 500, (1973).

49. T.H. Whitesides and R.A. Budnik, J. Chem. Soc. Chem. Comm. 87, (1973).

50. O. Gambino, M. Valle, S. Aime and G.A. Vaglio, Inorg. Chim. Acta **8**, 71, (1974)

51. K. Kitching, C.J. Moore and D. Doddrell, Inorg. Chem. **9**, 541, (1970).

52. R.T. Boere and C.J. Willis, Inorg. Chem. **24**, 1059, (1985).

53. J.A. Davies, Adv. Inorg. Chem. Radiochem. **24**, 115, (1981).

54. A. Mercer and J. Trotter, J. Chem. Soc. Dalton Trans. 2480, (1975).

55. K. Eriks, C.B. Shoemaker and R. Thomas, Acta Crystallogr. **21**, 12, (1966).

56. C.E. Johnson and F.A. Bovey, J. Chem. Phys. **24**, 1012,

(1958).

57. A.M.Z. Slawin, D.J. Williams, J. Crosby, J.A. Ramsden and C. White, J. Chem. Soc. Dalton Trans. 2491, (1988).

58. J.A. Bailey, S.L. Grundy and S.R. Stobart, Personal Communication.

59. A.M. McNair and K.R. Mann, Inorg. Chem. **25**, 2519, (1986).

60 F. Basola, Inorg. Chim. Acta **100**, 33, (1985).

61. D.L. Kerschner and F. Basolo, J. Am. Chem. Soc. **109**, 7396, (1987).

62. C.M. Carr, D.M. Davies, M. Gower, I.A.P. Kane-Maguire and D.A. Sweigart, J. Chem. Soc. Dalton Trans. 923, (1981).

63. J.A. Bailey, S.L. Grundy and S.R. Stobart, Personal Communication.

64. F.A. Cotton and M.H. Chisholm, Chem. Eng. News **60**, 40, (1982).

65. M.A. Bennett, T. Huang, T.W. Matheson and A.K. Smith, Inorg. Synth. **21**, 75, (1982).

# VITA

Surname: BEASLEY Given Names: TIMOTHY JOHN

Place of Birth: PAISLEY, SCOTLAND

Date of Birth: AUGUST 15, 1963

Educational Institutes attended:

| | |
|---|---|
| UNIVERSITY OF LEEDS, ENGLAND | 1981 to 1984 |
| UNIVERSITY OF VICTORIA, CANADA | 1986 to 1989 |

Degrees awarded:

| | | |
|---|---|---|
| B.Sc.(HONOURS) CLASS 1 | 1984 | UNIVERSITY OF LEEDS, ENGLAND |

Honours and Awards:

| | |
|---|---|
| UNIVERSITY OF VICTORIA FELLOWSHIP | 1985-1986 |
| UNIVERSITY OF VICTORIA FELLOWSHIP | 1986-1987 |
| LEWIS J. CLARK MEMORIAL FELLOWSHIP | 1986-1987 |
| UNIVERSITY OF VICTORIA FELLOWSHIP | 1987-1988 |

PARTIAL COPYRIGHT LICENSE

I hereby grant the right to lend my dissertation (the title of which is given below) to users of the University of Victoria Library, and to make single copies only for such users or in response to a request from the Library of any other University, or similar institution, on its behalf or for one of its users. I further agree that permission for extensive copying of this thesis for scholarly purposes may be granted by me or a member of the University designated by me. It is understood that copying or publication of this thesis for financial gain shall not be allowed without my written permission.

Title of Dissertation:

SYNTHESIS OF POLYCYCLIC HYDROCARBON METAL SYSTEMS AND RUTHENIUM PYRAZOLE SYSTEMS.

Author: [redacted]

Timothy. J. Beasley

January 24, 1989.

ISBN 0-315-50157-X